INVESTIGATION OF THE EFFECTIVE ELASTIC PROPERTIES OF COMPOSITE MATERIALS

Thesis submitted towards the degree

"Doctor of Philosophy"

by

YACOV KANTOR

Submitted to the Senate of Tel-Aviv University

August 1983

This work was carried out
under the supervision of
Professor David J. Bergman

ACKNOWLEDGEMENTS

I am deeply grateful to Professor David J. Bergman for his dedicated guidance, patience and support. I have benefited enormously from his broad knowledge and deep scientific insight.

I have learned a lot from Professors Amnon Aharony, Guy Deutscher, Mark Azbel, Yoseph Imry and Ora Entin-Wohlman. My choices of the directions of investigation in this Thesis were guided by the numerous works of Professor Zvi Hashin.

I shall always remember the scientific and social connections with my friends and colleagues Doctors Michael Rappaport, Moshe Schwartz, Eshel Ben-Jacob, Daniel Blankschtein and Yonathan Shapir, and with Yuval Gefen, Aharon Kapitulnik and Alexander Palevski.

Most of all, I am indebted to my wife Mary for her infinite patience, and to my family for their help and encouragement.

ABSTRACT

A new method is presented for a systematic evaluation of the effective elastic constants of a composite material and for deriving rigorous bounds on them. A scattering-theory-like approach is used to expand the solution of the elastostatic problem in terms of a complete set of eigenstates of a certain integral operator. These eigenstates are the elastostatic resonances of the sample, i.e., states where the sample is internally deformed and strained even though the boundaries are undeformed. Each effective elastic constant is presented as a sum of simple poles. The locations of the poles are determined by the unphysical values of the elastic constants of the components at which the elastostatic resonances occur, while the residues can be found from a detailed knowledge of the strain fields of the resonance states.

The resonances of a multi-grain composite with a well defined microgeometry are found by stages. First one finds the resonances of individual, isolated grains, and only then the resonances of the entire composite are constructed as a superposition of the single grain resonances. I apply this procedure to 2D periodic arrays of cylinders - both hexagonal and square. Using simple matrix perturbation techniques, I obtain exact expansions for the elastic constants in powers of p_1, the volume fraction of the cylinders, that go up to order p_1^7 (p_1^{11}) in the case of the bulk modulus of the square (hexagonal) array and up to order p_1^5 in the case of the shear moduli for both arrays. For those microgeometries, I show that a Clausius-Mossotti-type approximation provides a good estimate of the exact solution. I derive such an approximation also for a 3D system of circular-cylinder inclusions with cubic symmetry.

I apply the pole representation of the effective elastic constants to the cases when only partial information is available on the microgeometry of the composite. The locations and strengths of the poles are treated as variational parameters, while different kinds of available information are

translated into constraints on these parameters, such as sum rules on moments of the pole spectrum. Some known bounds are rederived using this method. My new results include an extension of the range of validity of the Hashin-Shtrikman bounds to the case of composites made of isotropic materials but with an arbitrary microgeometry, for cases where the two-point correlation function of the microgeometry is not known. I also use information on the effective elastic constants of one composite in order to obtain improved bounds on the effective elastic constants of another composite with the same or a similar microgeometry.

I discuss some possible additional applications of the theory to quasi-random systems and to viscoelastic composites. I also discuss the relations between my theory and other approaches to the problem of calculating the (effective) elastic moduli of a composite material.

TABLE OF CONTENTS

SOME NOTATIONS AND ABBREVIATIONS

Symbol	Meaning	Page[+]
A_{ij}	Antisymmetric part of γ_{ij}	39
A_i	Numerical coefficient	40
AO or A	Compression dipole resonance state of cylinder	43
a	Index of grain	58
$\vec{a}$	Location of grain a	60
$\pm B\ell$ or B	B-type resonance state of cylinder	43,45
$B_{a\alpha}^{(n)}$ or $B_{\alpha}^{(n)}$	Expansion coefficient of a multi-grain resonance in terms of single-grain resonances	59,60
b	Index of grain	59
b	Lattice spacing	77
$\vec{b}$	Location of grain b	60
$b_{n\gamma}$	Parameter of $v_{n\gamma}$	99
C_{ijkl}	Elastic stiffness tensor (general notation)	16
$C(\vec{r})$	Local stiffness tensor	17
$C^{(o)}$	Spatially constant part of $C(\vec{r})$	18
$C^{(e)}$	Effective C	19
$C_{+}^{(e)}$	Value of $C^{(e)}$ for $s = s_{+}$	111
$C^{(n)}$	C of n-th component	28
$C^{(\gamma)}$	γ-part of decomposition of C	26
$C^{(n\gamma)}$	γ-part of decomposition of $C^{(n)}$	99
$C^{(1)}$,	Elastic stiffness of $C^{(1)}$ material for $s \neq 1$	29

+ 1. No. of page in which the symbol is defined or appears for the first time.

2. Several page numbers may appear if the symbol is redefined or if the definition is extended .

$C_+^{(1)}$	Value of $C^{(1)}$, for $s = s_+$	111
CT	Transverse compression dipole resonance	80
CL	Longitudinal compression dipole resonance	83
$\pm C\ell$ or C	C-type resonance state of cylinder	46
CMTA	Clausius-Mossotti-type approximation	72
Ch. V	Chapter V	
Ch. V.A	Section A in Ch. V	
δC	$C^{(1)} - C^{(2)}$	28
$\delta C^{(n\gamma)}$	$C^{(n\gamma)} - C^{(o\gamma)}$	99
c	Index of grain	125
$c(\vec{r})$	Spatially varying part of $C(\vec{r})$	18
D(s)	Characteristic function	95
D_α	Residue of pole d_α of D(s)	95
$\pm D\ell$ or D	D-type resonance state of cylinder	46
d	Dimensionality of space	22
d_α	Pole of D(s)	95
$\vec{E}$	Electric field	18
$E^{(\kappa)}$	Function of κ and μ	52
$E^{(\mu)}$	Function of κ and μ	52
$E^{(\gamma)}$	Either $E^{(\kappa)}$ or $E^{(\mu)}$	52
F(s)	Characteristic function	29,99,129
F_α	Residue of pole s_α of F(s)	33,99,129
$F_\ell(qp)$	Modified Bessel function or its derivative	79
f(x)	Continuous weight function	91
$f_{ij}(\vec{r})$	Volume average of two-point correlation function	50,103
$\tilde{f}_{ij}(\vec{k})$	Fourier transform $f_{ij}(\vec{r})$	50
G_{ijkl}	Tensor Green's function of ε	18,118

$\tilde{G}_{ijkl}(\vec{k})$	Fourier transform of G_{ijkl}	50,119
$\hat{G}$	Integral operator	31
$\hat{G}_a$	$\hat{G}$ of grain a	58
g_{ij}	Tensor Green's function of $\vec{u}$	117
$\tilde{g}_{ij}(\vec{k})$	Fourier transform of g_{ij}	119
H(s)	Characteristic function	105,131
H_α	Residue of pole h_α of H(s)	105,131
H_{ijkl}	KGK	121
$\hat{H}$	Integral operator	121
h_α	Pole of H(s)	105,131
I_{ijkl}	Symmetric unit tensor	16
$\hat{I}$	Identity operator	33,39
$\hat{J}$	Infinitesimal rotation generating operator	38,39
K_{ijkl}	"Square root tensor" of δC	121
$\vec{k}$	Fourier transform variable	50
$\vec{k}$	Bloch's k-vector	60
$\hat{k}$	Unit vector in $\vec{k}$-direction	50
L	Radius of a large circle around origin of coordinates	65
L	Length of cylinder	80
ℓ	Eigenvalue of $\hat{J}$	40
M_n	n-th moment of pole spectrum of F(s)	48,130
M_{nH}	n-th moment of pole spectrum of H(s)	106,132
$M_n^{(\gamma)}$	M_n for $\varepsilon^o = \varepsilon^{o\gamma}$	52
m	Shear modulus (general notation)	25
$m^{(e)}$	Effective m	47
m(12), m(23),etc.	Shear modulus	25

N	Number of cells in periodic sample	60,61
$\vec{n}$	Unit vector, normal to surface	17
$\vec{P}$	Electrostatic polarization density	18
$P_{ij}^{a(\alpha)}$	Elastostatic polarization density of grain a at resonance state α	65
p_n	Volume fraction of n-th component	47,48,101
$Q_{\beta,\alpha}$	Lattice sum of interactions	61
$Q_{b\beta,a\alpha}$	Interaction between resonances of two grains	60
$\vec{q}$	Wave-vector of plane wave	61
q	Eigenstate index of 3D resonance of cylinder	79
R	Radius of cylinder	38
R_{ijkl}	Directional average of $\tilde{G}$	51
$\vec{r}$	Location vector	17
S_{ijkl}	Elastic compliance tensor (general notation)	16
S	Total area of 2D sample	47
S	Surface area of sample	20
$S(\vec{r})$	Local compliance tensor	129
$S^{(o)}$	Spatially constant part of $S(\vec{r})$	129
$S^{(n)}$	S of n-th component	129
ST±	Transverse shear dipole resonance	81
SL±	Longitudinal shear dipole resonance	82
Sec. B	Section B in current chapter	
s	Continuous parameter that changes $C(\vec{r})$	27,129
s'	Smallest possible value of zero of $F(s)$	106
s_α	Eigenvalue of $\hat{G}$; pole of $F(s)$	32,33,129
$s_{a\alpha}$	Eigenvalue of $\hat{G}_a$	59
s_+	s for which $C^{(e)}$ is known	98
$\vec{T}$	Surface traction	17

$\vec{u}$	Displacement vector	16
$\vec{u}^h$	$\vec{u}$ in homogenous sample	117
$\vec{u}^{(\alpha)}$	$\vec{u}$ of right eigenstate of $\hat{G}$	34
V	Volume of sample	18
v	Volume of single inclusion	47
$v_{n\gamma}$	Function of s	99
W	Elastic energy density	19
w	Point in 2D complex plane $w=x_1 + ix_2$	38
w	1/s	
w_o	Location of the center of cylinder in complex plane	62
X	x_1	77
X_α	Resonance α of X-cylinder	80
x	Parameter which changes $C^{(1)}$,	112
x_i	i-th coordinate (i=1,2,...d)	20
Y_α	x_2	77
Y	Resonance α of Y-cylinder	80
Z	x_3	77
Z_α	Resonance α of Z-cylinder	80
2D	Two-dimensional	22
3D	Three-dimensional	22
α or β	Resonance state (index)	32,59
Γ	Analytic function of w in 2D elasticity	39,40
γ	Elastic modulus ($=\kappa, \mu$ or m)	49
γ_{ij}	Transformation of coordinates for infinitesimal rotation	38
$\gamma^{(n)}$	γ of n-th component	49

$\delta\gamma$	$\gamma^{(1)}-\gamma^{(2)}$	49
Δ	Analytic function of w in 2D elasticity	39,40
Δ	Variation of function or variable	101
∂_i	Partial derivative in x_i direction	16
δ_{ij}	Krönecker delta	16
δ_{ijkl}	=1, for i=j=k=l; =0, otherwise	26
ε_{ij}	Strain tensor (general notation)	16
ε^h	ε in a homogeneous sample	18
$\tilde{\varepsilon}$	Tensor complementary to ε	31
ε^o	Constant strain tensor which defines homogeneous boundary conditions	20
$\varepsilon^{o\kappa}$	Pure compression ε^o	23
$\varepsilon^{o\mu}$	Pure shear ε^o	25
$\varepsilon^{o\mu}(12)$, $\varepsilon^{o\mu}(23)$, etc.	Pure shear ε^o	25
$\varepsilon^{o\gamma}$	Particular choice of ε^o (= $\varepsilon^{o\kappa}$ or $\varepsilon^{o\mu}$ or ε^{om})	48
ε^{om}	Pure shear ε^o	25
$\varepsilon^{om}(12)$, $\varepsilon^{om}(23)$, etc	Pure shear ε^o	25
ε^{loc}	Local Lorentz strain	65
ε^{loc}_{near}	Near contribution to ε^{loc}	65
ε^{loc}_{far}	Far contribution to ε^{loc}	65
$\varepsilon^{macro}_{near}$	ε created by smeared near polarization	65
$\varepsilon^{macro}_{far}$	ε created by smeared far polarization	65

$\boldsymbol{\varepsilon}^{(\alpha)}$	Right eigenstate of $\hat{G}$	32
$\tilde{\boldsymbol{\varepsilon}}^{(\alpha)}$	Left eigenstate of $\hat{G}$	32
$\boldsymbol{\varepsilon}^{a(\alpha)}$	Right eigenstate of $\hat{G}_a$	59
$\tilde{\boldsymbol{\varepsilon}}^{a(\alpha)}$	Left eigenstate of $\hat{G}_a$	59
κ	Bulk modulus (general notation)	23
$\kappa^{(e)}$	Effective κ	47
$\kappa^{(n)}$	κ of n-th component	30,36
$\kappa^{(1)'}$	κ of $C^{(1)}$ material for $s\neq 1$	41
$\kappa_\alpha^{(1)'}$	Resonance value of $\kappa^{(1)'}$	41
$\kappa_+^{(1)}$	Value of $\kappa^{(1)'}$ for $s=s_+$	110
$\delta\kappa$	$\kappa^{(1)} - \kappa^{(2)}$	30,36
λ	Lamé constant	22
$\lambda^{(n)}$	λ of n-th component	50
μ	Lamé constant	22
μ	Shear modulus (general notation)	25
$\mu(12), \mu(23)$ etc.	Shear modulus	25
$\mu^{(e)}$	Effective μ	47
$\mu^{(n)}$	μ of n-th component	30,36
$\mu^{(1)'}$	μ of $C^{(1)}$ material for $s\neq 1$	31
$\mu_\alpha^{(1)'}$	Resonance value of $\mu^{(1)'}$	41,43
$\mu_+^{(1)}$	Value of $\mu^{(1)'}$ for $s=s_+$	110
$\bar{\mu}_{av}$	Average shear modulus	54
$\delta\mu$	$\mu^{(1)} - \mu^{(2)}$	30,36
ρ	Radial cylindrical coordinate	79
ρ	$K\varepsilon$	121
ρ^o	$K\varepsilon^o$	121
$\rho^{(\alpha)}$	Right eigenstate of $\hat{H}$	122

$\rho'^{(\alpha)}$	Left eigenstate of $\hat{H}$	122
σ_{ij}	Stress tensor	16
θ_n	Step function of n-th component	28,99
θ_a	Step function of grain a	58
Φ	Analytic function of w in 2D elasticity	39,40
ϕ	Azimuthal angle in x_1, x_2 plane	39
Ψ	Analytic function of w in 2D elasticity	39,40
Ω_d	d-dimensional solid angle	50,51
ω	Infinitesimal angle	39
$< \mid$	Symbolic notation for bra state	31
$\mid >$	Symbolic notation for ket state	31
$< \mid >$	Scalar product	31
$< >_{av}$	Volume average	19
*	Complex conjugation	31
(III.7)	Equation 7 in Chapter III	
(B.2)	Equation 2 in Appendix B	
[27,28]	References nos. 27 and 28	

CHAPTER I. GENERAL INTRODUCTION

A. COMPOSITE MATERIALS AND THEIR MECHANICAL PROPERTIES

It is convenient for many purposes to distinguish between simple (or homogeneous) and composite (sometimes also called complex, heterogeneous or heterophase) materials. The "usual" crystalline and amorphous solids are classified as simple, while the materials made of large (on the atomic scale) homogeneous regions with different macroscopic physical properties, are classified as composites. Although borderline cases may be difficult to classify [1], typically, whenever the sizes of homogeneous regions are larger than about 100 Å, we can treat the material as a composite [2]. This definition of a composite includes a wide range of materials, e.g., materials obtained by physically combining two or more existing materials, polycrystalline solids, materials with cracks or holes or voids (either empty or filled with some liquid), etc. The last example includes such "natural composites" as porous rocks. On a macroscopic scale composites behave like homogeneous materials, thus enabling us to define the effective (also called overall or average) physical properties of these materials.

Mankind has made use of composite materials from the earliest times, e.g., mortar and concrete were used in extreme antiquity [1]. In more recent times, linoleum, asphalt agregate mixtures and aerated concrete are examples of composites which have assumed considerable importance [1]. The outstanding mechanical properties of fibre composites and especially the unique combination of low density with high strength and stiffness have led to a highly developed technology [2]. Examples of modern composites are alloys strengthened by a dispersion of hard particles, porous ceramics, ceramic-glass and ceramic-metal systems, glass-resin composites, fibrous materials made of glass, carbon and boron fibers imbedded in materials such as epoxy and aluminum, and many others [3]. Among the applications of composites [4,5] we can mention the use of fiberglass in the fabrication of small boats, because a material which is at the same time corrosion-resistant, rot-proof, thermally insulating, dielectric, and nonmagnetic [6] is needed there, and numerous aerospace applications of fibrous materials [5]

(helicopter rotor blades, wings, missile interstage adapters, etc.), because strong, stiff and light (at the same time) materials are needed.

All these technological developments, as well as the interest in the properties of polycrystals, have stimulated intensive theoretical studies of the mechanical and other [1,7] properties of composites during the past twenty years. Among the subjects which received theoretical attention we can mention thermoelastic properties, strength (fracture mechanics, crack propagation, etc.) and viscoelastic properties of composites [7]. However, the elastic properties of composites have been studied most extensively. These properties are important in themselves, and they are also closely connected to other mechanical properties: E.g., a simple relation connects the thermal expansion coefficients with the effective elastic moduli of a two-component composite [8], a simple correspondence principle connects the problems of linear viscoelasticity in composites with the regular elastic problems [9]. Some of the known theoretical approaches to the elastic problem of composites are described in the next section.

B. SOME OF THE KNOWN THEORETICAL APPROACHES TO THE EFFECTIVE ELASTIC PROPERTIES OF COMPOSITES.

The problem of determining effective elastic properties of composites has been attacked in numerous ways [10]. In this work we concentrate our attention only on the theoretical approaches which are related to our work. At this point we would like to mention several important methods and results, while more detailed discussions can be found in the following chapters.

The enormous complexity of the elastostatic problems in composite materials prevents an exact analytic solution even for rather simple microgeometries. However, a few exact solutions of non-trivial microgeometries are known: a) The bulk modulus of assemblages of composite-spheres [11] or of composite-cylinders [12] can be calculated exactly. A composite-sphere-assemblage is a composite material made of two isotropic components, in which the entire volume is comprised of coated spheres, each consisting of

a spherical particle of one component and a concentric spherical shell of the other component. These coated spheres all have the same volume ratio of coating to core, but they must come in many different sizes in order to fill up the entire volume. A composite-cylinder-assemblage consists of parallel coated cylinders which have a structure analogous to that of the coated spheres. b) If a composite consists of two isotropic components with equal shear moduli, then the effective bulk modulus is independent of the details of the microgeometry and it can be calculated exactly [13].

Simple microgeometries, such as lattices of parallel cylinders imbedded in a material with different elastic properties, can be solved numerically [14]. The numerical solutions are very important in practice. However, they are not very convenient: each choice of constituents requires a new numerical solution, even when the microgeometries are the same.

Various bounding methods [10] are very useful whenever the microgeometry of the composite is not exactly known, or when its complexity prevents an exact evaluation of the effective elastic properties. Hill has shown [15] that the volume averaged elastic stiffness tensor (Voigt average [16]) and the volume averaged elastic compliance tensor (Reuss average [17]) provide upper and lower bounds, respectively, on the effective stiffness tensor. The Voigt and Reuss bounds were considerably improved for isotropic mixtures by Hashin and Shtrikman [18], and by Hill [13]. Later, these bounds were rederived, modified and extended by numerous authors. Some details of the different bounding methods are presented in Ch.V. Usually, improvement of the Hashin-Shtrikman bounds requires more geometrical information on the composite than just the volume fractions of the components. In this work, additional information of a non-geometrical character is used to derive improved bounds.

Several approximate solutions of the elastostatic problem in composites are known. If the concentration of one component in a two-component composite is very small (dilute suspension), then approximate expressions for the effective elastic moduli can be found [19]. These expressions can be treated as first terms in the expansions of the effective moduli in power series of the concentration. When the concentrations are not low,

the self-consistent approach [20] is frequently used.

During the last ten years, an approach that is analogous to the quantum scattering theory in solid state physics has often been used [21-26]. Various previously known approximations and bounds were rederived using this approach, thus providing an additional point of view on those results. New results were also obtained. Our theory is mathematically somewhat related to this method. The details of this approach and its relations to our theory will be discussed in Chs.III-V.

The above incomplete list of existing theories shows that there is no lack of theoretical approaches to the problem of the effective elastic moduli of composite materials. Thus, any new approach, such as ours, to this problem should be tested by its ability to obtain results which could not have been derived (or their derivation would be extremely complicated) from the existing theories. We shall demonstrate the usefulness of our approach both by systematic derivations of the effective elastic moduli for several well defined microgeometries and by obtaining improved bounds on those moduli for a type of additional information which cannot be incorporated in the traditional bounding approaches in a tractable way.

C. OUTLINE OF THE THESIS AND SUMMARY OF THE RESULTS

In this Thesis I present a new method for the systematic evaluation of the effective elastic moduli and for deriving rigorous bounds on these moduli.

An attempt was made to present the entire theory and the results in a self-contained form. Therefore I devote Ch.II and App.A to some well known results and definitions of the mathematical theory of composite materials.

In Ch.III I present the new approach in a general form and investigate its main features. I consider a family of two-component composites with the same microgeometry but with different values of the elastic stiffness tensors, depending on a continuous parameter s. A scattering-theory-like

treatment in Sec.B leads to a representation of the effective elastic stiffness, which now depends on s, as a sum of simple poles. Each pole is obtained as an eigenvalue or resonance of the elastostatic problem, while the residue (or weight) is obtained from a detailed knowledge of the local, position dependentstrain tensor at that resonance. I show that both the locations and the weights of the poles are real quantities which are confined to certain intervals (Sec.C), and that they satisfy certain moment sum rules (Sec.E). A simple implementation of the theory for an isolated cylindrical inclusion is given is Sec. D. An alternative formulation of the general approach is presented in App.B.

In Ch.IV I apply this theory to various multi-grain systems. In Sec.B I use methods analogous to the tight-binding approach in solid state physics to construct the resonances of a multi-grain system from the resonances of individual, isolated grains. I demonstrate that only two-body interactions, which are proportional to the overlap integrals between different resonances, need to be known in order to construct the resonances of the entire system. This approach becomes particularly simple in the case of periodic systems. Some difficulties arising from the long range interactions that exist between certain types of resonances are discussed and solved in Sec.C and App.C. The method is applied in Sec.D to two-dimensional (hexagonal and square) arrays of cylindrical inclusions. Elastostatic analogs of the electrostatic Clausius-Mossotti approximation are found. I compare these approximations with numerical solutions of the problem and show the high accuracy of these simple approximations. Using simple matrix perturbation techniques I obtain systematic expansions for the elastic constants in powers of p_1, the volume fraction of the cylinders, that go up to order p_1^{11} in the case of the bulk modulus of an hexagonal array, and to a somewhat lower order in the case of the shear modulus of that array. The bulk and (two) shear moduli of the square array are also calculated to a rather high order in p_1. In Sec.E Clausius-Mossotti-type expressions are obtained for the bulk and (two) shear moduli of a three-dimensional system of cylindrical inclusions which form three mutually perpendicular sets of square arrays of parallel cylinders (i.e., the three-dimensional symmetry is cubic).

In Ch.V I use the formalism derived in Ch.III, as well as an extended version, to derive various bounds. In Sec.B, and also in App.D , I use the sum rules which were obtained in Ch.III to rederive some well known bounds (the Voigt, Reuss and Hashin-Shtrikman bounds). I extend the range of validity of the usual expressions for Hashin-Shtrikman bounds to the case of a composite with an arbitrary microgeometry for which the two-point correlation function of the microgeometry is not known. In Sec.C I extend the general approach to the case of multi-component composites and also make it more flexible. This is applied in Secs.D and E to derive improved bounds which require additional information of a non-geometrical character about composite: Known values of the effective elastic constants for one composite are used to derive improved bounds on the effective constants of another composite with the same microgeometry but made of different constituents.

In Chs.III-V I also discuss the new results and some further possible applications of the formalism (to quasi-random systems, to viscoelastic composites, etc.), as well as possible extensions of the formalism. I also discuss the relations between my theory and other approaches to the problem of calculating the (effective) elastic moduli of a composite material.

Most of the important results which are presented in this Thesis have already been published [27-29], although not in such a detailed form. All the details that are of a more technical nature appear here for the first time.

CHAPTER II. MAIN EQUATIONS AND DEFINITIONS

A. MATHEMATICAL MODEL OF A COMPOSITE MATERIAL AND THE MAIN EQUATIONS

The general composite material can be considered as a mixture of several homogeneous components with different elastic properties. Here the word "component" refers to the different regions of the composite, which have the same elastic properties in a fixed reference frame. Thus two crystals of the same material will be treated as different components, if, due to their different orientiations, their elastic stiffness tensors have different components in the same reference frame. From this point of view, a polycrystalline material is a composite with an infinite number of components.

We shall assume that each homogeneous region is large enough to be treated as a bulk continuum and that it has sharp, well defined boundaries. Under this assumption, any local elastic property of the composite becomes a piecewise constant function. In many cases, the sizes of homogeneous regions are really much larger than interatomic distances: E.g., in many ceramic systems the sizes of the grains range from a micron to several millimeters [30], and in concrete the grains range from 100 microns to several centimeters [31]. However, the validity of the above assumption can be questioned for dispersion-hardened systems [30], where the particle size is about 10 Å. In real composites the interface between two components is not mathematically sharp, i.e. the properties change gradually over several interatomic distances [32]. However, as long as this transition region is narrow compared to the grain sizes, the assumption of a sharp interface is valid. When the grains become very small (several interatomic distances) the validity of some of the above assumptions must be reexamined.

We shall consider the case of small deformations, i.e. the case where the geometrical shape of the sample is practically unchanged. This enables us to disregard all the complications that arise for finite deformations [33]. In that case, the state of the deformed body can be described by a

linearized strain tensor [34]

$$\varepsilon_{ij} = \tfrac{1}{2}(\partial_i u_j + \partial_j u_i), \tag{II.1}$$

where $\vec{u}$ is the displacement vector, while in the case of finite deformations a non-linear term $(\partial_i u_k)(\partial_j u_k)$ occurs in the definition of ε_{ij} and it is necessary to distinguish between the Eulerian and Lagrangian modes of description [35], i.e. between the fixed reference frame and the frame which is distorted by the deformation. Moreover, for small deformations the stress tensor σ depends linearly on the strain ε at the same point, i.e. the generalized Hooke's law [34] is valid:

$$\sigma_{ij} = C_{ijkl}\varepsilon_{kl}, \tag{II.2}$$

where C_{ijkl} is the elastic stiffness tensor of the material. Here and subsequently we use the Einstein summation convention on repeated tensorial indices. Both σ and ε are symmetric second rank tensors, while C is a fourth rank tensor which has the following symmetries [34]:

$$C_{ijkl} = C_{jikl} = C_{ijlk} = C_{klij}. \tag{II.3}$$

The relation (II.2) can also be written in the following form:

$$\varepsilon_{ij} = S_{ijkl}\sigma_{kl}, \tag{II.4}$$

where S is the elastic compliance tensor, which is the (symmetric) inverse of C, i.e.,

$$S_{ijkl}C_{klmn} = I_{ijmn}, \tag{II.5}$$

where

$$I_{ijmn} = \tfrac{1}{2}(\delta_{im}\delta_{jn} + \delta_{in}\delta_{jm}) \tag{II.6}$$

is the symmetric fourth rank unit tensor and δ_{ij} denotes a Kronecker delta. Both C and S of any real solid material must be positive definite tensors [34].

We shall also assume the absence of "frozen" stresses, i.e., when the boundaries of the composite sample are undeformed, then both σ and ε vanish everywhere, and we shall neglect the body forces (e.g., the weight of the materials).

When the composite is in equilibrium, the stress satisfies the following equation [34]

$$\partial_j \sigma_{ij} = 0. \tag{II.7}$$

This relation, together with (II.1) and (II.2), supplemented by appropriate boundary conditions, determines the state of a homogeneous material. In a composite these equations must hold in each one of the homogeneous regions separately. However, in addition to that, continuity conditions must be satisfied at the interfaces. We shall use the simplest assumption of rigid contact between the different regions, i.e., both the displacement vector $\vec{u}$ and the surface traction $\vec{T}$, defined by [34]

$$T_i = \sigma_{ij} n_j, \tag{II.8}$$

where $\vec{n}$ is a unit vector normal to the interface, are continuous. This assumption is usually valid for small deformations [36], although different assumptions are sometimes also made: E.g., surface tractions are continuous, while the displacements change discontinuously across the interface by given increments [37].

In formal calculations it is convenient to use a different approach: We rewrite (II.2) and (II.7) in the following form:

$$\partial_j [C_{ijkl}(\vec{r})\ \varepsilon_{kl}(\vec{r})] = 0, \tag{II.9}$$

where $C(\vec{r})$ is the local elastic stiffness tensor at the point $\vec{r}$. If we require this equation to be satisfied <u>everywhere</u>, including the interfaces, then the continuity of $\vec{u}$ and $\vec{T}$ will be automatically ensured. The derivatives of the discontinuous tensor now are interpreted in the sense of

generalized functions or distributions [38] (i.e., Dirac delta-functions).

Sometimes it is convenient to express the local elastic stiffness tensor $C(\vec{r})$ as a sum of a spatially constant and a spatially varying term:

$$C(\vec{r}) = C^{(o)} + c(\vec{r}). \tag{II.10}$$

In this equation, and often also in subsequent discussions, we have suppressed the tensorial indices. By substituting (II.10) into (II.9) we arrive at the following equation:

$$C^{(o)}_{ijkl}\ \partial_j \varepsilon_{kl} = -\partial_j c_{ijkl}\varepsilon_{kl}. \tag{II.11}$$

Note the analogy between this equation and the equation of electrostatics [39]

$$\partial_i E_i = -4\pi \partial_i P_i, \tag{II.12}$$

where $\vec{E}$ is the electric field and $\vec{P}$ is the polarization. The fact that $c_{ijkl}\varepsilon_{kl}$ plays the role of polarization will be used in Ch.IV.

The strain tensor in a composite material is also a solution of a linear integral equation [40], which replaces (II.1),(II.11) and the boundary conditions on the displacement vector

$$\varepsilon_{ij}(\vec{r}) = \varepsilon^h_{ij}(\vec{r}) + \int G_{ijkl}(\vec{r},\vec{r}';C^{(o)})\, c_{klmn}(\vec{r}')\varepsilon_{mn}(\vec{r}')\, dV'. \tag{II.13}$$

Here G is the tensor Green's function of the problem — it depends on $C^{(o)}$ and on the shape of the sample, ε^h is the strain, which would exist in a homogeneous system with elastic stiffness $C^{(o)}$ subject to the same boundary conditions on the displacement $\vec{u}$ as the actual inhomogeneous sample, and the integral is performed over the entire volume V of the sample. As our work relies heavily on the properties of Green's tensor, we give a brief derivation and a list of some important properties of G in App.A.

B. HOMOGENEOUS BOUNDARY CONDITIONS AND THE DEFINITION OF THE EFFECTIVE STIFFNESS TENSOR

This work will be concerned with the determination of the effective elastic stiffness tensor $C^{(e)}$. This quantity is supposed to be the analogue of C, which appears in the generalized Hooke's law (II.2) for homogeneous materials, when we are interested in the properties of the composite on large scales. It is generally believed that such a quantity exists and that it is unique whenever all the relevant length scales (the size of the sample, the distance over which an external loading changes by appreciable amounts, etc.) are large compared to the scale on which the sample "becomes homogeneous". However, no exact mathematical proof of the statement exists.

There are two options for defining $C^{(e)}$. It can be defined by means of volume averages of the stress tensor σ and the strain tensor ε in the sample

$$\langle\sigma\rangle_{av} = \langle C\varepsilon\rangle_{av} \equiv C^{(e)}\langle\varepsilon\rangle_{av}, \tag{II.14}$$

where $\langle\ \rangle_{av}$ denotes the volume average. Thus we require the volume averages of σ and ε to satisfy the Hooke's law (II.2). An alternative definition uses the expression for the elastic energy density [34]

$$W(\vec{r}) = \tfrac{1}{2}\varepsilon(\vec{r})\sigma(\vec{r}) = \tfrac{1}{2}\varepsilon(\vec{r})C(\vec{r})\varepsilon(\vec{r}) \tag{II.15}$$

and requires that the elastic energy that would exist in a homogeneous sample with elastic stiffness tensor $C^{(e)}$ be equal to the elastic energy of the actual sample, when the average strains are the same, i.e.,

$$2\langle W\rangle_{av} = \langle\varepsilon\sigma\rangle_{av} = \langle\varepsilon C\varepsilon\rangle_{av} \equiv \langle\varepsilon\rangle_{av}C^{(e)}\langle\varepsilon\rangle_{av}. \tag{II.16}$$

Both definitions of $C^{(e)}$, namely (II.14) and (II.16), coincide whenever the decomposition

$$\langle\varepsilon\sigma\rangle_{av} = \langle\varepsilon\rangle_{av}\langle\sigma\rangle_{av} \tag{II.17}$$

is valid. Kröner [41] has shown that this decomposition can be made under quite general circumstances: The elastic compliances and the surface forces have to be bounded, the body has to be macroscopically homogeneous and no body forces or "frozen" strains may be present. From (II.4) we could construct a definition of the effective compliance similar to (II.14) and (II.16). However, (II.14) and (II.16) are more convenient to our purposes.

In the previous section we did not specify the boundary conditions on the displacement vector $\vec{u}$. We will use homogeneous boundary conditions [42]:

$$u_i = \varepsilon^o_{ij} x_j, \text{ for } \vec{r} = (x_1, x_2, x_3) \text{ on the boundary,} \qquad \text{(II.18)}$$

where ε^o_{ij} is some constant symmetric tensor (i.e., ε^o has the same value over the entire boundary). These boundary conditions would cause the strain ε to be a uniform constant $\varepsilon = \varepsilon^o$ over the entire volume in the case of a homogeneous material. This can be shown by assuming (II.18) to be valid over the entire volume. Equations (II.9) and (II.1) will be trivially satisfied when C is a constant tensor, and the boundary conditions (II.18) are also obviously satisfied. In the case of an inhomogeneous material only the volume average of $\varepsilon(\vec{r})$ is equal to ε^o, as can be shown by direct calculation:

$$\begin{aligned} \langle \varepsilon_{ij} \rangle_{av} &= \frac{1}{2V} \int (\partial_i u_j + \partial_j u_i)\, dV = \frac{1}{2V} \oint (u_j n_i + u_i n_j)\, dS = \\ &= \frac{1}{2V} \oint (\varepsilon^o_{jk} x_k n_i + \varepsilon^o_{ik} x_k n_j)\, dS = \frac{1}{V} \int \varepsilon^o_{ij}\, dV = \varepsilon^o_{ij}, \end{aligned} \qquad \text{(II.19)}$$

where we used the definition (II.1), performed the volume-to-surface and surface-to-volume transformations (dS denotes surface element) of the integral (i.e., applied twice Gauss' theorem) and used (II.18) for the value of $\vec{u}$ on the surface.

For homogeneous boundary conditions the decomposition (II.17) is valid exactly:

$$<\varepsilon_{ij}\sigma_{ij}>_{av} = \frac{1}{2V}\int(\partial_i u_j + \partial_j u_i)\sigma_{ij}dV = \frac{1}{2V}\oint(u_j n_i + u_i n_j)\sigma_{ij}dS =$$

$$= \frac{1}{2V}\oint(\varepsilon^o_{jk}x_k n_i + \varepsilon^o_{ik}x_k n_j)\sigma_{ij}dS = \frac{1}{V}\int\varepsilon^o_{ij}\sigma_{ij}dV = \varepsilon^o_{ij}<\sigma_{ij}>_{av}, \quad \text{(II.20)}$$

where we performed a transformation of the same type as in (II.19), and the additional volume integrals of the type $\int u_j \partial_i \sigma_{ij}dV$, which should have appeared in the volume-to-surface transformations, vanish due to (II.7). Thus both definitions of $C^{(e)}$, namely (II.14) and (II.16), coincide exactly for any sample, i.e. even when the sample is small and cannot be treated as macroscopically homogeneous. By applying homogeneous boundary conditions we thus obtain a well defined quantity $C^{(e)}$, while its applicability to general boundary conditions and for large samples becomes a separate question.

In this work we will use the definition (II.16) of $C^{(e)}$, which under the conditions (II.18) and using (II.19) and (II.20) assumes the form

$$\varepsilon^o C^{(e)}\varepsilon^o = \varepsilon^o<C\varepsilon>_{av}. \quad \text{(II.21)}$$

Finally, we would like to make a remark on the size of ε^o in (II.18). In the previous section we resricted the validity of the main equations to the case of small (strictly speaking, infinitesimally small) deformations, which would imply $\varepsilon^o_{ij} << 1$. However, once we assumed the validity of the equations (II.1) and (II.9) (or (II.13)), we can use strains of arbitrary sizes, because the equations are linear and (II.21) is not affected by a multiplication of ε^o in (II.19) by a constant factor.

C. EFFECTIVE ELASTIC MODULI IN TWO- AND THREE- DIMENSIONAL COMPOSITES

Symmetries of C_{ijkl} (see (II.3)) restrict the number of its independent components to 21, in the most general case. The crystal symmetry of a homogeneous material reduces the number of components drastically [34]. For orthotropic media (symmetric under reflections through the x_1x_2, x_2x_3

and x_1x_3 coordinate planes) there are only 9 independent non-zero components. This number is reduced to 2 in the isotropic case:

$$C_{ijkl} = \lambda\delta_{ij}\delta_{kl} + 2\mu I_{ijkl}, \qquad \text{(II.22)}$$

where λ and μ are the Lamé constants.

The elastic symmetry of $C^{(e)}$ of a composite material depends both on the microgeometry and on the crystal symmetry of the constituents. Thus in the most general case the symmetry of $C^{(e)}$ may be very low, as it usually must be a sub-group of both the geometrical and the crystal symmetry groups. However, in many cases the symmetry of $C^{(e)}$ is higher than that: For instance, a polycrystalline material in which the crystals are oriented in all possible directions with equal probabilities will, in fact, be isotropic. All the specific examples in this work will consider composites with isotropic constituents, and therefore the symmetry will be determined entirely by the microgeometry of the composite.

Different choices of ε^0 in (II.21) can isolate different parts of $C^{(e)}$. In this work the scalar quantities obtained from $\varepsilon^0 C \varepsilon^0$ will be referred to as elastic moduli or elastic constants. In general, an elastic modulus will be a linear combination of several components of the tensor C_{ijkl}. The elastic moduli which are defined in this way must be positive in any real (solid) material, because the elastic energy density (II.15) must be positive [34].

Some results in this work are valid for a general dimensionality d of the system. While the case $d > 3$ is a mathematical abstraction, both two-dimensional (2D) and three-dimensional (3D) cases have physical meaning. In this context we should point out that the d=2 case does not really mean a 2D material, but rather a situation in which the stresses and the strains as well as the microgeometry of the composite do not depend on the x_3 coordinate. The composite itself then has the form of parallel fibers. Moreover, we shall restrict our discussion to a plane strain problem [43], in which the u_3 component of the displacement vector $\vec{u}$ vanishes. This choice is especially convenient, because the 2D elastic stiffness tensor

coincides with that part of the usual 3D tensor, in which the indices are only 1 or 2. E.g., in the isotropic case the 2D Lamé constants λ and μ in (II.22) are the same as the usual 3D Lamé constants. The components σ_{13}, σ_{23} and σ_{33} of the stress tensor in a plane strain problem can be derived trivially from the solution of the 2D problem [43].

A different situation would occur if we considered a plane stress problem, in which the σ_{13}, σ_{23} and σ_{33} components of the stress tensor vanish. However, the plane strain and plane stress problems are related [43]: E.g., in a homogeneous isotropic material the replacement of λ by $2\lambda\mu/(\lambda + 2\mu)$ suffices to convert the plane strain problem to a plane stress problem.

Clearly, the solution of the 2D plane strain problem determines only part of the components of the full $C^{(e)}$ of the 3D sample. However, it has been shown by Hill [44] that in important cases, such as transverse isotropic symmetry or transverse square symmetry, the remaining elastic constants are simply related to the 2D or transverse elastic constants of the sample.

Different possible choices of ε^0, and thus different elastic moduli $\varepsilon^0 C \varepsilon^0$ of a material characterised by a stiffness tensor C, were extensively discussed by Hashin [42]. We shall limit ourselves to a partial set of elastic moduli, and thus to few ε^0. This set suffices for the description of highly symmetric (isotropic, cubic (in 3D), square (in 2D)) materials. The choice

$$\varepsilon^0_{ij} = \varepsilon^{0K}_{ij} \equiv \frac{1}{d}\delta_{ij} \tag{II.23}$$

selects the d-dimensional bulk modulus

$$\kappa \equiv \varepsilon^{0K} C \varepsilon^{0K} = \frac{1}{d^2} \cdot C_{iikk} \quad . \tag{II.24}$$

In 2D this expression yields the transverse bulk modulus. In Fig. II.1a the deformation caused by ε^{0K} is depicted for a 2D case - it corresponds to an isotropic compression. In the isotropic case, the bulk modulus is

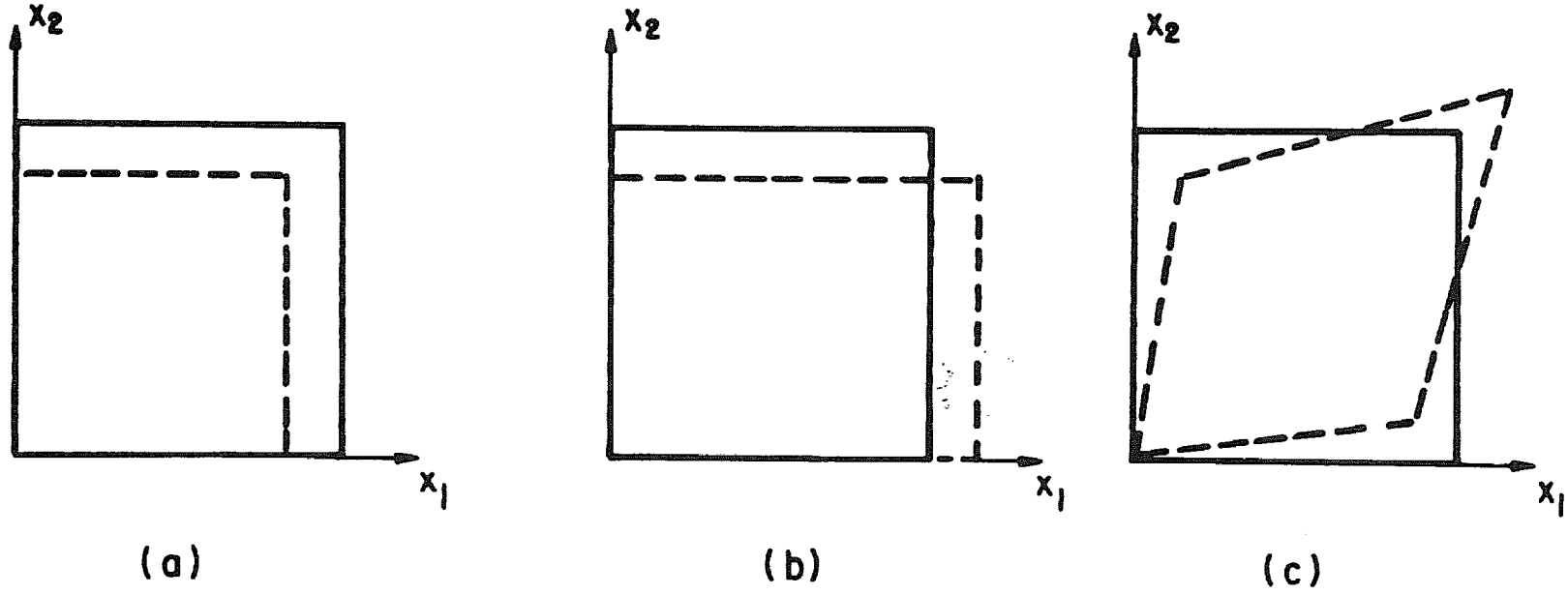

Fig. II. 1 Schematic representation of the deformations of a 2D square sample imposed by (a) pure (isotropic) compression (II.23) and (b), (c) pure shear deformations (II.29) and (II.28), respectively, of the boundaries. Continuous lines show the original shape while the broken lines depict the deformed state.

simply related to Lamé constants

$$\kappa = \lambda + \frac{2}{d}\mu \,. \tag{II.25}$$

In a 2D system we can choose two pure shears,

$$\varepsilon^{o} = \varepsilon^{o\mu} \equiv I_{ij12} \tag{II.26}$$

and

$$\varepsilon^{o} = \varepsilon^{om} \equiv \tfrac{1}{2}(I_{ij11} - I_{ij22}), \tag{II.27}$$

which will define two shear moduli,

$$\mu \equiv \varepsilon^{o\mu} C \varepsilon^{o\mu} = C_{1212} \tag{II.28}$$

and

$$m \equiv \varepsilon^{om} C \varepsilon^{om} = \tfrac{1}{4}(C_{1111} + C_{2222} - 2C_{1122}), \tag{II.29}$$

respectively. These shear deformations are depicted in Fig.II.1b,c. The definitions (II.26)-(II.29) can also be applied to a 3D system. However, in that case we can construct a whole set of shears,

$$\varepsilon^{o\mu}(12) \equiv I_{ij12},\ \varepsilon^{o\mu}(13) \equiv I_{ij13},\ \varepsilon^{o\mu}(23) \equiv I_{ij23},$$

$$\varepsilon^{om}(12) \equiv \tfrac{1}{2}(I_{ij11}-I_{ij22}),\ \varepsilon^{om}(13) \equiv \tfrac{1}{2}(I_{ij11}-I_{ij33}),$$

$$\varepsilon^{om}(23) \equiv \tfrac{1}{2}(I_{ij22}-I_{ij33}), \tag{II.30}$$

which defines the shear moduli $\mu(12)$, $\mu(13)$, $\mu(23)$, $m(12)$, etc. In the case of cubic symmetry, $\mu(12) = \mu(13) = \mu(23)$ and $m(12) = m(13) = m(23)$ and thus we are left with only two shear moduli, μ and m.

In the case of cubic (square in 2D) symmetry the elastic stiffness tensor has the following form in terms of the three elastic moduli:

$$C_{ijkl} = \kappa\delta_{ij}\delta_{kl} + 2\mu(I_{ijkl} - \delta_{ijkl}) + 2m(\delta_{ijkl} - \frac{1}{d}\delta_{ij}\delta_{kl})$$

$$\equiv C^{(\kappa)} + C^{(\mu)} + C^{(m)}, \qquad \text{(II.31)}$$

where

$$\delta_{ijkl} \equiv \begin{cases} 1, \text{ for } i=j=k=l \\ \\ 0, \text{ otherwise.} \end{cases} \qquad \text{(II.32)}$$

In the isotropic case (transverse isotropic in 2D), both shear moduli, μ and m, are equal and they coincide with the Lamé constant μ in (II.22). The equation (II.31) then reduces to

$$C_{ijkl} = \kappa\delta_{ij}\delta_{kl} + 2\mu(I_{ijkl} - \frac{1}{d}\delta_{ij}\delta_{kl}) \equiv C^{(\kappa)} + C^{(\mu)}, \qquad \text{(II.33)}$$

which can also be obtained directly by substituting (II.25) into (II.22).

When the symmetry of a material is low, additional ε^0's may be needed to describe completely the tensor C. These can always be constructed as linear combinations of the different ε^0's which were defined in this section.

CHAPTER III. SPECTRAL REPRESENTATION OF THE EFFECTIVE ELASTIC MODULI

A. INTRODUCTION

The integral equation (II.13) for the strain tensor in the composite has the form of the scattering equation in quantum mechanics. Over the last ten years, an approach that is analogous to quantum scattering theory in solid state physics [45] has often been used [21-26]. In some works [22,23,25], (II.13) is iterated and, the resulting series is then resummed to obtain a formal solution for ε. An unknown operator (T-matrix) then appears in the formal solution. Approximate solutions based on perturbation theory have been developed [22,23], which enabled a rederivation of some known results, including approximate solutions [16,17,20] and bounds [18]. In approaches of this kind, one usually begins by solving the one grain (either static or dynamic) scattering problem (frequently, in Born or long-wave approximations). This is then extended to a solution of the multi-inclusion problem by multiple scattering techniques. Such a procedure is successful when the concentration of inclusions is low, or when the elastic constants of the inclusions do not differ strongly from those of the host medium, i.e. when the scattering is weak.

We also start from a scattering-theory-like representation of the elastostatic problem. Following a similar approach to one that was used in the electrostatic case [46,47], we expand the solution of the elastostatic problem in a set of eigenstates of the integral operator which appears in (II.13) [27,28]. In this way we obtain a (spectral) representation of the effective elastic constants in the form of a sum of elastostatic resonance terms, each of which can be calculated from a knowledge of the appropriate eigenstate. This way of calculation influences our treatment of a multi-grain system, i.e. we will use the elastostatic resonances of individual, isolated grains to obtain the resonances of the entire system [27] (see Ch.IV).

In this chapter we introduce the general approach to the elastostatic

problem of a two-component composite [27,28] (Sec.B) and investigate the main properties of the spectral representation which is obtained (Secs.C and E). A simple implementation of the formalism [27] is presented in Sec.D. The entire chapter is a theoretical preparation to the implementations which will be presented in the following chapters. Although we usually assume that both components of the composite are elastic, i.e. the elastic stiffness tensors are real, the formalism is valid, though with some reservations, in the viscoelastic case too, i.e. when the stiffness tensors are complex. The validity of the theory in viscoelastic cases is discussed, along with other subjects, in Sec.F.

B. THE GENERAL APPROACH

In this section we present our formalism for the calculation of the effective elastic moduli of a two-component composite [27,28]. Elastostatic resonances are introduced and used to represent the effective elastic moduli as a sum of simple poles.

The position dependent local elastic stiffness tensor $C(\vec{r})$ of a two-component composite made of homogeneous materials with stiffness tensors $C^{(1)}$ and $C^{(2)}$ can be written with the help of a step function θ_1:

$$C(\vec{r}) = C^{(2)} + \theta_1(\vec{r})(C^{(1)} - C^{(2)}) \equiv C^{(2)} + \theta_1(\vec{r})\delta C, \qquad \text{(III.1)}$$

where

$$\theta_1(\vec{r}) \equiv \begin{cases} 1, \text{ for } \vec{r} \text{ inside } C^{(1)} \text{ material,} \\ 0, \text{ for } \vec{r} \text{ outside } C^{(1)} \text{ material.} \end{cases} \qquad \text{(III.2)}$$

The choice, which constituent will be denoted $C^{(1)}$ and which one $C^{(2)}$, is completely arbitrary. At this formal stage there is no need to relate, say, $C^{(1)}$ to the inclusions and $C^{(2)}$ to the host material. Thus the formal theory will be completely symmetric from this point of view. However, in some practical applications certain choices may be more convenient than

others.

We shall use a somewhat more general form of (III.1)

$$C(\vec{r};s) = C^{(2)} + \frac{1}{s}\theta_1(\vec{r})\delta C. \tag{III.3}$$

By allowing s to take arbitrary values, we are actually replacing the $C^{(1)}$ material by a different material, characterized by a stiffness tensor

$$C^{(1)'} = C^{(2)} + \frac{1}{s}\delta C = \frac{1}{s}C^{(1)} + \frac{s-1}{s}C^{(2)}. \tag{III.4}$$

As s varies, $C^{(1)'}$ moves along a straight line in the space of elastic moduli as it is depicted in Fig. III.1. We note that when s lies in certain ranges, the tensor $C^{(1)'}$ becomes <u>unphysical</u>, i.e. it ceases to be positive semidefinite.

When the local stiffness $C(\vec{r};s)$ given by (III.3) is used in the definition of the effective elastic stiffness tensor $C^{(e)}$ (see (II.21)) we arrive at the following form:

$$\varepsilon^0 C^{(e)}(s)\varepsilon^0 = \frac{1}{V}\int \varepsilon^0 (C^{(2)} + \frac{1}{s}\theta_1\delta C)\varepsilon^0 dV, \tag{III.5}$$

where ε^0 defines the homogeneous boundary conditions (II.18) and the integration is performed over the entire volume of the composite. Consequently, we define the characteristic function F(s) by

$$F(s) \equiv \varepsilon^0 C^{(e)}(s)\varepsilon^0 - \varepsilon^0 C^{(2)}\varepsilon^0 = \frac{1}{sV}\int \theta_1 \varepsilon^0 \delta C \varepsilon dV. \tag{III.6}$$

Obviously, F(s) is a scalar quantity that depends on the choice of ε^0.

If we compare (III.3) with the general expression (II.10) for $C(\vec{r})$ we can identify the spatially constant term $C^{(o)}$ and the varying term $c(\vec{r})$ of (II.10) in our specific case (III.3):

$$C^{(o)} = C^{(2)}, \tag{III.7a}$$

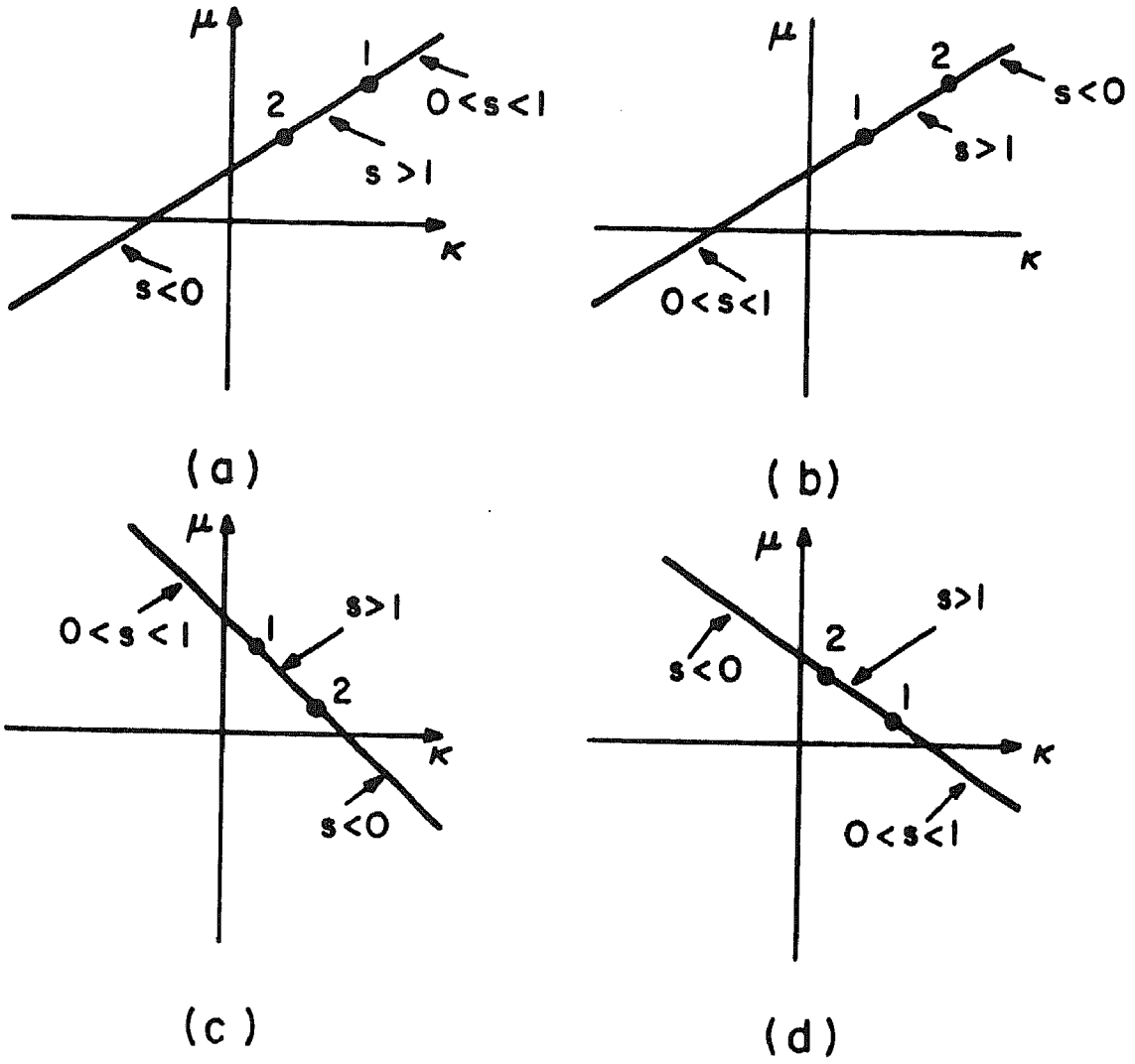

Fig. III.1 Possible locations of $C^{(1)}$, defined by (III.4) in the space of elastic moduli κ and μ. Points 1 and 2 show the locations of two isotropic materials $C^{(1)} = (\kappa^{(1)}, \mu^{(1)})$ and $C^{(2)} = (\kappa^{(2)}, \mu^{(2)})$. Four different cases are shown: (a) $\delta\kappa \equiv \kappa^{(1)} - \kappa^{(2)} > 0$, $\delta\mu \equiv \mu^{(1)} - \mu^{(2)} > 0$, (b) $\delta\kappa < 0$, $\delta\mu < 0$, (c) $\delta\kappa < 0$, $\delta\mu > 0$, (d) $\delta\kappa > 0$, $\delta\mu < 0$. For various values of s, various locations of $C^{(1)}$, along the solid line are obtained. Intervals of the line, corresponding to the intervals $s < 0$, $0 < s < 1$ and $s > 1$ are indicated by arrays.

$$c(\vec{r}) = \frac{1}{s}\theta_1(\vec{r})\delta C. \qquad \text{(III.7b)}$$

Thus the integral equation (II.13) for the strain tensor assumes the form:

$$\varepsilon_{ij}(\vec{r}) = \varepsilon^0_{ij} + \frac{1}{s}\int \theta_1(\vec{r}')\, G_{ijkl}(\vec{r},\vec{r}';C^{(2)})\delta C_{klmn}\varepsilon_{mn}(\vec{r}')dV', \qquad \text{(III.8)}$$

where we used the fact that in a homogeneous body subject to homogeneous boundary conditions (II.18) the strain is constant, i.e. $\varepsilon^h(\vec{r}) = \varepsilon^0$ in (II.13). In a more concise bra-and-ket notation

$$|\varepsilon> = |\varepsilon^0> + \frac{1}{s}\hat{G}|\varepsilon>, \qquad \text{(III.9)}$$

where the linear integral operator $\hat{G}$ acts as follows:

$$\hat{G}|\varepsilon> \equiv \int \theta_1(\vec{r}')G(\vec{r},\vec{r}')\delta C\varepsilon(\vec{r}')dV'. \qquad \text{(III.10)}$$

In order to simplify the notation, we now introduce two definitions: For any second rank tensor ε we define a complementary tensor $\tilde{\varepsilon}$

$$\tilde{\varepsilon} \equiv (\varepsilon\delta C)^*, \qquad \text{(III.11)}$$

where the asterisk denotes complex conjugation, and we also define a scalar product between two arbitrary second rank tensors

$$<\varepsilon|\varepsilon'> \equiv \int \theta_1(\vec{r})\varepsilon^*_{ij}(\vec{r})\varepsilon'_{ij}(\vec{r})dV. \qquad \text{(III.12)}$$

Note that the integration is confined to the volume of $C^{(1)}$ material. Thus the definition of the scalar product (III.12) depends on the microgeometry of the composite, while the definition of the complementary tensor (III.11) depends on the difference in the elastic properties of the constituents. We can now rewrite (III.6) in the form:

$$F(s) = \frac{1}{sV}<\tilde{\varepsilon}^0|\varepsilon>. \qquad \text{(III.13)}$$

The use of non-real (i.e., complex) tensors is mandatory only if s or C's are complex. Otherwise we can always restrict ourselves to real $\varepsilon, \tilde{\varepsilon}$ (see Sec.C). However, even then it is sometimes convenient to allow complex $\varepsilon, \tilde{\varepsilon}$.

Now we formally solve (III.9)

$$|\varepsilon> = \frac{s}{s-\hat{G}}|\varepsilon^0>, \tag{III.14}$$

and substitute this solution in (III.13) to obtain

$$F(s) = \frac{1}{V}<\tilde{\varepsilon}^0|\frac{1}{s-\hat{G}}|\varepsilon^0>. \tag{III.15}$$

In order to make further progress, we introduce the eigenstates of the operator $\hat{G}$. Although the Green's tensor G is symmetric (see (A.8)), the integral operator $\hat{G}$ defined by (III.10) is non-hermitian under the scalar product (III.12). Thus there exists a set of right eigenstates $|\varepsilon^{(\alpha)}>$ such that

$$\hat{G}|\varepsilon^{(\alpha)}> = s_\alpha|\varepsilon^{(\alpha)}> \tag{III.16}$$

and a different set of left eigenstates. However, from (A.8), (III.10)-(III.12) we can easily see that the complementary tensor $\tilde{\varepsilon}^{(\alpha)}$ of a right eigenstate $\varepsilon^{(\alpha)}$ is a left eigenstate of $\hat{G}$ with the same eigenvalue, i.e.

$$<\tilde{\varepsilon}^{(\alpha)}|\hat{G} = <\tilde{\varepsilon}^{(\alpha)}|s_\alpha \quad . \tag{III.17}$$

The two sets satisfy the bi-orthogonality relations [48]

$$<\tilde{\varepsilon}^{(\alpha)}|\varepsilon^{(\beta)}> = 0, \text{ for } s_\alpha \neq s_\beta \ . \tag{III.18}$$

When there is degeneracy of eigenvalues, we can always choose the eigenstates so that they are mutually bi-orthogonal. The only property which is not automatically ensured for such operators is normalizability, i.e.

$$<\tilde{\varepsilon}^{(\alpha)}|\varepsilon^{(\alpha)}> \neq 0 \ . \tag{III.19}$$

In the next section we will prove that this property holds for all relevant eigenstates of $\hat{G}$, and that they form a complete set of eigenstates inside $C^{(1)}$ material.

By comparing (III.16) with (III.9) we can identify the physical significance of the right eigenstates of $\hat{G}$. These are the elastostatic resonances of the sample, i.e., states where the sample is internally deformed and strained even though the boundaries are undeformed. Such a situation cannot occur for any physically allowed values of the elastic constants, and therefore $C^{(1)}$' in (III.3) must assume unphysical values for $s = s_\alpha$, i.e. it cannot be positive definite. We now use the complete bi-orthogonal set of normalized eigenstates of $\hat{G}$ in order to write the following expansion for the identity operator

$$\hat{I} = \sum_\alpha |\varepsilon^{(\alpha)}><\tilde{\varepsilon}^{(\alpha)}| \,. \tag{III.20}$$

Using this operator we can bring (III.15) to the following form

$$F(s) = \sum_\alpha \frac{F_\alpha}{s-s_\alpha} \,, \tag{III.21}$$

where

$$F_\alpha \equiv \frac{1}{V}<\tilde{\varepsilon}^{o}|\varepsilon^{(\alpha)}><\tilde{\varepsilon}^{(\alpha)}|\varepsilon^{o}> = \frac{1}{V}(<\tilde{\varepsilon}^{o}|\varepsilon^{(\alpha)}>)^2 \,. \tag{III.22}$$

Thus the problem of calculation of $C^{(e)}$ has been reduced to the problem of calculation of elastostatic resonances of the sample: Once all $\varepsilon^{(\alpha)}$ and s_α are known we can reconstruct the function F(s), and from its value at s=1 the effective modulus can be found (see (III.6)).

It is important to note that because the scalar product (III.12) involves integration only over the volume of $C^{(1)}$ material, it is only inside this subvolume that the bi-orthogonal set of eigenstates forms a complete set. Thus (III.20) is an identity operator only in this subvolume. However, this fact does not affect the validity of the above procedure: Since (III.15) involves a scalar product, we actually need the

correct strains only inside the $C^{(1)}$ material.

In the next section we shall discuss some properties of the poles s_α and their residues F_α.

Finally we would like to mention that the formalism presented above can be somewhat modified [27]: Equation (III.9) can be replaced by an analogous equation in which a symmetric operator (sometimes it is even hermitian) appears instead of $\hat{G}$. This approach is described in App.B. Although we used the modified approach in our original paper [27], it has become clear that the approach presented in this section is less complicated.

C. LOCATIONS AND WEIGHTS OF POLES IN THE SPECTRAL REPRESENTATION

In this section we prove that all the eigenvalues s_α of the operator $\hat{G}$, i.e. the poles of $F(s)$, and all weights F_α are real, and that the product $F_\alpha \cdot s_\alpha$ is always negative [27]. We also prove the normalizability of the eigenstates of $\hat{G}$.

Let $|\varepsilon^{(\alpha)}\rangle$ be an eigenstate of $\hat{G}$. From (II.9), (III.3) and the definition of the resonance state it follows that the strain tensor $\varepsilon^{(\alpha)}$ satisfies

$$\partial_j[(C^{(2)}_{ijkl} + \frac{1}{s_\alpha}\theta_1\delta C_{ijkl})\varepsilon^{(\alpha)}_{kl}] = 0, \qquad \text{(III.23)}$$

and the corresponding displacement vector $\vec{u}^{(\alpha)}$ vanishes at the surface of the sample. We now form the following integral

$$\int u_i^{(\alpha)*}\partial_j[(C^{(2)}_{ijkl} + \frac{1}{s_\alpha}\theta_1\delta C_{ijkl})\varepsilon^{(\alpha)}_{kl}]\, dV \qquad \text{(III.24)}$$

and add to it a similar expression but with the subscripts i and j interchanged. Integrating by parts, we transfer the ∂_j operator to $u_i^{(\alpha)*}$, the surface integral vanishes, and we are left with

$$\int \varepsilon^{(\alpha)*} (C^{(2)} + \frac{1}{s_\alpha} \theta_1 \delta C) \varepsilon^{(\alpha)} dV = 0 \ . \qquad \text{(III.25a)}$$

If we would perform the same operation with $u_i^{(\alpha)}$, instead of $u_i^{(\alpha)*}$, the resulting expression

$$\int \varepsilon^{(\alpha)} (C^{(2)} + \frac{1}{s_\alpha} \theta_1 \delta C) \varepsilon^{(\alpha)} dV = 0 \qquad \text{(III.25b)}$$

would have a simple physical meaning: The integral gives the total elastic energy of the sample for undeformed boundaries, and therefore it must vanish. Since $C^{(2)}$ and δC in (III.25a) are real symmetric matrices, the eigenvalue s_α must be a real number.

Since $\varepsilon^{(\alpha)}$ is an eigenstate of a real integral operator (see (III.10)), and s_α is a real eigenvalue, the real and imaginary parts of $\varepsilon^{(\alpha)}$ are also eigenstates with the same eigenvalue. If the eigenvalue is non-degenerate, the real and imaginary parts of the eigenstate are proportional and we can choose $\varepsilon^{(\alpha)}$ to be a real tensor. If the eigenvalue is degenerate then a set of real bi-orthogonal tensors can be constructed by a Gram-Schmidt-type orthogonalization process. The set of real eigenstates thus obtained must be normalized as follows:

$$1 = \langle \widetilde{(A_\alpha \varepsilon^{(\alpha)})} \, | A_\alpha \varepsilon^{(\alpha)} \rangle = A_\alpha^2 \int \theta_1 \varepsilon^{(\alpha)} \delta C \varepsilon^{(\alpha)} \, dV \ . \qquad \text{(III.26)}$$

From this follows that the normalization constant A_α is a pure real or pure imaginary number, depending upon the sign of the integral $\int \theta_1 \varepsilon^{(\alpha)} \delta C \varepsilon^{(\alpha)} dV$. Comparing (III.25) with (III.26) we find, since $C^{(2)}$ is positive semi-definite matrix,

$$\text{sgn } A_\alpha^2 = \text{sgn} \int \theta_1 \varepsilon^{(\alpha)} \delta C \varepsilon^{(\alpha)} dV = -\text{sgn } s_\alpha \ . \qquad \text{(III.27)}$$

From (III.22) we find

$$F_\alpha = \frac{A_\alpha^2}{V} \left(\int \varepsilon^{o} \delta C \varepsilon^{(\alpha)} dV \right)^2 , \qquad \text{(III.28)}$$

and hence that F_α is real and that sgn F_α = -sgn s_α. Actually, F_α or s_α can also vanish, therefore the general statement is

$$F_\alpha \cdot s_\alpha \leqslant 0. \tag{III.29}$$

In the case of degenerate eigenvalue s_α, this statement is only guaranteed to hold for the total weight F_α of the resonance s_α.

We can rewrite (III.25a) in the following form

$$\int \varepsilon^{(\alpha)} (1-\frac{1}{s_\alpha}\theta_1) C^{(2)} \varepsilon^{(\alpha)} dV + \int \varepsilon^{(\alpha)*} \frac{1}{s_\alpha} \theta_1 C^{(1)} \varepsilon^{(\alpha)} dV = 0. \tag{III.30}$$

Since $C^{(1)}$ and $C^{(2)}$ are positive semidefinite tensors, we see that s_α cannot exceed 1. If δC is a positive (negative) semidefinite tensor, then s_α is negative (positive), as can be seen from (III.27). The summary of these results is

$$s_\alpha \leqslant 0, \quad \text{for } \delta C \geqslant 0, \tag{III.31a}$$

$$0 \leqslant s_\alpha < 1, \quad \text{for } \delta C \leqslant 0, \tag{III.31b}$$

where $\delta C \geqslant 0$ ($\delta C \leqslant 0$) means that δC is a positive (negative) semidefinite tensor. Moreover, since for a real <u>solid</u> material $C^{(2)}$ is positive definite (<u>not semi</u>definite), we can see that for sufficiently negative s_α, the l.h.s. of (III.25a) is positive and therefore the locations of the poles are also bounded from below.

The physical significance of these results can be easily seen from a simple example shown in Fig.III.1. Points 1 and 2 denote the locations $C^{(1)} = (\kappa^{(1)}, \mu^{(1)})$ and $C^{(2)} = (\kappa^{(2)}, \mu^{(2)})$, respectively, of two isotropic materials in the space of elastic moduli. Although the example is restricted to isotropic materials, the general case is analogous. Four different cases are shown: a) $\delta\kappa \equiv \kappa^{(1)} - \kappa^{(2)} > 0$ and $\delta\mu \equiv \mu^{(1)} - \mu^{(2)} > 0$, i.e. $\delta C \geqslant 0$, b) $\delta\kappa < 0$ and $\delta\mu < 0$, i.e. $\delta C \leqslant 0$, c) and d) $\delta\kappa \cdot \delta\mu < 0$, i.e. δC is a non-definite tensor. Only the first quadrant of the plane ($\kappa > 0$, $\mu > 0$) corresponds to the physically allowed values of the elastic stiffness, i.e. no resonances of $C^{(e)}$ can exist while $C^{(1)}$ is in that area. Note that in

all four cases the interval $s \geq 1$ lies in the physical region. Thus there are no poles for $s \geq 1$. Similarly, the inequalities (III.31 a,b) can be verified by observing Fig.III.1a,b.

By analogy with the electrostatic problem in a composite material [49], we believe that the pole spectrum in (III.21) is discrete as long as the total volume is finite and all interfaces between different components are smooth (i.e. no corners or contact points). To the best of our knowledge, a rigorous proof of this conjecture exists only for the case where the two materials are both isotropic and have equal Poisson ratios [50].

Note that a part of the l.h.s. of (III.25b), namely $\int \theta_1 \varepsilon^{(\alpha)} \delta C \varepsilon^{(\alpha)} dV$, is actually $\langle \tilde{\varepsilon}^{(\alpha)} | \varepsilon^{(\alpha)} \rangle$ as it appeared in (III.19). If $\varepsilon^{(\alpha)}$ is real or pure imaginary and $C^{(2)}$ is a positive definite tensor, then $\int \varepsilon^{(\alpha)} C^{(2)} \varepsilon^{(\alpha)} dV$ does not vanish. Thus, we conclude from (III.25b) that, as long as $s_\alpha \neq 0$, (III.19) holds, i.e. the eigenstates are normalizable. The normalizability of a general bi-orthogonal set of eigenstates then follows from the possibility of expanding any member of this set in a bi-orthogonal set of real or pure imaginary tensors.

This proof of normalizability fails whenever $s_\alpha = 0$. Such an eigenstate can still be normalizable, however the above treatment is no longer valid. In the case of $s_\alpha = 0$ it is possible to have an eigenstate of $\hat{G}$ for which the displacement vector does not vanish at the boundary [51]. The solution $|\varepsilon(s)\rangle$ of the integral equation (III.9) depends on the value of the parameter s. It is clear that the limit $|\varepsilon(0)\rangle \equiv |\varepsilon(s \to 0)\rangle$ is an eigenstate of $\hat{G}$ with an eigenvalue $s_\alpha = 0$. Multiplying (III.9) by $\langle \tilde{\varepsilon}(0)|$ we find that $\langle \tilde{\varepsilon}(0) | \varepsilon(s) \rangle = \langle \tilde{\varepsilon}(0) | \varepsilon^0 \rangle$, for any s, and in particular $\langle \tilde{\varepsilon}(0) | \varepsilon(0) \rangle = \langle \tilde{\varepsilon}(0) | \varepsilon^0 \rangle$. Thus $|\varepsilon(0)\rangle$ is normalizable as long as $\langle \tilde{\varepsilon}(0) | \varepsilon^0 \rangle \neq 0$. If the last scalar product vanishes, then $\langle \tilde{\varepsilon}(0) | \varepsilon(s) \rangle = 0$ for any s, i.e. $\langle \tilde{\varepsilon}(0) |$ is orthogonal to the solution of (III.9), and thus we can ignore this eigenstate altogether. Finally, any other $s_\alpha = 0$ eigenstate $|\varepsilon'\rangle$ of $\hat{G}$ must also satisfy $\langle \tilde{\varepsilon}' | \varepsilon(s) \rangle = \langle \tilde{\varepsilon}' | \varepsilon^0 \rangle$ for any s. If $\langle \tilde{\varepsilon}' |$ is orthogonal to $|\varepsilon(0)\rangle$, i.e. $\langle \tilde{\varepsilon}' | \varepsilon(0) \rangle = 0$, then also $\langle \tilde{\varepsilon}' | \varepsilon^0 \rangle = 0$ and therefore $\langle \tilde{\varepsilon}' |$ is orthogonal to the solution of (III.9) and can be ignored. A detailed discussion of the physical significance of $s_\alpha = 0$ eigenstates will be given

in Ch.IV.E.

An additional possibility of failure of the normalizability proof occurs when the tensor $C^{(2)}$ has at least one vanishing eigenvalue (or elastic modulus), i.e. when it is positive semidefinite. In that case the entire theory fails (e.g. Green's tensor G may not exist). Such a case can be treated as a (careful!) limit of positive definite $C^{(2)}$ in which some of the eigenvalues approach zero.

Thus in the case of positive definite $C^{(2)}$ all the eigenstates of $\hat{G}$ which are not orthogonal to the solution of (III.9) are normalizable and therefore they form a complete set [48], i.e. the solution can be expanded in these eigenstates inside $C^{(1)}$ material.

D. ISOLATED CYLINDRICAL INCLUSION

In this section we discuss the problem [27] of a single infinitely long cylinder with radius R and stiffness tensor $C^{(1)}$, embedded in an infinite medium with elastic tensor $C^{(2)}$. Both $C^{(1)}$ and $C^{(2)}$ are assumed to be isotropic and their bulk and shear moduli will be denoted $\kappa^{(1)}$, $\mu^{(1)}$ and $\kappa^{(2)}$, $\mu^{(2)}$ respectively. We shall concentrate on the 2D elastic problem in the plane perpendicular to the cylinder axis (see the remarks on 2D systems in Ch.II.C). We shall calculate the elastic resonances and the effective moduli of this system. the results will constitute a simple implementation of the formalism described in the previous sections. They will also be used in the next chapter where we shall calculate the elastic moduli of a system of many cylindrical inclusions.

It is convenient to represent both components of the 2D displacement vector $\vec{u}(x_1,x_2)$ as functions of the complex variable [43] $w = x_1 + ix_2$. Initially we shall also allow the eigenstates of (III.16) to be complex functions, as our formalism does not limit us to real functions.

Since this 2D problem is invariant under rotations about the cylinder axis, some of the eigenvalues of (III.16) may be degenerate. In

constructing a complete set of bi-orthogonal eigenstates of $\hat{G}$, it is convenient to choose them to be eigenstates of the infinitesimal rotation generating operator $\hat{J}$ as well. The form in which $\hat{J}$ operates on a strain tensor is found from the following considerations: Let $\gamma_{ij}(\omega)$ be a transformation of coordinates which corresponds to a 2D rotation of the reference frame through an infinitesimal angle ω about the origin [52], i.e. the transformed coordinates x_i' are related to the original coordinates x_i by $x_i' = \gamma_{ij}(\omega)x_j$, where $\gamma_{ij} = \delta_{ij}+\omega A_{ij}$ and $A_{ij} = \begin{pmatrix} 0 & 1 \\ -1 & 0 \end{pmatrix}$. The rotation of the entire strain field through the angle ω is given (disregarding the terms $O(\omega^2)$) by [53]

$$\begin{aligned}
\varepsilon'_{ij}(x_m) &= \gamma_{ik}(-\omega)\,\gamma_{jl}(-\omega)\,\varepsilon_{kl}(\gamma_{mn}(\omega)x_n) \\
&= (\delta_{ik} - \omega A_{ik})(\delta_{jl} - \omega A_{jl})\varepsilon_{kl}(x_m + \omega A_{mn}x_n) \\
&= [\delta_{ik}\delta_{jl} - \omega(\delta_{ik}A_{jl} + \delta_{jl}A_{ik})](\varepsilon_{kl} + \omega A_{mn}x_n\partial_m\varepsilon_{kl}). \\
&= \varepsilon_{ij} - \omega(\delta_{ik}A_{jl} + \delta_{jl}A_{ik})\varepsilon_{kl} + \omega x_n A_{mn}\partial_m\varepsilon_{ij} = (\hat{I} - \omega\hat{J})\varepsilon \quad , \qquad \text{(III.32a)}
\end{aligned}$$

where $\hat{I}$ is an identity operator and $\hat{J}$ has the form

$$\hat{J}\varepsilon = \left[i\begin{pmatrix} 0 & 0 & -2 \\ 0 & 0 & 2 \\ 1 & -1 & 0 \end{pmatrix} - i\frac{\partial}{\partial\phi} \right] \cdot \begin{pmatrix} \varepsilon_{11} \\ \varepsilon_{22} \\ \varepsilon_{12} \end{pmatrix} \quad , \qquad \text{(III.32b)}$$

where we replaced $x_n A_{mn}\partial_m = x_2\partial_1 - x_1\partial_2$ by $-\frac{\partial}{\partial\phi}$ (ϕ is the azimuthal angle in the x_1 x_2 plane). The matrix on the r.h.s. of (III.32b) already takes account of the fact that $\varepsilon_{12} = \varepsilon_{21}$. It can be easily verified that $\hat{J}$ is hermitian under the scalar product defined by (III.12) and that $\hat{G}$ and $\hat{J}$ commute. The fact that $\hat{J}$ is hermitian ensures that its eigenstates create an orthogonal set. However, we need a bi-orthogonality relation between the right eigenstates and their complementary states. Thus, this fact still has to be verified for the final results which will be obtained.

In order to solve for eigenstates, we use the methods commonly used in

2D elastostatic problems [43], which are s[illegible] because, at this stage we allow the eigenstates to be complex. The most general solution of a 2D elastostatic problem in an isotropic medium may be expressed in the form

$$u_1(w) = \frac{1}{2\mu}(\chi\Phi - w^*\Phi' - \Psi + \chi\Delta^* - w\Delta'^* - \Gamma^*)$$
$$u_2(w) = \frac{i}{2\mu}(-\chi\Phi - w^*\Phi' - \Psi + \chi\Delta^* + w\Delta'^* + \Gamma^*) \quad , \qquad \text{(III.33)}$$

where u_1 and u_2 are the components of the 2D displacement vector, the elastostatic potentials Φ, Ψ, Δ and Γ are analytic functions of the complex variable w, a prime denotes differentiation and $\chi = 1 + 2\mu/\kappa$.

The eigenvalues of $\hat{J}$ are all the integers $\ell = 0, \pm1, \pm2, \ldots$, and the elastostatic potentials corresponding to its $\ell \geq 0$ eigenstates are

$$\Phi^{(\ell)} = A_1 w^{\ell+1}, \quad \Psi^{(\ell)} = A_2 w^{\ell-1}, \quad \Delta^{(\ell)} = A_3/w^{\ell-1}, \quad \Gamma^{(\ell)} = A_4/w^{\ell+1}, \quad \text{for } \ell \geq 2$$
$$\Phi^{(1)} = A_5 w^2, \quad \Psi^{(1)} = A_6 \ln w + A_7, \quad \Delta^{(1)} = A_8 \ln w + A_9, \quad \Gamma^{(1)} = A_{10}/w^2, \quad \text{for } \ell=1$$
$$\Phi^{(0)} = A_{11} w, \quad \Psi^{(0)} = A_{12}/w, \quad \Delta^{(0)} = A_{13} w, \quad \Gamma^{(0)} = A_{14}/w, \quad \text{for } \ell=0 \qquad \text{(III.34)}$$

For negative ℓ eigenstates, the displacement vector is given by) = $(\vec{u}^{(|\ell|)})^*$, i.e., by the complex conjugate of the displacement field of the positive $|\ell|$ eigenstate. The coefficients are arbitrary if we only require these functions to be eigenstates of $\hat{J}$. Their values are however determined when we require that these functions also be eigenstates of $\hat{G}$: a) The eigenstates must decrease to zero for $|w| \to \infty$, and they must be nonsingular everywhere else. b) Both the displacement vector $\vec{u}$ and the surface traction $\vec{T}$ must be continuous at the surface of the cylinder. The normal and tangential components T_n and T_t of the surface traction at the surface of the cylinder for a displacement given by (III.33) can be found by repeating the standard 2D procedure [43] modified to include complex displacements:

$$T_n = 2(\Phi' + \Delta'^*) - (w^*\Phi'' + \Psi')e^{2i\phi} - (w\Delta''^* + \Gamma'^*)e^{-2i\phi}$$

$$T_t = -i(w^*\Phi'' + \Psi')e^{2i\phi} + i(w\Delta''^* + \Gamma'^*)e^{-2i\phi} \quad . \tag{III.35}$$

The first requirement restricts the (different) choices of non-vanishing coefficients A_i in (III.34) both for $|w| < R$ and for $|w| > R$, i.e. inside and outside the cylinder, while from the second requirement (continuity conditions) we finally get four homogeneous equations with four unknowns (the coefficients A_i) for every value of ℓ. Setting the determinant equal to zero leads to the resonance values $\kappa^{(1)'}$, $\mu^{(1)'}$ in terms of $\kappa^{(2)}$, $\mu^{(2)}$.

For $\ell = 0$ the resonance values satisfy the equation

$$\kappa^{(1)'} = -\mu^{(2)} . \tag{III.36}$$

These resonances are located on the vertical line in Fig.III.2, denoted by A. For $|\ell| = 1$, the resonance values satisfy

$$\frac{\mu^{(1)'}\kappa^{(1)'}}{\kappa^{(1)'} + 2\mu^{(1)'}} = -\mu^{(2)} , \tag{III.37}$$

and they are located on the two hyperbola branches in Fig.III.2, denoted by C and D. Finally, for $|\ell| \geq 2$, the resonance values satisfy either (III.37) or

$$\mu^{(1)'} = \frac{\mu^{(2)}\kappa^{(2)}}{\kappa^{(2)} + 2\mu^{(2)}} . \tag{III.38}$$

The last results are located on the horizontal line in Fig.III.2, denoted by B. Note that all the resonances are found in the non-physical part of the κ,μ plane. For a problem with given $\kappa^{(1)}$, $\kappa^{(2)}$, $\mu^{(1)}$, $\mu^{(2)}$ the values

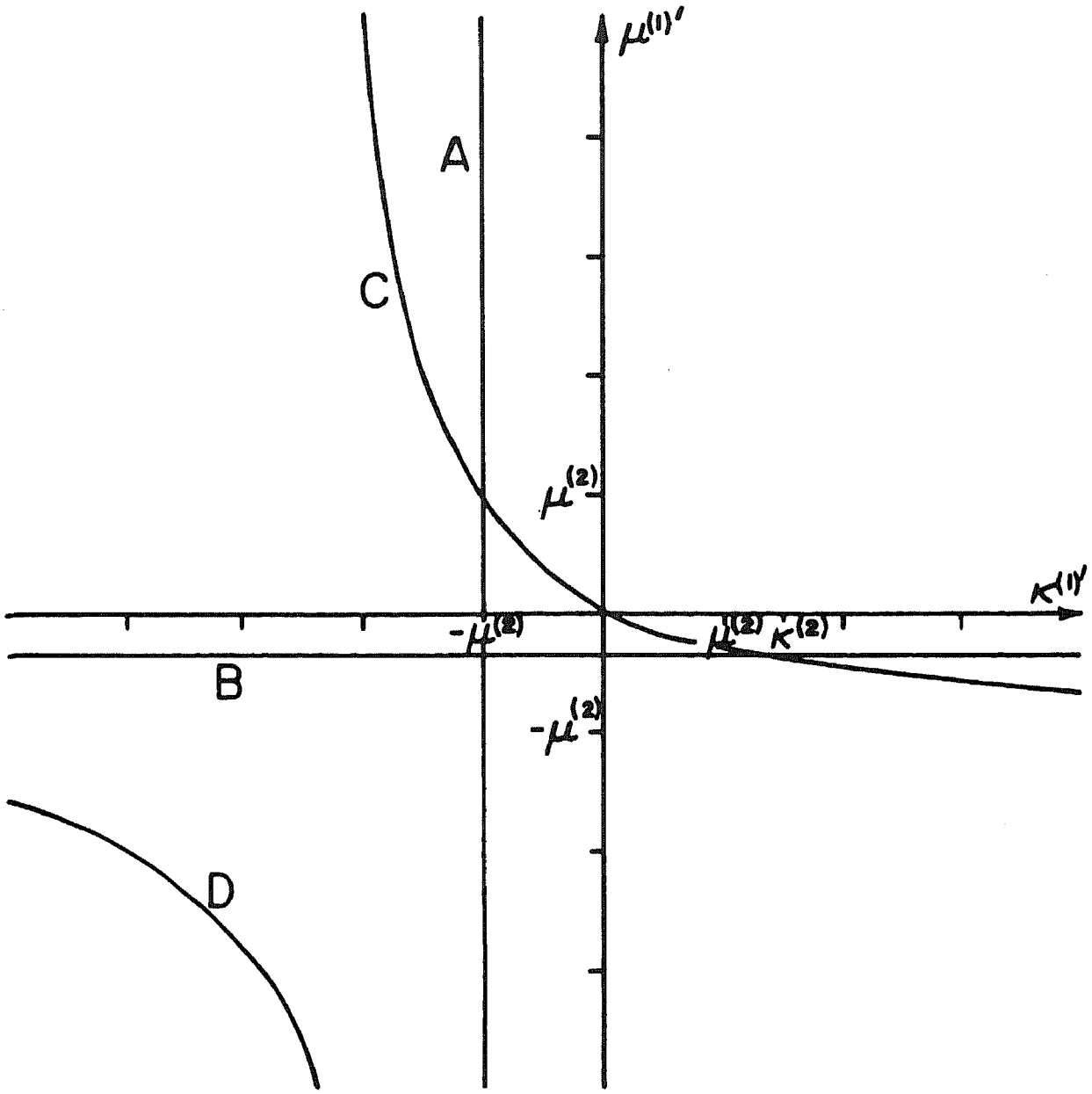

Fig. III.2 Location of the resonance values $\kappa^{(1)\prime}$ and $\mu^{(1)\prime}$ of the cylinder material in the κ,μ plane. The curves are defined by Eqs. (III.36) (line A), (III.38) (line B), (III.37) (hyperbola branches C and D). In order to draw this set of curves, we assumed the particular relationship $\kappa^{(2)} = 1.5\mu^{(2)}$, but otherwise the values of $\kappa^{(1)}$, $\kappa^{(2)}$, $\mu^{(1)}$, $\mu^{(2)}$ are arbitrary.

taken by $\kappa^{(1)'}$ and $\mu^{(2)'}$ must also lie on the straight lines given by

$$\kappa^{(1)'} = \kappa^{(2)} + \frac{1}{s}\delta\kappa \ ,$$
$$\mu^{(1)'} = \mu^{(2)} + \frac{1}{s}\delta\kappa \qquad \text{(III.39)}$$

(see (III.4)). Consequently, the actual resonance values of $\kappa^{(1)'}$ and $\mu^{(1)'}$ in a given problem are the intersection points of that straight line with the four curves of Fig.III.2. Thus there are at most four different eigenvalues, denoted by s_A, s_B, s_C, s_D in correspondence with the curves of Fig.III.2. Correspongingly, there are four pairs of resonance elastic constants, $\kappa_A^{(1)'}$, $\mu_A^{(1)'}$; $\kappa_B^{(1)'}$, $\mu_B^{(1)'}$; etc.

Instead of using complex ε's we shall use the linear combinations $(\varepsilon^{(\ell)}+\varepsilon^{(-\ell)})$ and $-i(\varepsilon^{(\ell)}-\varepsilon^{(-\ell)})$, i.e. the real and imaginary parts of $|\ell|\geq 1$ states (the $\ell=0$ state is non-degenerate, and therefore ε is automatically real). It can be directly verified that these states together with their complementary tensors form a bi-orthogonal set. These real states are no longer eigenstates of $\hat{J}$, but they are still eigenstates of $\hat{J}^2$, and at the same time, eigenstates of the reflection operator through the x_1 axis. The real and imaginary parts of $\varepsilon^{(\ell)}$ have eigenvalues +1 and -1, respectively, for this operator.

From (III.36) and (III.39) we obtain

$$s_A = -\frac{\delta\kappa}{\kappa^{(2)}+\mu^{(2)}} \ , \qquad \text{(III.40)}$$

and the corresponding right eigenstate is

$$\varepsilon^{(A0)} = \begin{pmatrix} \varepsilon_{11}^{(A0)} \\ \varepsilon_{22}^{(A0)} \\ \varepsilon_{12}^{(A0)} \end{pmatrix} = \begin{cases} \dfrac{1}{2R\sqrt{\pi\delta\kappa}} \begin{pmatrix} 1 \\ 1 \\ 0 \end{pmatrix} \ , \text{ for } |w| \leq R \\ \dfrac{R}{2\sqrt{\pi\delta\kappa}} \ \mathrm{Re} \begin{pmatrix} -1 \\ 1 \\ i \end{pmatrix} \dfrac{1}{w^2} \ , \text{ for } |w| > R. \end{cases} \qquad \text{(III.41)}$$

(The superscript 0 signifies the fact that this is an eigenstate of $\hat{J}$ with eigenvalue $\ell = 0$.) This is the only eigenstate that has the eigenvalue s_A, i.e. s_A is non-degenerate. The displacement vector field $\vec{u}$ of this eigenstate is depicted in Fig.III.3a. Inside the cylinder it corresponds to a pure, uniform compression (compare with (II.23)), while outside it is proportional to $1/|w|$. We call this state a "compression dipole".

From (III.38) and (III.39) we obtain

$$s_B = -\frac{\delta\mu(\kappa^{(2)} + \mu^{(2)})}{2\mu^{(2)}(\kappa^{(2)}+\mu^{(2)})} \quad . \tag{III.42}$$

There are ifinitely many right eigenstates corresponding to this eigenvalue:

$$\varepsilon^{(\pm B\ell)} = \begin{cases} A_{B\ell}\ \begin{Bmatrix}\mathrm{Re}\\ \mathrm{Im}\end{Bmatrix} \begin{pmatrix}-1\\ 1\\ i\end{pmatrix} w^{\ell-2} \quad , & \text{for } |w| \leq R \\ \dfrac{A_{B\ell}\cdot R^{2(\ell-1)}\kappa^{(2)}}{\kappa^{(2)}+2\mu^{(2)}} \begin{Bmatrix}\mathrm{Re}\\ \mathrm{Im}\end{Bmatrix} \left[\dfrac{2\mu^{(2)}}{\kappa^{(2)}} \begin{pmatrix}1\\ 1\\ 0\end{pmatrix} + \right. & \\ \left. + \begin{pmatrix}1\\ -1\\ i\end{pmatrix} \left[\frac{\ell w}{w^{*\ell+1}} - \frac{(\ell+1)R^2}{w^{*\ell+2}}\right]\right], & \text{for } |w| > R. \end{cases} \tag{III.43a}$$

$$A_{B\ell} \equiv \left(\frac{\ell-1}{\pi\delta\mu}\right)^{\frac{1}{2}} \cdot \frac{1}{2R^{\ell-1}} \tag{III.43b}$$

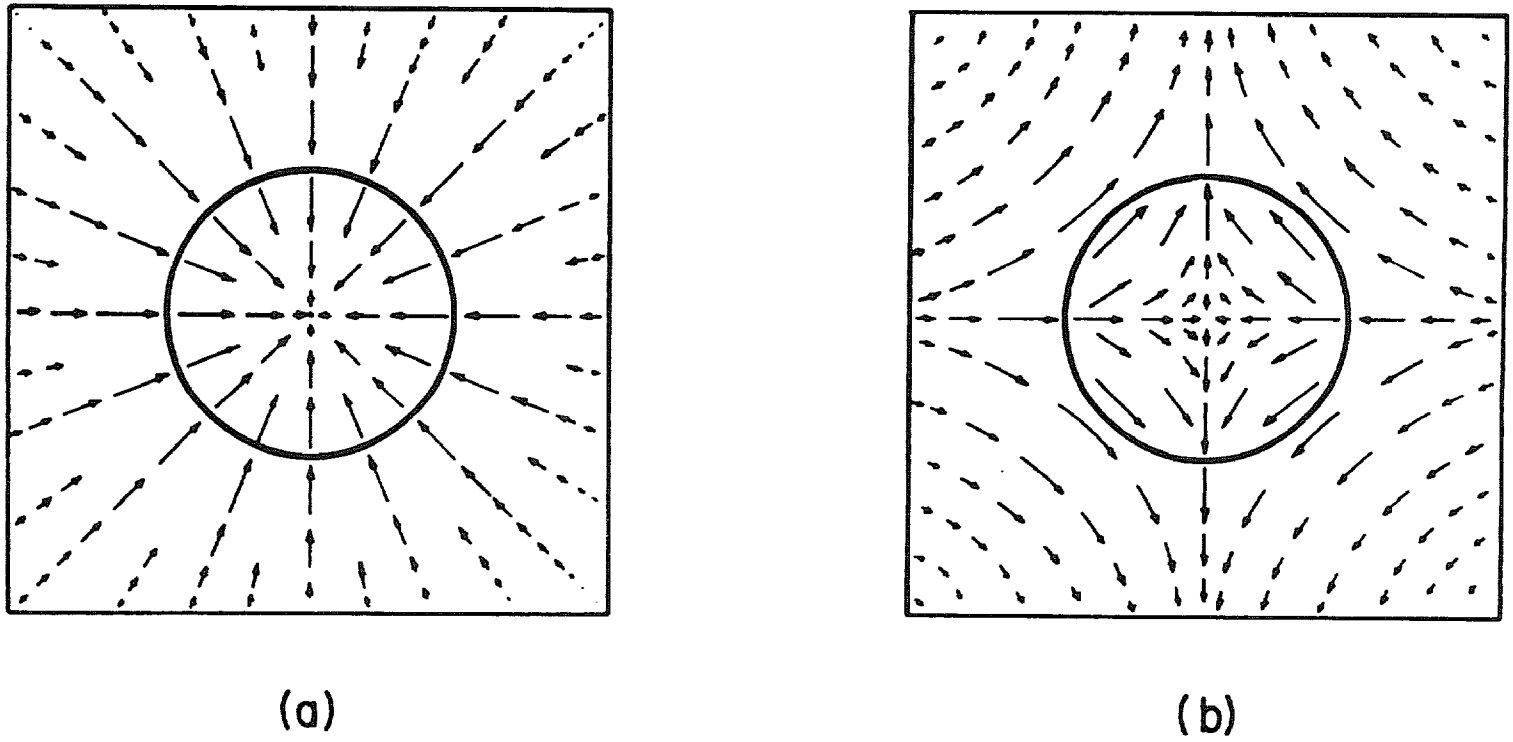

Fig. III. 3 The displacement vector field $\vec{u}$ of (a) the compression-dipole and (b) one of the shear-dipole resonance states (the other one has the same form, but rotated by an angle $\pi/4$).

where $\ell = 2,3,\ldots$, and where $(\pm)$ corresponds to $\{{}^{\mathrm{Re}}_{\mathrm{Im}}\}$ on the r.h.s. Each of these states is also an eigenstate of $\hat{J}^2$, with an eigenvalue equal to ℓ^2, and an eigenstate of the reflection operator through the x_1-axis with the eigenvalue ± 1. The $\vec{u}$-field of the $\varepsilon^{(+B2)}$ state is depicted in Fig. III.3 b. The $\vec{u}$-field of the $\varepsilon^{(-B2)}$ is given by the same figure but rotated by $\pi/4$. Inside the cylinder these two states correspond to a pure, uniform shear (compare with (II.27) and (II.26), respectively), while outside it they decrease asymptotically like $1/|w|$. We will call these states (first and second) "shear dipoles".

From (III.37) and (III.39), two different eigenvalues (intersections of the straight line (III.39) and the hyperbola branches C and D) are found for s, determined by the following quadratic equation:

$$s_{C,D}^2\, 2\mu^{(2)}(\mu^{(2)}+\kappa^{(2)}) + s_{C,D}[2\mu^{(2)}\delta\kappa + (\kappa^{(2)}+2\mu^{(2)})\delta\mu] + \delta\mu\delta\kappa = 0 \quad \text{(III.44)}$$

and they are both infinitely degenerate. These right eigenstates are

$$\varepsilon^{(\pm C,D\ell)} = \begin{cases} A_{C,D\ell}\ \{{}^{\mathrm{Re}}_{\mathrm{Im}}\}\left[\dfrac{2\mu^{(1)}_{C,D}}{\kappa^{(1)}_{C,D}}\begin{pmatrix}1\\1\\0\end{pmatrix} w^{\ell} + \right. \\ \qquad \left. + \begin{pmatrix}-1\\1\\-i\end{pmatrix}[\ell w^{*} w^{\ell-1} - (\ell-1)R^2 w^{\ell-2}]\right], \quad \text{for } |w| \leqslant R \\ A_{C,D\ell}\ R^{2(\ell+1)}\ \dfrac{\mu^{(1)}_{C,D}}{\mu^{(2)}}\ \{{}^{\mathrm{Re}}_{\mathrm{Im}}\}\begin{pmatrix}1\\-1\\-i\end{pmatrix}\dfrac{1}{w^{*\ell+2}}, \quad \text{for } |w| > R\,. \end{cases} \quad \text{(III.45a)}$$

$$A_{C,D\ell} \equiv \left[\frac{\ell+1}{\pi\left[2\delta\kappa\left(\dfrac{\mu^{(1)}_{C,D}}{\kappa^{(1)}_{C,D}}\right)^2 + \delta\mu\right]}\right]^{\frac{1}{2}} \cdot \frac{1}{2R^{\ell+1}} \quad \text{(III.45b)}$$

where $\ell = 1,2,\ldots$ and where $\mu^{(1)}_{C,D}$ and $\kappa^{(1)}_{C,D}$ are the values of $\mu^{(1)}$ and $\kappa^{(2)}$ for $s = s_{C,D}$. The superscripts ℓ and $(\pm)$ have the same meaning as for the B-type states. Outside the cylinder all of these states decrease with distance faster than the dipolar states $\varepsilon^{(A0)}$ and $\varepsilon^{(\pm B2)}$.

Using these results, we can easily write down the effective elastic constants for a composite that has just one inclusion. Of course, in the limit of an infinite volume for the host material, the effective constants approach those of the host. Therefore we are really interested in the corrections of order $p_1 = v/V$, where v is the volume of the cylinder and V is the total volume of the system. To order p_1 we find that there is only one non-zero term in (III.21). Choosing $\varepsilon^0 = \varepsilon^{0\kappa}$, we get

$$F(s) = \frac{1}{S}\frac{(\langle\tilde{\varepsilon}^{0\kappa}|\varepsilon^{(A0)}\rangle)^2}{s - s_A} = \frac{1}{S}\frac{\pi R^2\delta\kappa}{s + \delta\kappa/(\kappa^{(2)}+2\mu^{(2)})} \quad , \quad \text{(III.46)}$$

where S is the total area of the 2D sample. Taking $s = 1$ and noting that the volume fraction is given by $p_1 = \pi R^2/S = v/V$, we finally get

$$\kappa^{(e)} = \kappa^{(2)} + \frac{p_1}{\frac{1}{\delta\kappa} + \frac{1}{\kappa^{(2)}+\mu^{(2)}}} \quad . \quad \text{(III.47)}$$

Similarly, taking $\varepsilon^0 = \varepsilon^{0\mu}$, we get

$$\mu^{(e)} = \mu^{(2)} + \frac{p_1}{\frac{1}{\delta\mu} + \frac{\kappa^{(2)} + 2\mu^{(2)}}{2\mu^{(2)}(\kappa^{(2)}+\mu^{(2)})}} \quad . \quad \text{(III.48)}$$

It is obvious that $m^{(e)} = \mu^{(e)}$ in this case, and this can also be verified by a direct calculation with $\varepsilon^0 = \varepsilon^{0m}$.

Equations (III.47) and (III.48) can also be derived by considering one cylindrical inclusion in a uniform external field [54]. Our method of derivation looks quite complicated for such a simple problem. The advan-

tages of our method will be seen in the next chapter, where we will consider systems with many cylindrical inclusions.

E. SUM RULES

Besides the inequalities (III.29) or (III.31), the parameters F_α and s_α appearing in (III.21) must satisfy certain (moment) sum rules. This section will be devoted to the derivation of some of them [28]. Sum rules provide a useful tool for checking different approximations and can also be used for the derivation of different bounds on the effective elastic moduli, as will be shown in Chs. IV and V.

We start by expanding two different representations of F(s), namely (III.15) and (III.21), in powers of 1/s

$$F(s) = \sum_\alpha \frac{F_\alpha}{s-s_\alpha} = \sum_{n=0}^{\infty} \sum_\alpha F_\alpha \cdot (\frac{s_\alpha}{s})^n = \frac{1}{V}\langle \varepsilon^0 | \frac{1}{s-\hat{G}} | \varepsilon^0 \rangle =$$

$$= \frac{1}{V} \sum_{n=0}^{\infty} \langle \tilde{\varepsilon}^{0} | (\frac{\hat{G}}{s})^n | \varepsilon^0 \rangle \ . \qquad \text{(III.49)}$$

Equating the expansions order by order, we obtain the following expression for the n-th moment of the pole spectrum:

$$M_n \equiv \sum_\alpha F_\alpha s_\alpha^n = \frac{1}{V} \langle \tilde{\varepsilon}^{0} | \hat{G}^n | \varepsilon^0 \rangle \ . \qquad \text{(III.50)}$$

In general, M_n is a scalar quantity whose value depends on the choice of ε^0 as well as on the detailed microgeometry. However, a knowledge of the volume fraction p_1 of the $C^{(1)}$ material suffices for the calculation of the zero moment sum rule

$$M_0 \equiv \sum_\alpha F_\alpha = \frac{1}{V}\langle \tilde{\varepsilon}^{0} | \varepsilon^0 \rangle = \frac{1}{V} \int \theta_1 \varepsilon^0 \delta C \varepsilon^0 dV = p_1 \varepsilon^0 \delta C \varepsilon^0 \ . \qquad \text{(III.51)}$$

If we make a particular choice $\varepsilon^0 = \varepsilon^{0\gamma}$, where γ represents either κ or μ or m (see the definitions (II.24), (II.26) and (II.27)), then (III.51) will

have the form

$$M_0^{(\gamma)} = p_1 \delta\gamma, \tag{III.52}$$

where $\delta\gamma \equiv \gamma^{(1)} - \gamma^{(2)}$ and the superscript of M_0 indicates the particular choice of ε^0.

Higher moment sum rules generally depend on the microgeometry of the sample. Thus from (III.10)-(III.12) and (III.50) we arrive at the following expression for the first moment sum rule:

$$M_1 \equiv \sum_\alpha F_\alpha s_\alpha = \frac{1}{V}\langle \tilde{\varepsilon}^0 | \hat{G} | \varepsilon^0 \rangle = \frac{1}{V}\int \theta_1(\vec{r})\theta_1(\vec{r}')\varepsilon^0 \delta C G(\vec{r},\vec{r}')\delta C \varepsilon^0 dV dV' \quad . \tag{III.53}$$

In App.A we show that the integral $\int G(\vec{r},\vec{r}')dV'$ vanishes whenever the integration is performed over the entire volume of the sample (see (A.10)). Thus subtraction of a constant from $\theta_1(\vec{r})\theta_1(\vec{r}')$ in (III.53) will not change the result of integration, and we can rewrite (III.52) in the following form [55]:

$$M_1 = \frac{1}{V}\int (\theta_1(\vec{r})\theta_1(\vec{r}') - p_1^2)\varepsilon^0 \delta C G(\vec{r},\vec{r}')\delta C \varepsilon^0 dV dV'. \tag{III.54}$$

The constant p_1^2 was subtracted from the geometric correlation function $\theta_1(\vec{r})\theta_1(\vec{r}')$ in order to make the average correlation decay to zero for large separations $|\vec{r}-\vec{r}'|$ and thus have a non-singular Fourier transform. This statement is correct in the absence of long range correlations, e.g. when the composite has a random structure. If this is not the case, e.g. if the inclusions form a regular lattice, then the Fourier transform may have singularities. However, even in this case the Fourier transform will be non-singular at the origin of Fourier transform space.

In the infinite volume limit the tensor Green's function becomes translationally invariant, i.e. $G(\vec{r},\vec{r}') = G(\vec{r}-\vec{r}')$, and we may perform one volume integration trivially in (III.54) to obtain

$$M_1 = \varepsilon^0 \delta C \int f_{11}(\vec{r}) G(\vec{r}) dV \; \delta C \varepsilon^0 \quad , \tag{III.55}$$

where

$$f_{11}(\vec{r}) = \frac{1}{V} \int \theta_1(\vec{r}+\vec{r}') \theta_1(\vec{r}') dV' - p_1^2 \quad . \tag{III.56}$$

If we substitute Fourier integrals for $f_{11}(\vec{r})$ and $G(\vec{r})$ in (III.55), we arrive in the general d-dimensional case at the following form for M_1:

$$M_1 = \frac{1}{(2\pi)^d} \varepsilon^0 \; \delta C \int \tilde{f}_{11}(-\vec{k}) \tilde{G}(\vec{k}) d^d k \; \delta C \varepsilon^0 , \tag{III.57}$$

where $\tilde{f}(\vec{k})$, $\tilde{G}(\vec{k})$ are the Fourier transforms. In general, the evaluation of M_1 requires the knowledge of the volume average of the two point correlation function of the microgeometry $\theta_1(\vec{r}) \theta_1(\vec{r}')$ - see (III.55) or (III.57). When the volume of the sample is small $\theta_1(\vec{r}) \theta_1(\vec{r}')$ itself, and not its volume average, has to be known (see (III.54)). However, in some infinite-volume cases, M_1 can be evaluated with less detailed information.

When $C^{(2)} = (\kappa^{(2)}, \mu^{(2)})$ is an isotropic material, the infinite-volume Green's function $G(\vec{r}; C^{(2)})$ has a relatively simple form. Its Fourier transform (see App.A) depends only on the direction of $\vec{k}$

$$\tilde{G}_{mnij}(\vec{k}) = \frac{\lambda^{(2)}+\mu^{(2)}}{\mu^{(2)}(\lambda^{(2)}+2\mu^{(2)})} \frac{k_m k_n k_i k_j}{k^4} - \frac{1}{4\mu^{(2)} k^2} (\delta_{mi} k_n k_j + \delta_{ni} k_m k_j + \delta_{mj} k_n k_i + \delta_{nj} k_m k_i) , \tag{III.58}$$

where $\lambda^{(2)}$ and $\mu^{(2)}$ are the Lamé constants of the $C^{(2)}$ material. This expression is valid for any space dimensionality d.

If the sample has an isotropic microgeometry, i.e. $f_{11}(\vec{r}) = f_{11}(|\vec{r}|)$ and its Fourier transform $\tilde{f}_{11}(\vec{k}) = \tilde{f}_{11}(|\vec{k}|)$, then , by combining this property with the fact that $\tilde{G}$ depends only on the unit vector $\hat{k} \equiv \vec{k}/k$, we can rewrite (III.57) in the form

$$M_1 = \varepsilon^0 \delta C f_{11}(0) \frac{1}{\Omega_d} \int \tilde{G}(\hat{k}) d\Omega_d \; \delta C \varepsilon^0 \quad , \tag{III.59}$$

where Ω_d is the d-dimensional solid angle in k-space, and $f_{11}(0) = p_1 - p_1^2$. The average of $\tilde{G}(\hat{k})$ over all directions

$$R_{mnij} \equiv \frac{1}{\Omega_d} \int \tilde{G}_{mnij}(\hat{k})\, d\Omega_d \tag{III.60}$$

can be easily evaluated once we realize that the integrals which appear are of only two types, and that they can be found without actually performing any integration (see (III.58)):

$$\frac{1}{\Omega_d} \int \frac{k_i k_j}{k^2}\, d\Omega_d = \frac{1}{d}\delta_{ij} \quad , \tag{III.61}$$

$$\frac{1}{\Omega_d} \int \frac{k_m k_n k_i k_j}{k^4}\, d\Omega_d = \frac{1}{d(d+2)}(\delta_{ij}\delta_{mn} + 2I_{ijmn}) . \tag{III.62}$$

The result (III.61) is obtained from the following consideration: Under rotations the integral must behave like an invariant second rank symmetric tensor. Thus the only possibility is

$$\frac{1}{\Omega_d} \int \frac{k_i k_j}{k^2}\, d\Omega_d = A \cdot \delta_{ij} . \tag{III.63}$$

The value of the constant multiplier A is determined by considering the trace of the tensor:

$$\frac{1}{\Omega_d} \int \frac{k_i k_i}{k^2}\, d\Omega_d = \frac{1}{\Omega_d} \int d\Omega_d = 1 = A \cdot \delta_{ii} = A \cdot d. \tag{III.64}$$

By analogous reasoning, the integral (III.62) must be proportional to $\delta_{ij}\delta_{mn} + \delta_{mi}\delta_{nj} + \delta_{mj}\delta_{ni} = \delta_{ij}\delta_{mn} + 2I_{ijmn}$, with a coefficient B whose value is easily found by the following consideration:

$$\frac{1}{\Omega_d} \int \frac{k_m k_m k_i k_i}{k^4}\, d\Omega_d = \frac{1}{\Omega_d} \int d\Omega_d = 1 = B \cdot (\delta_{ii}\delta_{mm} + 2I_{iimm}) =$$

$$= B(d^2 + 2d) . \tag{III.65}$$

Using these results we finally obtain from (III.58), (III.60)-(III.62), and

(II.25)

$$R_{mnij} = \frac{d\kappa^{(2)} + (d-2)\mu^{(2)}}{d(d+2)\mu^{(2)}[d\kappa^{(2)}+2(d-1)\mu^{(2)}]}\delta_{mn}\delta_{ij} - \frac{d(\kappa^{(2)} + 2\mu^{(2)})}{(d+2)\mu^{(2)}[d\kappa^{(2)}+2(d-1)\mu^{(2)}]}I_{mnij} \quad , \tag{III.66}$$

Thus M_1 can be calculated from the expression

$$M_1 = p_1(1-p_1)\varepsilon^0_{kl}\delta C_{klmn}R_{mnij}\delta C_{ijrt}\varepsilon^0_{rt} \tag{III.67}$$

for any isotropic mixture of components one of which ($C^{(2)}$) is isotropic. Note that this expression can be used also in the case of non-isotropic $C^{(1)}$.

When both components are isotropic we can use $\varepsilon^0=\varepsilon^{0\kappa}$ to obtain from (III.66) and (III.67) the following expression for the first moment sum rule:

$$M_1^{(\kappa)} = -p_1(1-p_1)\,\delta\kappa^2 E^{(\kappa)}(C^{(2)}), \tag{III.68a}$$

$$E^{(\kappa)}(C^{(2)}) \equiv 1/(\kappa^{(2)} + 2\frac{d-1}{d}\mu^{(2)}), \tag{III.68b}$$

while for $\varepsilon^0 = \varepsilon^{0\mu}$ we obtain

$$M_1^{(\mu)} = -p_1(1-p_1)E^{(\mu)}(C^{(2)}), \tag{III.69a}$$

$$E^{(\mu)}(C^{(2)}) \equiv 2(\kappa^{(2)}+2\mu^{(2)})/[(d+2)\mu^{(2)}(\kappa^{(2)}+2\frac{d-1}{d}\mu^{(2)})]. \tag{III.69b}$$

The sum rules (III.68) and (III.69) will be used in Ch.V to derive bounds on the effective elastic constants. Therefore, we would like to extend the validity of these expressions (and therefore the validity of the bounds) as far as possible. The above derivation was restricted to an isotropic composite with isotropic constituents. However, the validity of these results can be extended beyond the special case of isotropic mixtures. First we note that when both constituents are isotropic and $\varepsilon^0 = \varepsilon^{0\kappa}$ then the expression

$$\varepsilon^0 \delta C \tilde{G}(\hat{k}) \delta C \varepsilon^0 = -\delta\kappa^2 E^{(\kappa)} \qquad \text{(III.70)}$$

is a constant (i.e., independent of $\hat{k}$) and therefore $\varepsilon^0 \delta C G(\vec{r}) \delta C \varepsilon^0$ is proportional to a δ-function. Thus the integration (III.55) is trivial and (III.68) is universally valid regardless of the microgeometry of the composite!

There is no such simple rule for M_1 when an arbitrary shear is applied to an arbitrary composite. However, we can find simple rules for a particular linear combination of the shears. In 2D we can use $\varepsilon^0 = \varepsilon^{0\mu}$ and $\varepsilon^0 = \varepsilon^{0m}$ as defined by (II.26) and (II.27) to define two different functions F(s) and two different first moments $M_1^{(\mu)}$ and $M_1^{(m)}$, respectively. The expression

$$\frac{1}{2}(\varepsilon^{0\mu} \delta C \tilde{G}(\hat{k}) \delta C \varepsilon^{0\mu} + \varepsilon^{0m} \delta C \tilde{G}(\hat{k}) \delta C \varepsilon^{0m}) = -\delta\mu^2 E^{(\mu)} \qquad \text{(III.71)}$$

is a constant (i.e. independent of $\hat{k}$) and therefore an expression similar to (III.69) is again valid for the quantity $\frac{1}{2}(M_1^{(\mu)} + M_1^{(m)})$ regardless of the symmetry of $f_{11}(\vec{r})$.

A similar procedure can be followed for shears in 3D composites, but now we have to consider 6 different shears as defined by (II.30). In order to obtain a constant term similar to (III.70), we must now use the linear combination $[2(M_1^{m(12)}+M_1^{m(23)}+M_1^{m(13)}) + 3(M_1^{\mu(12)}+M_1^{\mu(23)}+M_1^{\mu(13)})]/15$, where the shear moduli m(12), μ(12), etc. are defined by (II.30). We thus conclude that (III.69) is valid for the above linear combination for a composite with arbitrary microgeometry. For a microgeometry with cubic symmetry this combination reduces to the simpler form $(2M_1^{(m)}+3M_1^{(\mu)})/5$.

The above statements can be rephrased as follows: Suppose we have several spectral functions $F^{(\gamma_1)}(s)$, $F^{(\gamma_2)}(s)$, etc., where $\gamma_1, \gamma_2, \ldots$ denote different elastic moduli, i.e. different choices of ε^0. Instead of talking about a sum rule which is satisfied by some weighted average of the n-th moments $(\sum_i a_i M_n^{(\gamma_i)})/(\sum_i a_i)$, we can talk about the n-th moment of the averaged function $(\sum_i a_i F^{(\gamma_i)}(s))/(\sum_i a_i)$. Thus if we define "average shear

moduli"

$$\mu_{av} = \frac{1}{2}(\mu^{(e)} + m^{(e)}) \quad , \quad \text{in the general 2D case,} \tag{III.72a}$$

$$\mu_{av} = \frac{1}{15}[3(\mu^{(e)}(12) + \mu^{(e)}(23) + \mu^{(e)}(13)) + 2(m^{(e)}(12) + m^{(e)}(23) + m^{(e)}(13)]\,, \tag{III.72b}$$

in the general 3D case,

$$\mu_{av} = \frac{1}{5}(3\mu^{(e)} + 2m^{(e)}), \quad \text{in the 3D case with cubic symmetry,} \tag{III.72c}$$

we can say that μ_{av} satisfies the sum rules (III.52) and (III.69).

Integrals involving both Green's function G and the microgeometric correlation function $\theta_1(\vec{r})\theta_1(\vec{r}')$, such as the expression for M_1 in (III.53), have been considered before [22,23]. However, no connection with a pole-expansion, not to mention sum rules, was ever made prior to this work. An explicit evaluation of the above-mentioned integral for M_1 existed previously only for the special case of isotropic and ellipsoidal microgeometry [56].

F. DISCUSSION

In this chapter we have presented a completely new approach to the calculation of the effective elastic constants of composites. Both the formal theory and its simple implementation, as well as an analysis of some important properties of the spectral representation (III.21) were given. Clearly, our approach is related to some previous scattering-theory-like approaches. E.g., the elastostatic resonances of the system also appear implicitly as singularities of the T-matrix of the system [22,23]. It is in the construction of the resonance states of the entire system from the resonances of individual grains, which will be presented in the next chapter, that we use a procedure that is entirely different from the multiple scattering methods which were used in the T-matrix approach [22,23].

In the previous sections we assumed that both constituents are elastic. However, our theory is also applicable when they are viscoelastic,

i.e., when the elastic stiffness tensors are complex [9]. Any of the results obtained above can be directly translated into a viscoelastic case simply by replacing the values of the elastic moduli by appropriate complex numbers. The only difference between the elastic and viscoelastic cases is that both s_α and F_α of (III.21) now cease to be real, i.e., the proof which was presented in Sec.C for the reality of s_α, F_α is no longer valid. However, even in that case the locations of the poles s_α are confined to certain regions of the complex plane, which can be found by a procedure similar to the one presented in Sec.C but modified to take account of the fact that the tensors are complex.

The main application of the moment sum rules of Sec.E is in the derivation of various bounds — this will be done in Ch.V. However, these sum rules also provide a convenient check of various approximate solutions. Such checks will be performed in Ch.IV. Note that M_0 in (III.52) contains the factor p_1. Therefore any approximate solution which does not satisfy the M_0 sum rule is incorrect already at order p_1. The first moment sum rule (see (III.68), (III.69)) includes the factor $p_1(1-p_1)$, thus enabling us to check any solution up to order p_1^2 whenever an explicit expression for M_1 is available.

We have focussed our attention on a calculation of the effective elastic constants. However the range of applicability of our formalism is much broader: Using the identity operator (III.20) in (III.14) we can get the following expression for $|\varepsilon>$:

$$|\varepsilon> = \sum_\alpha |\varepsilon^{(\alpha)}> \frac{s}{s-s_\alpha} <\tilde{\varepsilon}^{(\alpha)}|\varepsilon^0> \ , \qquad \text{(III.74)}$$

which is valid only <u>inside</u> $C^{(1)}$ material, as was explained in Sec. B ($\hat{I}$ of (III.20) is an identity operator only inside $C^{(1)}$ material). In order to get an expansion that is also valid <u>outside</u> $C^{(1)}$ material, we substitute (III.74) on the r.h.s. of (III.9), to get

$$|\varepsilon\rangle = |\varepsilon^0\rangle + \frac{1}{s}\hat{G}\sum_{\alpha}|\varepsilon^{(\alpha)}\rangle\frac{s}{s-s_\alpha}\langle\tilde{\varepsilon}^{(\alpha)}|\varepsilon^0\rangle$$

$$= |\varepsilon^0\rangle + \sum_{\alpha}|\varepsilon^{(\alpha)}\rangle\frac{s_\alpha}{s-s_\alpha}\langle\tilde{\varepsilon}^{(\alpha)}|\varepsilon^0\rangle \qquad \text{(III.75)}$$

(Note that the definition of $\hat{G}$ in (III.10) contains θ_1-function, thus enabling to perform of the above substitution.) The knowledge of the strain (and the stress) field at any point in the composite is useful for the investigation of other mechanical properties of the composite. E.g., this knowledge is necessary (although not sufficient) for investigations of the strength of the composite [57].

CHAPTER IV. EFFECTIVE ELASTIC MODULI OF MULTI-GRAIN SYSTEMS

A. INTRODUCTION

In this chapter we apply our general approach to several well defined microgeometries [27,29]. We use the elastostatic resonances of individual, isolated grains to construct the resonances of a multi-grain system. In Sec.B we develop the formalism of this procedure for general multi-grain systems and obtain a rather simple prescription for constructing the resonances of a periodic composite. This procedure is applied in Secs. C and D to periodic hexagonal and square arrays of parallel circular cylinders, and in Sec.E to a more complicated 3D system of cylinders. In lowest order we obtain Clausius-Mossotti-type approximations for the bulk modulus as well as for the shear moduli. Some higher order corrections to these constants are also calculated — all of them by using some very simple techniques of perturbation theory [64]. In this way, we obtain expressions for the bulk modulus correct to order p_1^{11} and p_1^7 for hexagonal and square arrays, respectively. For the shear moduli we obtain expressions which are correct to order p_1^5 for both types of arrays. In the 3D case our results are correct (at least) to order p_1^2. At the end of the chapter we shall discuss the advantages of our method as compared to the T-matrix techniques, and possible applications of our approach to quasi-random systems.

Usually, theoretical models of composites have oversimplified microgeometries. A typical model consists of a host medium with inclusions which have the following properties [58]: a) each inclusion is an <u>infinite</u> fibre; b) all fibers are exactly <u>parallel</u>; c) all fibers are <u>identical</u> and have a <u>simple</u> cross section (circular, elliptical, square, rhombic); d) fibers form a <u>periodic</u> 2D lattice (hexagonal, square, rectangular). Usually, none of the underlined properties is exactly valid, and the main reason for such choices is the mathematical simplicity of the model, which allows numerical solution of the elasticity equations in a repeated element of the composite [14]. However, numerous examples can be found, for which such simple geometries are good approximations: In many cases the fibers are very long, their cross sections are close to some simple geometrical

form (e.g., circle) and the distribution of the cross section sizes is quite narrow [59]. Usually, the fibers are distributed quite randomly. However, there are cases when they form simple geometrical structures, e.g., periodic hexagonal lattices [60].

We apply our methods to two very extensively investigated [61-63] simple mcrogeometries: square and hexagonal periodic arrays of indentical, parallel, circular-cylinder inclusions. Our analytical results will be compared with the results of existing numerical calculations. Many composite materials have more complicated 3D structures, among which we can find fibrous composites consisting of fibers with different (frequently, random) spatial orientations. The number of analytical investigations of 3D fibrous composites is very limited, and those approaches usually combine some exact elastic relations with various barely justified approximations [65]. In Sec.E we derive a Clausius-Mossotti-type approximation for a simple 3D model of a fibrous composite.

B. A SYSTEM OF MANY INCLUSIONS

It is convenient to set up the problem of many inclusions of one elastic material embedded in another elastic medium in terms of the eigenstates of the isolated inclusions [27]. In our discussion of this we follow a similar discussion recently given for the electrostatic problem of many inclusions [46,47].

For a system consisting of many non-overlapping inclusions we can write the θ_1-function defined in (III.2) as a sum of θ-functions of individual grains:

$$\theta_1 = \sum_a \theta_a \,, \tag{IV.1}$$

where **a** is a grain index. Similarly, the operator $\hat{G}$ can be written as a sum of individual grain operators (see (III.10)):

$$\hat{G} = \sum_a \hat{G}_a . \tag{IV.2}$$

Each isolated grain has its own set of eigenvalues and right eigenstates

$$\hat{G}_a|\varepsilon^{a(\alpha)}\rangle = s_{a\alpha}|\varepsilon^{a(\alpha)}\rangle, \tag{IV.3}$$

which together with the set of left eigenstates $\tilde{\varepsilon}^{a(\alpha)}$ form a complete bi-orthogonal set of eigenstates inside the **a**-th grain. We use these states to expand any eigenstate $\varepsilon^{(n)}$ of the entire system inside the grains

$$\theta_1|\varepsilon^{(n)}\rangle = \sum_{a\alpha} B^{(n)}_{a\alpha}\theta_a|\varepsilon^{a(\alpha)}\rangle . \tag{IV.4}$$

The various θ-functions have to appear in this equation because the states $\varepsilon^{a(\alpha)}$ for a given **a** form a complete set of states only inside the grain **a**. We now use this expansion in order to rewrite (III.16) as a matrix equation for the expansion coefficients $B^{(n)}_{a\alpha}$. The equation for the eigenstate of the entire system is

$$\begin{aligned} s_n|\varepsilon^{(n)}\rangle = \hat{G}|\varepsilon^{(n)}\rangle = \hat{G}\theta_1|\varepsilon^{(n)}\rangle = \hat{G}\sum_{a\alpha} B^{(n)}_{a\alpha}\theta_a|\varepsilon^{a(\alpha)}\rangle = \\ = \sum_{a\alpha} B^{(n)}_{a\alpha}\hat{G}_a|\varepsilon^{a(\alpha)}\rangle = \sum_{a\alpha} B^{(n)}_{a\alpha}s_{a\alpha}|\varepsilon^{a(\alpha)}\rangle, \end{aligned} \tag{IV.5}$$

where s_n is the eigenvalue of $\varepsilon^{(n)}$, and where the identities $\hat{G}\theta_1 \equiv \hat{G}$ and $\hat{G}\theta_a \equiv \hat{G}_a$, which follow directly from the definition (III.10) and from (IV.1), were used. By multiplying (IV.5) by $\langle\tilde{\varepsilon}^{b(\beta)}|\theta_b$ we arrive at the following equation:

$$(s_n - s_{b\beta})B^{(n)}_{b\beta} = \sum_{\substack{a\alpha \\ a\neq b}} \langle\tilde{\varepsilon}^{b(\beta)}|\theta_b\hat{G}\theta_a|\varepsilon^{a(\alpha)}\rangle B^{(n)}_{a\alpha} \tag{IV.6}$$

The matrix element appearing on the r.h.s. can be written explicitly in terms of an overlap integral between the individual grain eigenstates as follows:

$$Q_{b\beta,a\alpha} \equiv \langle \tilde{\varepsilon}^{b(\beta)} | \theta_b \hat{G} \theta_a | \varepsilon^{a(\alpha)} \rangle = s_{a\alpha} \langle \tilde{\varepsilon}^{b(\beta)} | \theta_b | \varepsilon^{a(\alpha)} \rangle = s_{a\alpha} \int \theta_b \varepsilon^{b(\beta)} \delta C \varepsilon^{a(\alpha)} dV$$

$$= s_{b\beta} \langle \tilde{\varepsilon}^{b(\beta)} | \theta_a | \varepsilon^{a(\alpha)} \rangle = s_{b\beta} \int \theta_a \varepsilon^{b(\beta)} \delta C \varepsilon^{a(\alpha)} dV \ ,$$

$$\text{for } b \neq a. \qquad \text{(IV.7)}$$

Note that the integrand includes summation over the tensorial indices, and that the integration is only over the volume of one grain. We shall call this matrix element "an interaction between the resonances of two grains". It can easily be seen from (IV.7) that the interaction is symmetric, i.e. $Q_{b\beta,a\alpha} = Q_{a\alpha,b\beta}$.

Having found the normalized right eigenvectors $B^{(n)}_{b\beta}$ as well as the eigenvalues of the secular equation (IV.6), we can again use (III.21) for F(s), with the weights now being expressed as follows (see (III.22)):

$$F_n = \frac{1}{V} \Big(\sum_{a\alpha} B^{(n)}_{a\alpha} \langle \tilde{\varepsilon}^{0} | \varepsilon^{a(\alpha)} \rangle \Big)^2 \ . \qquad \text{(IV.8)}$$

Since the overlap integrals decrease with the distance between two grains, to leading order in the volume fraction p_1 (i.e., to order p_1^0) we can neglect the r.h.s. of (IV.6), i.e., we can neglect the interactions between the grains. In that order, the eigenstates are equal to the individual grain eigenstates. That is why (III.46) and (III.47), if used for any system of parallel cylindrical fibers, are correct to order p_1^1.

In attempting to calculate more accurate results, a great simplification occurs if the inclusions are all identical and form a periodic array in space. Clearly, in that case the matrix element $Q_{b\beta,a\alpha}$ of (IV.7) depends on the two grain indices **a** and **b** only through their vector separation $\vec{a}-\vec{b}$, and the individual grain eigenvalues $s_{a\alpha}=s_\alpha$ are independent of **a**. In that case, Bloch's theorem [66] immediately specifies the dependence of the eigenvectors on the grain index **a**

$$B^{(n)}_{a\alpha} = \frac{1}{\sqrt{N}} B^{(n)}_{\alpha}(\vec{k}) e^{i\vec{k}\cdot\vec{a}} \ , \qquad \text{(IV.9)}$$

where N is the number of unit cells in the periodic sample. Furthermore, since ε^0 is independent of $\vec{r}$, while $\varepsilon^{a(\alpha)}$ is only a function of $\vec{r}-\vec{a}$, the scalar product $\langle\tilde{\varepsilon}^0|\varepsilon^{a(\alpha)}\rangle$ is independent of **a**. Consequently, (IV.8) simplifies to

$$F_n = \frac{1}{VN}\left(\sum_{a\alpha} B_\alpha^{(n)}(\vec{k})\, e^{i\vec{k}\cdot\vec{a}}\langle\tilde{\varepsilon}^0|\varepsilon^{a(\alpha)}\rangle\right)^2 = \\ = \frac{N}{V}\,\delta_{\vec{k},0}\left(\sum_{\alpha} B_\alpha^{(n)}(\vec{k}=0)\,\langle\tilde{\varepsilon}^0|\varepsilon^{a(\alpha)}\rangle\right)^2, \tag{IV.10}$$

where there is no longer summation over grain indices. We see that only the $\vec{k}=0$ Bloch states can have non-zero weights, so that only those states need to be considered. For $\vec{k}=0$ eigenstates (IV.6) becomes

$$(s_n - s_\beta)B_\beta^{(n)} = \sum_\alpha Q_{\beta,\alpha} B_\alpha^{(n)}, \tag{IV.11}$$

where the lattice sum of interactions

$$Q_{\beta,\alpha} \equiv \sum_{\substack{a \\ a\neq b}} \langle\tilde{\varepsilon}^{b(\beta)}|\theta_b \hat{G}\theta_a|\varepsilon^{a(\alpha)}\rangle \quad . \tag{IV.12}$$

This quantity is also symmetric, i.e. $Q_{\beta,\alpha}=Q_{\alpha,\beta}$.

At this point it might be worthwhile to note the similarity of this approach to the tight-binding method for calculating quantum-mechanical states of an electron in a crystal lattice [67]. In principle, we would get a continuous band of eigenvalues $s_n(\vec{k})$, but only the $\vec{k}=0$ state turns out to be important. The $\vec{k}=0$ eigenstates are periodic, i.e., the strains in one unit cell coincide with the strains in any other unit cell. Only these eigenstates give non-zero contributions to the effective elastic constants, because ε^0 is a uniform constant tensor, i.e., it can be viewed as an infinite wavelength ($\vec{k}=0$) strain. If ε^0 would be some plane wave with wave-vector $\vec{q}$, then $\vec{k}=\vec{q}$ eigenstates would become important. Although this simple consideration indicates what might happen in a non-static case, it should be kept in mind that our eigenstates correspond to a static problem and a modification of the entire formalism is needed for the discussion of non-trivial dynamical problems [68].

C. THE EVALUATION OF LATTICE SUMS

We would like to apply the methods developed in the previous section to a calculation of the effective elastic constants of a composite in the form of a periodic array of parallel, identical, non-overlapping, circular-cylinder inclusions, when both inclusions and the host medium are taken to be made of isotropic materials.

We start from evaluation of the overlap integrals $\langle \varepsilon^{*b(\beta)} | \theta_b | \varepsilon^{a(\alpha)} \rangle$ between different eigenstates of individual grains (see (IV.7)). We locate the origin of our 2D reference frame at the symmetry axis of cylinder **b**, while the location of the symmetry axis of cylinder **a** will be denoted by $w_o = x_1^o + ix_2^o$ (as in Ch.III.D, we use the complex variable $w = x_1 + ix_2$). Thus we have to evaluate 2D integrals of the type $\int \theta_b \varepsilon^{b(\beta)} \delta C \varepsilon^{a(\alpha)} dx_1 dx_2$. We assume that both cylinders have the same radius R. Note that $\varepsilon^{b(\beta)}$ is the strain <u>inside</u> the cylinder at the origin, and therefore the $|w| \leqslant R$ case of the expressions (III.41), (III.43) and (III.45) must be used, while $\varepsilon^{a(\alpha)}$ is the "tail" of the eigenstate centered at w_o, and therefore the $|w| > R$ case of the same expressions must be used, but w in those expressions must be replaced by $w - w_o$. Thus the evaluation of the overlap integrals is actually an integration of expressions such as $\frac{w^k}{(w-w_o)^{*\ell}}$, $\frac{w^k (w-w_o)}{(w-w_o)^{*\ell}}$, $\frac{w^* w^k}{(w-w_o)^{\ell}}$, etc. inside the circle of radius R. This can be accomplished by numerous standard methods, e.g., by expansion of the expression in a Taylor-Laurent series around the origin and subsequent integration in polar coordinates. The resulting overlaps are listed below. In this list, $\binom{\ell}{n}$ is a binomial coefficient; $\mu^{(1)}_{C,D}$ and $\kappa^{(1)}_{C,D}$ are the resonance values of $\mu^{(1)}$ and $\kappa^{(1)}$, as defined in Sec. III.D; the grain indices **a** and **b** are omitted; the notation $|\varepsilon^{(\pm C,D\ell)}\rangle$ means that we can take any possible combination of superscripts, e.g. $|\varepsilon^{(+C\ell)}\rangle$, $|\varepsilon^{(-D\ell)}\rangle$, etc.; the location of the **a** cylinder which is not at the origin is now denoted by w; and the coefficients A were defined in (III.43b) and (III.45b).

$$<\tilde{\varepsilon}^{(A0)}|\theta_b|\varepsilon^{(A0)}> = 0 \qquad \text{(III.13a)}$$

$$<\tilde{\varepsilon}^{(+B\ell)}|\theta_b|\varepsilon^{(+Bn)}> = <\tilde{\varepsilon}^{(-B\ell)}|\theta_b|\tilde{\varepsilon}^{(-Bn)}> =$$

$$= A_{B\ell}A_{Bn}\frac{4\pi\delta\mu R^{2(\ell+n-2)}}{1+2\mu^{(2)}/\kappa^{(2)}}(-1)^n \mathrm{Re}\left[\binom{\ell+n}{n}\frac{R^2}{w^{\ell+n}} - \binom{\ell+n-2}{\ell-1}\frac{|w|^2}{w^{\ell+n}}\right] \qquad \text{(III.13b)}$$

$$<\tilde{\varepsilon}^{(-B\ell)}|\theta_b|\varepsilon^{(+Bn)}> = -<\tilde{\varepsilon}^{(+B\ell)}|\theta_b|\varepsilon^{(-Bn)}> =$$

$$= A_{B\ell}A_{Bn}\frac{4\pi\delta\mu R^{2(\ell+n-2)}}{1+2\mu^{(2)}/\kappa^{(2)}}(-1)^n \mathrm{Im}\left[\binom{\ell+n}{n}\frac{R^2}{w^{\ell+n}} - \binom{\ell+n-2}{\ell-1}\frac{|w|^2}{w^{\ell+n}}\right] \qquad \text{(III.13c)}$$

$$<\tilde{\varepsilon}^{(\pm C,D\ell)}|\theta_b|\varepsilon^{(\pm C,Dn)}> = 0 \qquad \text{(III.13d)}$$

$$<\tilde{\varepsilon}^{(A0)}|\theta_b|\varepsilon^{(\pm C,D\ell)}> = 0 \qquad \text{(III.13e)}$$

$$<\tilde{\varepsilon}^{(A0)}|\theta_b|\varepsilon^{(\pm B\ell)}> = A_{B\ell}\frac{2\sqrt{\pi\delta\kappa}\,R^{2\ell-1}}{1+\kappa^{(2)}/2\mu^{(2)}}(-1)^{\ell}\left\{\begin{matrix}\mathrm{Re}\\ \mathrm{Im}\end{matrix}\right\}\frac{1}{w^{*\ell}} \qquad \text{(III.13f)}$$

$$<\tilde{\varepsilon}^{(+B\ell)}|\theta_b|\varepsilon^{(A0)}> = A_{B\ell}2R^{2\ell-1}\delta\mu\sqrt{\frac{\pi}{\delta\kappa}}\,\mathrm{Re}\frac{1}{w^{\ell}} \qquad \text{(III.13g)}$$

$$<\tilde{\varepsilon}^{(+B\ell)}|\theta_b|\varepsilon^{(+C,Dn)}> = -<\tilde{\varepsilon}^{(-B\ell)}|\theta_b|\varepsilon^{(-C,Dn)}> =$$

$$= A_{B\ell}A_{C,Dn}\frac{4\pi\delta\mu R^{2(\ell+n)}\mu^{(1)}_{C,D}}{(\ell-1)\mu^{(2)}}(-1)^{n+1}\binom{\ell+n-1}{\ell-2}\mathrm{Re}\,\frac{1}{w^{\ell+n}} \qquad \text{(III.13h)}$$

$$<\tilde{\varepsilon}^{(-B\ell)}|\theta_b|\varepsilon^{(+C,Dn)}> = -<\tilde{\varepsilon}^{(+B\ell)}|\theta_b|\varepsilon^{(-C,Dn)}> =$$

$$= A_{B\ell}A_{C,Dn}\frac{4\pi\delta\mu R^{2(\ell+n)}\mu^{(1)}_{C,D}}{(\ell-1)\mu^{(2)}}(-1)^{n+1}\binom{\ell+n-1}{\ell-2}\mathrm{Im}\,\frac{1}{w^{\ell+n}} \qquad \text{(III.13i)}$$

The interaction between two eigenstates can be calculated with the help of the overlap integral in two different ways, as shown in (IV.7). Thus the above list, which does not include all possible overlaps, suffices to evaluate all interactions.

We still have to evaluate sums over interactions in order to get the lattice sum $Q_{\beta\,\ell}{}^{\alpha}$ of (IV.12). This will involve summation of terms such as $1/w^{\ell}$ or $|w|^2/w^{\ell}$ over all points of the periodic lattice of the centers of cylinders, a task which will usually have to be accomplished numerically. As the effective elastic constants do not depend on the choice of the unit length, we can measure the distance and the radius of cylinders in, say, the units of lattice constant, and thus the summations of the terms $1/w^{\ell}$ or $|w|^2/w^{\ell}$ can be performed once and for all on a standard lattice with unit lattice constant.

A special problem arises in the summation of overlap integrals between two dipole states: There appear lattice sums of terms of the form $|w|^2/w^4$ and $1/w^2$, which are only semiconvergent, for which the distant contributions are just as important as the nearby ones. However, the states of grains that are near the surface of the system are not accurately given by the results of Ch.III.D, where we assumed that the isolated cylinder was infinitely far away from the surface. Therefore, we can only use the overlap integrals of (IV.13) to sum over the nearby lattice sites, and we must resort to a different stratagem for dealing with the distant contributions. E.g., the overlap between two $\varepsilon^{(AO)}$ states (compression dipoles) of different cylinders always vanishes. Nevertheless, we shall see that the sum of such interactions between all pairs of cylinders is nonzero: This is caused by the deviation from the infinite volume expressions as one of the cylinders approaches the surface of the system. Problems arising from semiconvergence of dipole-dipole interactions are well known, and have been discussed quite extensively in recent years in the context of elasticity and fluid mechanics [69].

It seems, however, that the analogous problem in electrostatics was already solved at the beginning of this century by means of the concept of

the local Lorentz field [70]. This concept is often used to sum over electrostatic dipole-dipole interactions, and we use an analogous approach in the elastostatic case.

The important properties of the elastic dipole states of an isolated cylinder are that $\varepsilon^{(\alpha)}$ is constant inside the cylinder, and that the eigenvalue $s_{a\alpha}=s_{\alpha}$ is independent of the cylinder radius. Following the elastostatic-electrostatic analogy (see (II.11) and (II.12)), we define the elastic polarization density of the cylinder by

$$P_{ij}^{a(\alpha)} \equiv \frac{1}{s_{a\alpha}} \theta_a \delta C_{ijkl} \varepsilon_{kl}^{a(\alpha)} \quad . \tag{IV.14}$$

We can then find ε everywhere else by solving the equation

$$\partial_j C^{(2)}_{ijkl} \varepsilon_{kl}^{a(\alpha)} = -\partial_j P_{ij}^{a(\alpha)} \quad , \tag{IV.15}$$

which is simply a special case of (II.11). The sum of dipole-dipole interactions between all the other cylinders and the one at the origin can be written in terms of an overlap integral over the volume of that cylinder, in which the integrand is the product of ε of that cylinder, δC and the ε due to all other cylinder-dipoles. The latter quantity (local Lorentz strain), denoted by ε^{loc}, is calculated by considering separately the contribution of the nearby cylinders, i.e., those that lie within a circle of radius L around the origin (L must be much larger than the cylinder radii and the intergrain separations), and that of the distant cylinders:

$$\varepsilon^{loc} = \varepsilon^{loc}_{near} + \varepsilon^{loc}_{far} \quad . \tag{IV.16}$$

In order to calculate the far contribution, we may replace the actual inhomogeneous polarization density for r>L in (IV.15) by its volume average, i.e., we smear the polarization. That would lead to a solution for ε denoted by $\varepsilon^{macro}_{far}$. If we made the same replacement for r<L in (IV.15), we would obtain the solution denoted by $\varepsilon^{macro}_{near}$. Finally, if we replace the inhomogeneous P_{ij} everywhere by its (homogeneous) volume average, the r.h.s. of (IV.15) would vanish, and the solution would simply be $\varepsilon \equiv 0$ (due to the zero boundary conditions). Therefore the sum

$\varepsilon^{\text{macro}}_{\text{near}} + \varepsilon^{\text{macro}}_{\text{far}}$ must vanish, and we can conclude that

$$\varepsilon^{\text{loc}}_{\text{far}} = \varepsilon^{\text{macro}}_{\text{far}} = -\varepsilon^{\text{macro}}_{\text{near}} , \tag{IV.17}$$

and hence

$$\varepsilon^{\text{loc}} = \varepsilon^{\text{loc}}_{\text{near}} - \varepsilon^{\text{macro}}_{\text{near}} . \tag{IV.18}$$

In order to evaluate $\varepsilon^{\text{macro}}_{\text{near}}$ close to the origin, we note that this is again a strain field in a kind of cylindrical inclusion at the origin (a very large one - its radius is L!) that is entirely due to the uniform polarization density $\frac{1}{s_{b\alpha}} p_1 \delta C \varepsilon^{b(\alpha)}$ inside that cylinder. This is reminiscent of the situation we described earlier for the actual cylindrical inclusion at the origin **b**, where the strain field could be viewed as resulting from a uniform polarization density $\frac{1}{s_{b\alpha}} \delta C \varepsilon^{b(\alpha)}$ inside the cylinder. Consequently, we may conclude that $\varepsilon^{\text{macro}}_{\text{near}}$ is the same as $\varepsilon^{b(\alpha)}$, except for the factor p_1, namely

$$\varepsilon^{\text{macro}}_{\text{near}} = p_1 \varepsilon^{b(\alpha)} \tag{IV.19}$$

at all points that are inside both cylinders (the large one and the small one).

When this result is used to substitute for the sum of contributions to ε from all the dipoles except the one at the origin, we find:

$$\begin{aligned} Q_{\beta,\alpha} &= \sum_{0 \neq |\vec{a}-\vec{b}|} {}_a \langle \hat{\varepsilon}^{b(\beta)} | \theta_b \hat{G} \theta_a | \varepsilon^{a(\alpha)} \rangle = \\ &= \sum_{0 \neq |\vec{a}-\vec{b}| < L} {}_a \langle \hat{\varepsilon}^{b(\beta)} | \theta_b \hat{G} \theta_a | \varepsilon^{a(\alpha)} \rangle - p_1 \langle \hat{\varepsilon}^{b(\beta)} | \theta_b \hat{G} \theta_b | \varepsilon^{b(\alpha)} \rangle = \\ &= \sum_{0 \neq |\vec{a}-\vec{b}| < L} {}_a \langle \hat{\varepsilon}^{b(\beta)} | \theta_b \hat{G} \theta_a | \varepsilon^{a(\alpha)} \rangle - p_1 s_{b\alpha} \delta_{\alpha\beta} . \end{aligned} \tag{IV.20}$$

In this equation, L must be large enough so that the use of an average polarization density for r>L is a good approximation. In practice, one sums the series over a set of circles with larger and larger L until convergence is obtained, i.e.

$$Q_{\beta,\alpha} = \lim_{L\to\infty} \sum_{0\neq|\vec{a}-\vec{b}|<L} {}_{a} <\tilde{\varepsilon}^{b(\beta)} | \theta_b \hat{G} \theta_a | \varepsilon^{a(\alpha)}> - p_1 s_\alpha \delta_{\alpha\beta} \cdot \qquad \text{(IV.21)}$$

This method of evaluation of elastostatic dipole-dipole interactions is not limited to the case of a periodic lattice of parallel cylinders: In App.C we will use it for a more general case, where the cylinders may be oriented in three perpendicular spatial directions. It can also be used in, say, a 3D periodic lattice of spheres. Moreover, the result (IV.21) is an exact evaluation of the dipole-dipole interaction between one cylinder and all the others in a non-periodic sample, because in the entire proof we actually did not use the periodicity of the system. However, in the non-periodic case the result depends on **b**, because the first term on the r.h.s. of (IV.21) depends on the relative locations of the cylinders, and the entire result loses the meaning of lattice sum as it was used in (IV.11).

D. PERIODIC ARRAYS OF CYLINDERS

In this section we apply the methods developed in Secs.B and C to a calculation of the effective elastic constants of hexagonal and square arrays of parallel, identical, non-overlapping cylindrical inclusions [27]. Those configurations, which are depicted in Fig. IV.1, are very frequently used to model the elastic behaviour of fibrous materials. The transverse effective elastic stiffness of a square array is characterized by the bulk modulus $\kappa^{(e)}$ and two shear moduli $\mu^{(e)}$ and $m^{(e)}$ while in the case of a hexagonal lattice, $\mu^{(e)}=m^{(e)}$, because its elastic properties are transversely isotropic [34]. Thus we will use $\varepsilon^o = \varepsilon^{o\kappa}$, $\varepsilon^o = \varepsilon^{o\mu}$ and $\varepsilon^o = \varepsilon^{om}$ to determine these effective moduli. It follows from (IV.10) that we actually need only those parts of the eigenvector $B_\alpha^{(n)}$, for which $<\tilde{\varepsilon}^o | \tilde{\varepsilon}^{(\alpha)}>$ does not

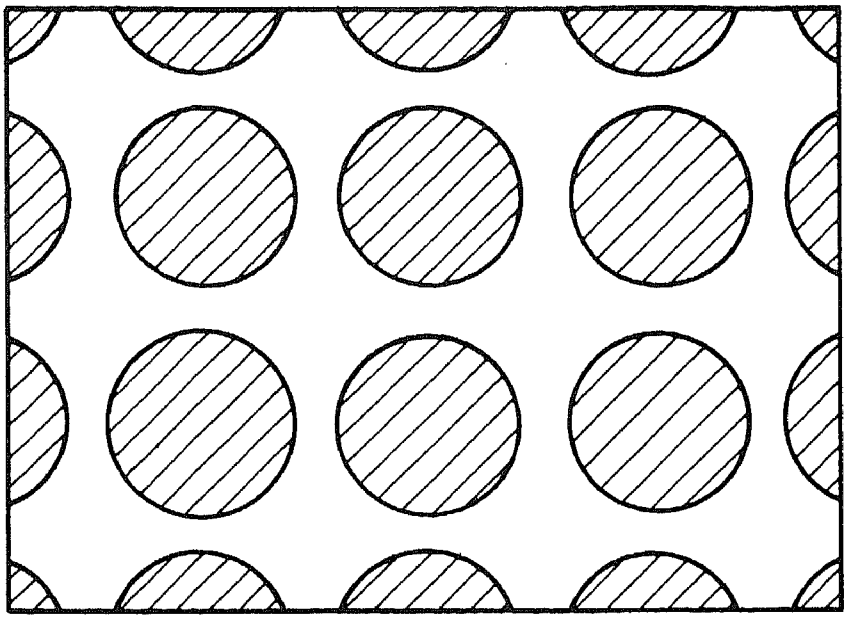

(a)

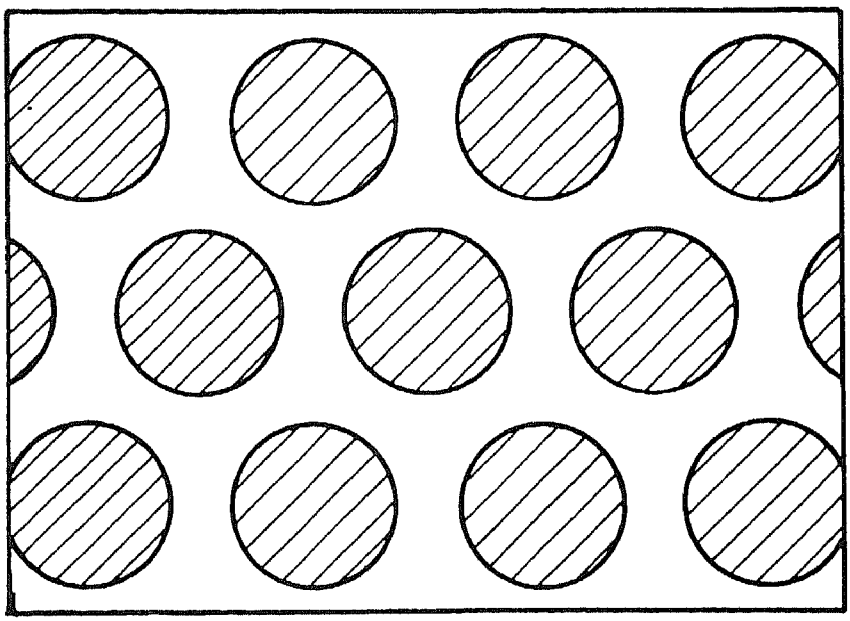

(b)

Fig. IV.1. Cross sections of (a) square and (b) hexagonal periodic arrays of parallel, identical, circular cylinders in the plane perpendicular to the cylinder axis.

vanish. For each of the above choices of ε^o there is only one non-vanishing term, namely

$$\langle \tilde{\varepsilon}^{o\kappa} | \varepsilon^{(A0)} \rangle = p_1 \delta\kappa \quad , \tag{IV.22a}$$

$$\langle \tilde{\varepsilon}^{o\mu} | \varepsilon^{(-B2)} \rangle = \langle \tilde{\varepsilon}^{om} | \varepsilon^{(+B2)} \rangle = p_1 \delta\mu \quad . \tag{IV.22b}$$

Thus we need only the $B_{A0}^{(n)}$, $B_{\pm B2}^{(n)}$ components of the eigenvectors of (IV.11).

The lattice sums $Q_{\beta,\alpha}$ for the dipole-dipole interactions will be evaluated using the prescription (IV.21). If both states are compression dipoles $\varepsilon^{(A0)}$ then all terms of the sum in a circle of size L vanish and we find

$$Q_{A0,A0} = -p_1 s_A \quad . \tag{IV.23}$$

The values of the other Q's already depend on the point symmetry of the lattice. If the lattice is invariant under reflection through the x_1-axis, then

$$Q_{A0,+B2} = Q_{A0,-B2} = Q_{+B2,-B2} = Q_{-B2,+B2} = 0 \tag{IV.24}$$

This can easily be concluded from the expressions for the overlap integrals (IV.13).

In the case of a hexagonal lattice we find for the remaining dipolar Q's that the lattice sums over a finite circle vanish, and we are left with

$$Q_{+B2,+B2} = Q_{-B2,-B2} = -p_1 s_B . \tag{IV.25}$$

Thus, taking into account only the strongest (dipole-dipole) interactions, the secular equation (IV.11) for the hexagonal lattice is already in diagonal form:

$$\begin{pmatrix} s_A(1-p_1) & 0 & 0 \\ 0 & s_B(1-p_1) & 0 \\ 0 & 0 & s_B(1-p_1) \end{pmatrix} \begin{pmatrix} B_{A0}^{(n)} \\ B_{+B2}^{(n)} \\ B_{-B2}^{(n)} \end{pmatrix} = s_n \begin{pmatrix} B_{A0}^{(n)} \\ B_{+B2}^{(n)} \\ B_{-B2}^{(n)} \end{pmatrix} . \qquad \text{(IV.26)}$$

The effective elastic constants will have a similar form to those of a single cylinder (see (III.47) and (III.48)) but with shifted poles:

$$\kappa^{(e)} = \kappa^{(2)} + \frac{p_1}{\frac{1}{\delta\kappa} + \frac{1-p_1}{\kappa^{(2)} + \mu^{(2)}}} \qquad \text{(IV.27)}$$

$$\mu^{(e)} = m^{(e)} = \mu^{(2)} + \frac{p_1}{\frac{1}{\delta\mu} + (1-p_1)\frac{\kappa^{(2)} + 2\mu^{(2)}}{2\mu^{(2)}(\kappa^{(2)}+\mu^{(2)})}} . \qquad \text{(IV.28)}$$

These results are equivalent to the well-known expressions for the Hashin-Shtrikman bounds on $\kappa^{(e)}$ and $\mu^{(e)}$ for transversely isotropic composite materials [71]. An identical expression for $\kappa^{(e)}$ was obtained by Hashin and Rosen [12] as an exact result for a composite-cylinder-assemblage. Identical expressions for both $\kappa^{(e)}$ and $\mu^{(e)}$ can be obtained for dilute isotropic suspensions in 2D, i.e. aligned cylindrical inclusions [54,72].

In the case of a square lattice, the remaining dipolar Q's involve lattice sums that do not vanish. Consequently, we find

$$Q_{\pm B2,\pm B2} = [\pm \frac{1}{1 + \frac{2\mu^{(2)}}{\kappa^{(2)}}} \lim_{L\to\infty} \mathrm{Re}(2R^4 \cdot \sum_{\substack{w \\ 0<|w|<L}} \frac{1}{w^4} - 2R^2 \cdot \sum_{\substack{w \\ 0<|w|<L}} \frac{|w|^2}{w^4}) - p_1]s_B$$

$$= (\pm \frac{1.92p_1^2 - 1.60p_1}{1 + \frac{2\mu^{(2)}}{\kappa^{(2)}}} - p_1)s_B \quad . \qquad \text{(IV.29)}$$

Note that the value of the semiconvergent sum of terms $|w|^2/w^4$ (equal to 2.5076... in units of the lattice constant) depends crucially on the particular type of summation (i.e., all the points inside a circle). The secular equation in this case is

$$\begin{pmatrix} s_A(1-p_1) & 0 & 0 \\ 0 & s_B\left(1-p_1-\frac{1.60p_1-1.92p_1^2}{1+2\mu^{(2)}/\kappa^{(2)}}\right) & 0 \\ 0 & 0 & s_B\left(1-p_1+\frac{1.60p_1-1.92p_1^2}{1+2\mu^{(2)}/\kappa^{(2)}}\right) \end{pmatrix} \begin{pmatrix} B_{A0}^{(n)} \\ B_{+B2}^{(n)} \\ B_{-B2}^{(n)} \end{pmatrix} =$$

$$= s_n \begin{pmatrix} B_{A0}^{(n)} \\ B_{+B2}^{(n)} \\ B_{-B2}^{(n)} \end{pmatrix}. \qquad \text{(IV.30)}$$

The effective bulk modullus is thus the same as in the hexagonal lattice, but the shear moduli are different:

$$\mu^{(e)} = \mu^{(2)} + \frac{p_1}{\frac{1}{\delta\mu} + (1-p_1)\frac{\kappa^{(2)}+2\mu^{(2)}}{2\mu^{(2)}(\kappa^{(2)}+\mu^{(2)})} + \frac{\kappa^{(2)}(1.60p_1-1.92p_1^2)}{\delta\mu(\kappa^{(2)}+2\mu^{(2)})}}, \qquad \text{(IV.31)}$$

$$m^{(e)} = \mu^{(2)} + \frac{p_1}{\frac{1}{\delta\mu} + (1-p_1)\frac{\kappa^{(2)}+2\mu^{(2)}}{2\mu^{(2)}(\kappa^{(2)}+\mu^{(2)})} - \frac{\kappa^{(2)}(1.60p_1-1.92p_1^2)}{\delta\mu(\kappa^{(2)}+2\mu^{(2)})}}. \qquad \text{(IV.32)}$$

Although the expression (IV.27) for the effective bulk modulus of both hexagonal and square arrays is only an approximation, it satisfies exactly the two sum rules (III.52) and (III.68). Similarly, the effective shear modulus of (IV.28) satisfies (III.52) and (III.69). In the case of the square array, these sum rules are satisfied exactly by μ_{av} (see (III.72a)) as they should be (see Ch.III.E). Actually, the results (IV.27) and

(IV.28) could have been "guessed" without any calculation: Had we assumed that the effective elastic modulus was given by a function F(s), which has only one pole, then the zero and first moment sum rules would have determined that function completely:

$$F(s) = \frac{M_0}{1 - M_1/M_0} \qquad \text{(IV.33)}$$

Substituting the expressions (III.52) and (III.68)(or (III.69)) for the moments M_0 and M_1, we would then have arrived at the expression (IV.27) (or (IV.28)).

Expressions (IV.27), (IV.28), (IV.31) and (IV.32) are the elastostatic analogues of Clausius-Mossotti or Maxwell-Garnett approximation in electrostatics [73]. In both cases (electrostatic and elastostatic) only dipole-dipole interactions are taken into account in the derivation of that approximation. However, there are several differences: In a 2D electrostatic case there are two dipolar resonances (one dipole points, say, in the x_1 direction and the second one the x_2 direction), while in the elastostatic problem there are three dipolar resonances (one compression dipole and two shear dipoles). Moreover, in the electrostatic case both square and hexagonal arrays of cylinders create an effective electrically isotropic medium, while in the elastostatic case the square array has a lower effective elastic symmetry than the hexagonal array.

In spite of their apparent simplicity, the Clausius-Mossotti-type approximations (CMTA's) are very accurate in a wide range of concentrations p_1. This fact is well known in electrostatics [73] and it also has been noted empirically in elastostatics [74] for (IV.27) and (IV.28) in the case of hexagonal arays of cylinders (although these expressions where known only as Hashin-Shtrikman bounds [71] or as exact solutions for composite-cylinder-assemblages [12] and not as CMTA's for other systems. In Fig. IV.2, the moduli $\kappa^{(e)}$ and $\mu^{(e)}$ of a hexagonal array of parallel cylinders are shown as a function of the cylinder volume fraction p_1. The elastic constants of the cylinders (fibers) are $(\kappa^{(1)}, \mu^{(1)}) = (6.95, 4.17)$ and those of the host medium are $(\kappa^{(2)}, \mu^{(2)}) = (0.578, 0.185)$, in arbitrary units. Solid lines depict the effective moduli as predicted by the CMTA's

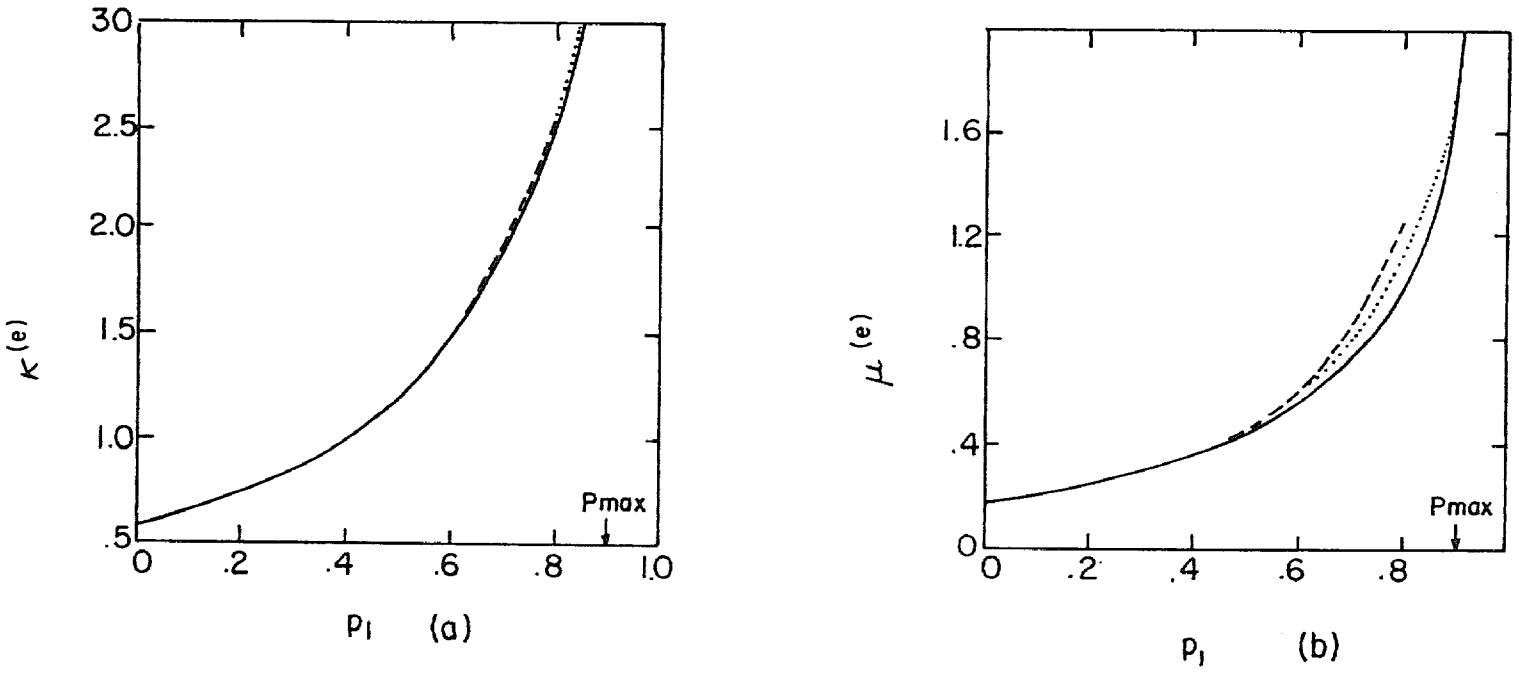

Fig. IV.2 Effective transverse elastic moduli (a) $\kappa^{(e)}$ and (b) $\mu^{(e)}$ of a periodic hexagonal lattice of parallel, identical, circular isotropic cylinders with $(\kappa^{(1)}, \mu^{(1)}) = (6.95, 4.17)$, embedded in an isotropic matrix with $(\kappa^{(2)}, \mu^{(2)}) = (0.578, 0.185)$, as a function of the fiber volume fraction p_1. Vertical array denotes maximal possible filling fraction $p_{max} = \pi/2\sqrt{3} \simeq 0.907$. CMTA predictions (IV.27) and (IV.28) (solid lines) are compared with improved approximations (IV.35) and (IV.36) (dotted lines) and with numerical results [61] (dashed lines) for $\kappa^{(e)}$ and $\mu^{(e)}$, respectively. The numerical results are know up to $p_1 = 0.8$, and they practically coincide with CMTA for $p_1 \lesssim 0.6$ in the case of $\kappa^{(e)}$, and for $p_1 \lesssim 0.4$ in the case of $\mu^{(e)}$. The improved approximations coincide with the numerical results over the entire range (where $\kappa^{(e)}$ is known numerically) in the case of $\kappa^{(e)}$, and for $p_1 \lesssim 0.6$ in the case of $\mu^{(e)}$.

(IV.27) and (IV.28), while the broken lines are results of numerical calculations [61]. Although the elastic constants of the host are smaller by an order of magnitude than the corresponding constants of the fibers, the results still coincide in a wide range of values of p_1: $\kappa^{(e)}$ almost coincides even for $p_1 = 0.8$, i.e. near the maximum filling fraction $p_{max} = \pi/2\sqrt{3} \simeq 0.907$, while $\mu^{(e)}$ is in good agreement up to $p_1 \simeq 0.6$.

A similar situation occurs also for the square lattice: E.g., for $(\kappa^{(1)}, \mu^{(1)}) = (6.67, 4.)$, $(\kappa^{(2)}, \mu^{(2)}) = (0.625, 0.2)$ and $p_1 = 0.6$ (i.e., quite close to the maximum filling fraction $p_{max} = \pi/4 \simeq 0.785$) the $\kappa^{(e)}$ of (IV.27) and the result of numerical calculation [61] are very close (1.55 and 1.51, respectively) while the shear modulus $m^{(e)}$ of (IV.32) and the numerical result [58] (0.66 and 0.81, respectively) differ by about 19%. Since expression (IV.28) has been known for a long time [12,71], it has sometimes been compared with numerical results for the shear modulus $m^{(e)}$ (or some other elastic constants that depend on $m^{(e)}$) of a <u>square</u> lattice of cylinders. Such a comparison is clearly wrong: The macroscopic elastic symmetry of a square lattice is <u>not isotropic</u>, and there is no reason to expect (IV.28) of a hexagonal lattice which has macroscopic <u>isotropic</u> elastic symmetry to be a fair approximation for $m^{(e)}$. If we use (IV.28) (instead of (IV.32)) to estimate $m^{(e)}$ in the square lattice mentioned above, we would obtain $m^{(e)} = 0.60$, which differs already by 26% from the numerical result [61]. This is a consequence of the fact that discrepancies between (IV.31), (IV.32) and (IV.28) start already in order p_1^2!

The reason for such good results, obtained from CMTA's, becomes clear when we try to increase the accuracy of the calculation. The order of the secular matrix, and with it the accuracy of the results, can be easily increased: Although $Q_{\beta,\alpha}$ is an infinite matrix, it is clear that the elements which connect higher ℓ states are of higher order in p_1. Therefore, when we truncate the matrix at some finite order ℓ, we actually get a result which is correct to some finite order in p_1. Furthermore, many of the matrix elements vanish because: a) overlap integrals between some types of states vanish (due to the cylindrical symmetry of individual grains); b) many sums vanish because of the lattice symmetry, e.g. $Q_{AO,+B\ell}$ vanishes for a hexagonal(square) lattice unless ℓ is an integral multiple of 6(4).

This allows us to obtain the elastic constants, to a rather high order in p_1 very easily. For instance, if we wish to improve the expression for $\kappa^{(e)}$ in a hexagonal lattice, taking it up to order p_1^{11}, we only need to diagonalize the following 2 x 2 matrix:

$$\begin{pmatrix} s_A(1-p_1) & -0.275\,\frac{\sqrt{\delta\kappa\,\delta\mu}}{\kappa^{(2)}+\mu^{(2)}}\,p_1^3 \\ -0.275\,\frac{\sqrt{\delta\kappa\,\delta\mu}}{\kappa^{(2)}+\mu^{(2)}}\,p_1^3 & s_B + \frac{\delta\mu\,\kappa^{(2)}(6.05p_1^5-6.09p_1^6)}{\mu^{(2)}(\kappa^{(2)}+\mu^{(2)})} \end{pmatrix} \begin{pmatrix} B_{A0}^{(n)} \\ B_{+B6}^{(n)} \end{pmatrix} = s_n \begin{pmatrix} B_{A0}^{(n)} \\ B_{+B6}^{(n)} \end{pmatrix} \tag{IV.34}$$

It can be shown that all other elements of the secular equation do not influence the state $\varepsilon^{(A0)}$ in that order. A similar calculation performed for the square lattice yields a result that is correct to order p_1^7. The bulk moduli for the two cases are then given by the following expressions:

$$\kappa^{(e)} = \kappa^{(2)} + p_1\delta\kappa\left[\frac{1-\frac{G}{(s_A'-s_B)^2}}{1-s_A'-\frac{G}{s_A'-s_B}} + \frac{\frac{G}{(s_A'-s_B)^2}}{1-s_B}\right] \tag{IV.35a}$$

$$s_A' = s_A(1-p_1) \tag{IV.35b}$$

$$G = 0.0754\,\frac{\delta\kappa\,\delta\mu}{(\kappa^{(2)}+\mu^{(2)})^2}\,p_1^6, \text{ for the hexagonal lattice} \tag{IV.35c}$$

$$G = 0.306\,\frac{\delta\kappa\,\delta\mu}{(\kappa^{(2)}+\mu^{(2)})^2}\,p_1^4, \text{ for the square lattice .} \tag{IV.35d}$$

From these equations, we see that the corrections to the previous result (IV.27) begin with order p_1^7 (p_1^5) for the hexagonal (square) lattice. This enables us to understand why (IV.27) gives such excellent agreement with more precise numerical calculations of $\kappa^{(e)}$ over a wide range of values of p_1. The result (IV.35) is depicted by a dotted line in the Fig. IV.2a. We can see that it practically coincides with the numerical results depicted by a broken line.

Similarly, we can extend the results for the shear moduli to higher order in p_1. For instance, in the case of the hexagonal lattice, by diagonalizing a 2 x 2 matrix we can obtain $\mu^{(e)}$ correctly to order p_1^5:

$$\mu^{(e)} = \mu^{(2)} + \delta\mu p_1 \left[\frac{1 - G + G^2}{1-s_B(1-p_1)+Gs_B p_1} + \frac{G(1-G)}{1 - s_B}\right] \tag{IV.36a}$$

$$G = \left[\frac{\kappa^{(2)}}{\kappa^{(2)}+2\mu^{(2)}} (2.98p_1 - 3.18p_1^2)\right]^2 \tag{IV.36b}$$

Comparing this result [75] with (IV.28) we find that the corrections begin with order p_1^4. Again, this explains the reasonable agreement between (IV.28) and the numerical results. The result (IV.36) is depicted by a dotted line in Fig. IV.2b. We can see that it is quite close to the results of numerical calculations depicted by a broken line.

In the case of the square lattice, the deviation of $\mu^{(e)}$ and $m^{(e)}$ from (IV.31) and (IV.32) starts with order p_1^5. Oddly enough, these corrections begin at higher order than in the case of the hexagonal lattice. In this case a 4 x 4 matrix must be treated in order to obtain the corrections of order p_1^5. The shear modulus $\mu^{(e)}$ of the square lattice is given by:

$$\mu^{(e)} = \mu^{(2)} + p_1\delta\mu \left[\frac{1 - \frac{G}{A^2} - \frac{R_C}{(s_B-s_C)^2} - \frac{R_D}{(s_B-s_D)^2}}{1 - s_B - A - \frac{R_C}{s_B-s_C} - \frac{R_D}{s_B-s_D}} + \right.$$

$$\left. + \frac{\frac{G}{A^2}}{1 - s_B} + \frac{\frac{R_C}{(s_C-s_D)^2}}{1 - s_C} + \frac{\frac{R_D}{(s_D-s_B)^2}}{1 - s_D}\right] \tag{IV.37a}$$

$$G = \left[\frac{\delta\mu\ \kappa^{(2)}}{2\mu^{(2)}(\kappa^{(2)}+\mu^{(2)})} (2.74\ p_1^4 - 1.95\ p_1^3)\right]^2 \tag{IV.37b}$$

$$R_{C,D} = \frac{1.11(\mu_{C,D}^{(1)})^2 s_{C,D}^2}{(\mu^{(2)})^2 \left[\frac{\delta\kappa}{\delta\mu}\left(\frac{2\mu_{C,D}^{(1)}}{\kappa_{C,D}^{(1)}}\right)^2 + 2\right]} p^4 \tag{IV.37c}$$

$$A = Q_{-B2,-B2} \quad \text{(see (IV.29).} \tag{Iv.37d}$$

The other shear modulus $m^{(e)}$ is given by the same expression except that $Q_{-B2,-B2}$ must be replaced by $Q_{+B2,+B2}$.

We have demonstrated that we are able, by rather simple analytical perturbative methods, to obtain an expansion of the effective elastic constants in powers of p_1 up to a rather high order. We would like to stress, however, that we are by no means limited to expanding the elastic constants in powers of p_1. Using the overlap integrals (IV.13), we can take any finite portion of the matrix $Q_{\beta,\alpha}$ of (IV.11) and find its eigenvalues and eigenvectors numerically.

E. CLAUSIUS-MOSSOTTI-TYPE APPROXIMATION FOR A THREE DIMENSIONAL MODEL

In this section we derive CMTA's for the effective elastic moduli of a 3D periodic composite, which is made of 3 perpendicular sets of parallel cylinders [29]. Each set consists of a periodic square array of parallel, circular, identical, non-overlapping cylinders of radius R with a lattice spacing b, i.e. each set has the same structure as one of the problems discussed in the previous section. However, now we have <u>three</u> such sets: one set of cylinders in parallel to the $X=x_1$ axis, another set is parallel to the $Y = x_2$ axis, and the third set is parallel to the $Z=x_3$ axis. In this array, which has a simple-cubic space symmetry the axes of the X-cylinders intersect the Y,Z plane at the square array points [0,kb,nb] where k and n are integers. Similarly, the Y-cylinder axes intersect the X,Z plane at the points [kb,0,(n+½)b], and the Z-cylinder axes intersect the X,Y plane at the points [(k+½)b,(n+½)b,0]. All the cylinders in all three sets have the same radius R which must satisfy

$$R < b/4 \tag{IV.38}$$

in order to ensure that the cylinders are non-overlapping (see Fig. IV.3).

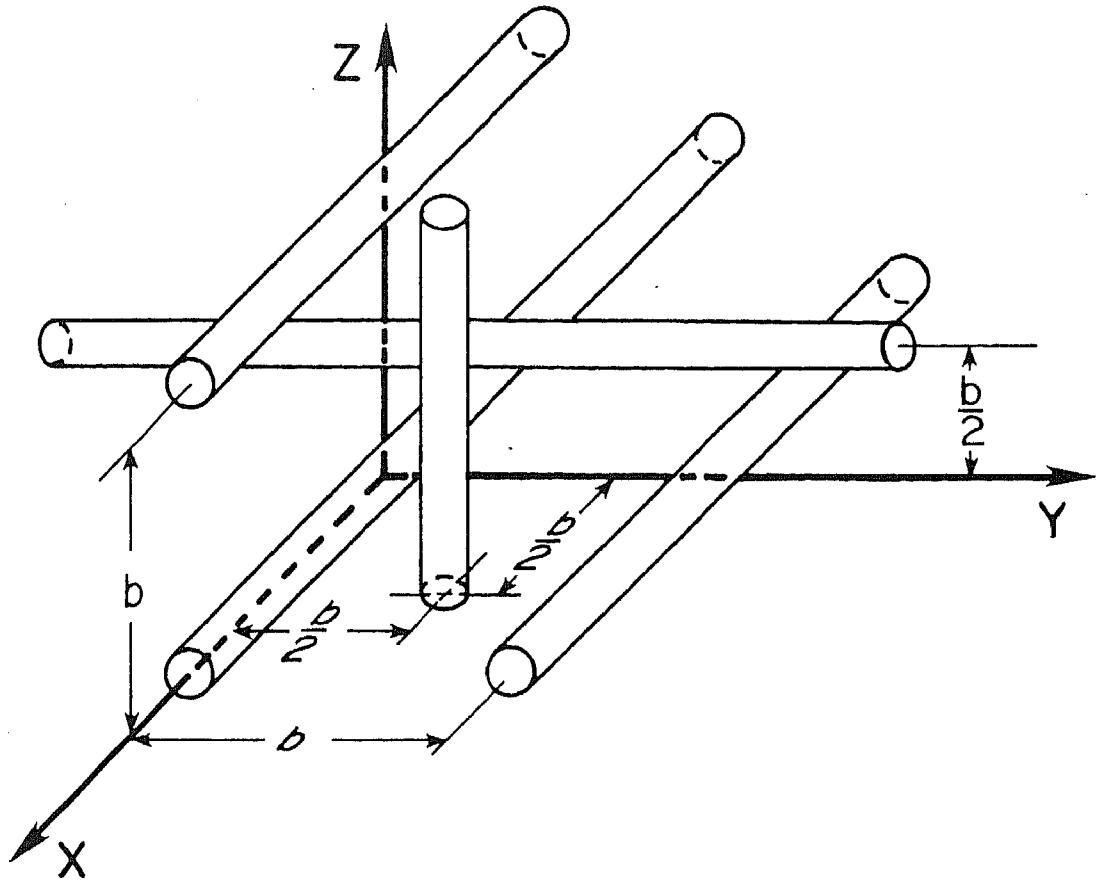

Fig. IV.3: Schematic drawing of some of the circular-cylindrical inclusions that form the cubic array. Depicted are three X-, one Y- and one Z-cylinder. The configuration avoids overlap so long as the radius of the cylinders R and the lattice constant b satisfy $R<\frac{1}{4}b$. The maximum filling fraction of the inclusions, attained when $R=\frac{1}{4}b$, is $3\pi/16 \simeq 0.59$.

Both $C^{(1)}$ of the cylinders and $C^{(2)}$ of the host medium, in which the entire structure is embedded, are assumed to be isotropic. Thus $C^{(1)}=(\kappa^{(1)},\mu^{(1)})$ and $C^{(2)}=(\kappa^{(2)},\mu^{(2)})$, where κ and μ now denote the three-dimensional bulk and shear moduli, respectively. The effective elastic properties of the composite will have cubic symmetry, and thus, they will be characterized by a bulk modulus $\kappa^{(e)}$ and two shear moduli $\mu^{(e)}$ and $m^{(e)}$.

The CMTA takes into account only the strongest (dipole-dipole) interactions in the secular equation (IV.11). Thus we are interested in the three-dimensional dipolar resonances of a single infinitely long isotropic cylinder embedded in an infinite isotropic medium. Generally speaking, the derivation of 3D eigenstates is analogous to the 2D problem (see Ch.III.D): Since the problem is invariant under rotations about the cylinder axis, i.e. some of the eigenstates may be degenerate, it is convenient to choose the eigenstates of $\hat{G}$ to be also eigenstates of the infinitesimal rotation generating operator $\hat{J}$. In order to solve for eigenstates, standard 3D elastostatic methods, which are adapted to cylindrical coordinates [76], are used. All components of the displacement vector of the resonance state will be sums of terms of the type $F_\ell(q\rho)e^{iqZ}e^{i\ell\phi}$, where ρ,ϕ and Z are the cylindrical coordinates, $F_\ell(q\rho)$ is a modified Bessel function (or its first derivative) of the first kind $I_\ell(q\rho)$ for $\rho<R$, or of the second kind $K_\ell(q\rho)$ for $\rho>R$ [77], $\ell=0,\pm1,\pm2,\ldots$, and $q=\frac{\pi n}{L}$ ($n=0,\pm1,\ldots$, and L is the length of the cylinder). The scalar product in (IV.10) between any $\tilde{\varepsilon}^{(0)}$ and an eigenstate with $q\neq0$ vanishes, because $\tilde{\varepsilon}^{(0)}$ does not depend on Z. Thus the important eigenstates for CMTA must be sought among the q=0 states. These eigenstates will have a power law dependence on ρ, which replaces the modified Besselfunctions $F_\ell(q\rho)$. We are interested only in the eigenstates which decrease slowly with the distance ρ from the cylinder axis. As in the 2D case (Ch.III.D) we expect these states to have a constant strain inside the cylinder (compare with the 2D compression dipole $\varepsilon^{(A0)}$ and shear dipoles $\varepsilon^{(\pm B2)}$ inside the cylinder). In the 2D case we had 3 dipolar states, because there are 3 linearly independent constant 2D strain tensors. Similarly, we expect to find 6 dipolar resonances in 3D, as this is the number of constant linearly independent strain tensors in 3D.

Actually, we already know some of the 3D resonances of the cylindrical inclusion: All the 2D resonances, which were found in Ch.III.D are also the 3D resonances of the system. Thus the 2D dipolar resonances are part of the set of 3D dipoles.

If a Z-cylinder is located at the origin, i.e., its axis intersects the X,Y plane at the origin of coordinates, then the 2D compression dipole $\varepsilon^{(AO)}$ (III.41) will have the following 3D form:

$$\varepsilon^{ZCT} = \begin{pmatrix} \varepsilon_{11} \\ \varepsilon_{22} \\ \varepsilon_{33} \\ \varepsilon_{12} \\ \varepsilon_{23} \\ \varepsilon_{13} \end{pmatrix} = \begin{cases} A_{CT} \begin{pmatrix} 1 \\ 1 \\ 0 \\ 0 \\ 0 \\ 0 \end{pmatrix} & , \text{ for } |w| \leq R \\ A_{CT}R^2 \begin{pmatrix} -\mathrm{Re} \\ \mathrm{Re} \\ 0 \\ \mathrm{Im} \\ 0 \\ 0 \end{pmatrix} \frac{1}{w^2} & , \text{ for } |w| > R \end{cases} \qquad \text{(IV.39a)}$$

$$A_{CT} \equiv \frac{1}{2R\sqrt{\pi(\delta\lambda + \delta\mu)L}} \quad , \qquad \text{(IV.39b)}$$

where λ and μ denote the Lamé constants, L is the length of the cylinder, and where we used the complex variable $w = X+iY$ to denote the coordinate in the directions perpendicular to the axis of the cylinder. The superscipt ZCT, which replaces the 2D notation AO, now indicates, that a) this is a Z-cylinder; b) this is a compression dipole; c) this is a transverse resonance, i.e. the compression is in the plane perpendicular to the cylinder axis. Note that $\delta\lambda+\delta\mu$, which appears in the normalization constant A_{CT}, is <u>not</u> $\delta\kappa$, as it may look, if we compare (IV.39) with (III.41), because the relation between κ, λ and μ depends on the dimensionality (see (II.25)): In order to translate the 2D case to a 3D case we first replace the 2D $\delta\kappa$ by its 2D expression $\delta\lambda + \delta\mu$ and <u>then</u> treat λ and μ as 3D constants (the Lamé constants of 2D plane strain problem coincide with the usual 3D

constants - see Ch.II.C). Thus the eigenvalue of the transverse compression dipole will be (see (III.20))

$$s_{CT} = -\frac{\delta\lambda + \delta\mu}{\lambda^{(2)}+2\mu^{(2)}} \tag{IV.40}$$

Note also that the 3D normalization requires the use of the cylinder length L in (IV.39), and that the displacements do not decrease to zero as we approach the boundary of the sample along the cylinder axis. However, in the limit of an infinite sample, in which the effective constant will be evaluated, the boundary corrections vanish.

Following the same lines of reasoning, we can convert the 2D shear dipoles $\varepsilon^{(\pm B2)}$ (III.43), into a 3D transverse (T) shear (S) dipoles

$$\varepsilon^{ZST\pm} = \begin{cases} A_{ST} \begin{Bmatrix} Re \\ Im \end{Bmatrix} \begin{pmatrix} 1 \\ -1 \\ 0 \\ i \\ 0 \\ 0 \end{pmatrix} & , \text{ for } |w| \leq R \\ A_{ST} \frac{\lambda^{(2)}+\mu^{(2)}}{\lambda^{(2)}+3\mu^{(2)}} R^2 \begin{Bmatrix} Re \\ Im \end{Bmatrix} \left[\frac{2\mu^{(2)}}{\lambda^{(2)}+\mu^{(2)}} \begin{pmatrix} 1 \\ 1 \\ 0 \\ 0 \\ 0 \\ 0 \end{pmatrix} \frac{1}{w^2} + \begin{pmatrix} 1 \\ -1 \\ 0 \\ i \\ 0 \\ 0 \end{pmatrix} \left(\frac{2w}{w^{*3}} - \frac{3R^2}{w^{*4}}\right)\right] & \\ \text{for } |w| > R \end{cases} , \tag{IV.41a}$$

$$A_{ST} \equiv \frac{1}{2R\sqrt{\pi\ \delta\mu\ L}} , \tag{IV.41b}$$

where the $\pm$ has the same meaning as in the 2D case and it corresponds to $\begin{Bmatrix} Re \\ Im \end{Bmatrix}$ on the r.h.s. of the equality. The corresponding eigenvalue will be (see (III.42)):

$$s_{ST} = - \frac{\delta\mu(\lambda^{(2)}+3\mu^{(2)})}{2\mu^{(2)}(\lambda^{(2)}+2\mu^{(2)})} \quad . \tag{IV.42}$$

This result terminates the list of 2D dipoles which can be directly translated into 3D.

A pair of additional dipole resonances can be easily found. These are longitudinal (L) shear (S) dipoles. The u_1 and u_2 components of the displacement vector $\vec{u}$ vanish in these states, while the u_3 component behaves like a potential of a 2D electrostatic dipolar resonance, i.e.

$$u_3^{ZSL\pm} = \begin{cases} A_{SL} \begin{Bmatrix} Re \\ Im \end{Bmatrix} w & , \text{ for } |w| \leq R \\ A_{SL} R^2 \begin{Bmatrix} Re \\ Im \end{Bmatrix} \frac{1}{w^*} & , \text{ for } |w| > R \end{cases} \tag{IV.43}$$

Thus the corresponding strain tensor is

$$\varepsilon^{ZSL\pm} = \begin{cases} A_{SL} \begin{Bmatrix} Re \\ Im \end{Bmatrix} \begin{pmatrix} 0 \\ 0 \\ 0 \\ 0 \\ i \\ 1 \end{pmatrix} & , \text{ for } |w| \leq R \\ A_{SL} R^2 \begin{Bmatrix} Re \\ Im \end{Bmatrix} \begin{pmatrix} 0 \\ 0 \\ 0 \\ 0 \\ i \\ -1 \end{pmatrix} \frac{1}{w^{*2}} & , \text{ for } |w| > R \end{cases} \tag{IV.44a}$$

$$A_{SL} \equiv \frac{1}{2R\sqrt{\pi\ \delta\mu\ L}} \quad , \tag{IV.44b}$$

while the eigenvalue of this resonance is

$$s_{SL} = - \frac{\delta\mu}{2\mu^{(2)}} \quad . \tag{IV.45}$$

The sixth dipolar resonance, which completes the list of dipole states, is somewhat special. We call it a longitudinal (L) compression (C) dipole and its strain tensor is

$$\varepsilon^{CL} = A_{CL} \begin{pmatrix} \delta\lambda \\ \delta\lambda \\ -2(\delta\lambda+\delta\mu) \\ 0 \\ 0 \\ 0 \end{pmatrix} \quad , \text{ for } |w| \gtrless R \tag{IV.46a}$$

$$A_{CL} \equiv \frac{1}{2R\sqrt{\pi\ \delta\mu\ (\delta\lambda+\delta\mu)(3\delta\lambda+2\delta\mu)L}} \quad , \tag{IV.46b}$$

and its eigenvalue is

$$s_{CL} = 0. \tag{IV.47}$$

This solution can be found, for instance, by looking for a constant strain tensor which is bi-orthogonol to the five dipolar resonances described earlier. It can also be found by a direct search for a resonance with a zero eigenvalue (the reasons why such a resonance must be present will be discussed later). The fact that ε^{CL} is constant over the entire system, and consequently does not decrease as one moves further away from the cylinder, causes no problems as far as interactions with other cylinders are concerned: Because the interaction between resonances on different cylinders (IV.7) is equal to an overlap integral multiplied by an eigenvalue, therefore the interaction between ε^{CL} and any other state always vanishes.

In order to clarify why an eigenstate with a vanishing eigenvalue must be present, we will calculate the 3D effective bulk modulus $\kappa^{(e)}$ of a large system in which one Z-cylinder is imbedded. As in the 2D case, we really evaluate only the corrections of order $p_1=v/V$ to the bulk modulus of the host medium. We shall use $\varepsilon^0=\varepsilon^{0K}$, i.e. isotropic compression of the boundaries. (Note that the system itself is not isotropic in 3D.) From

(III.21) and (III.22) we obtain

$$F(s) = \frac{1}{V}\left[\frac{(<\tilde{\varepsilon}^{0K}|\varepsilon^{ZCT}>)^2}{s - s_{CT}} + \frac{(<\tilde{\varepsilon}^{0K}|\varepsilon^{ZCL}>)^2}{s - s_{CL}}\right] =$$

$$= \frac{1}{V}\left[\frac{\frac{\pi R^2 L \delta\kappa^2}{\delta\lambda + \delta\mu}}{s + \frac{\delta\lambda + \delta\mu}{\lambda^{(2)}+2\mu^{(2)}}} + \frac{\frac{\pi R^2 L \delta\mu\delta\kappa}{3(\delta\lambda+\delta\mu)}}{s}\right] =$$

$$= \frac{\frac{p_1\delta\kappa^2}{\delta\lambda+\delta\mu}}{s + \frac{\delta\lambda + \delta\mu}{\lambda^{(2)}+2\mu^{(2)}}} + \frac{\frac{p_1\delta\mu\delta\kappa}{3(\delta\lambda+\delta\mu)}}{s}, \qquad \text{(IV.48)}$$

where $p_1 = \pi R^2 L/V$. (Note that this expression satisfies the M_0 and M_1 sum rules (III.52) and (III.68), respectively, correctly to order p_1.) The effective bulk modulus $\kappa^{(e)}$ can be obtained by substituting s=1 in (IV.48). The presence of the pole at s=0 in the second term of (IV.48) now can be understood as follows: Let us assume that $\delta\kappa > 0$ and $\delta\mu > 0$. Then, for $s \to 0^+$, $C^{(1)}$, defined by (III.4) will represent an infinitely rigid inclusion, i.e. $\kappa^{(1)}, \to +\infty$ and $\mu^{(1)}, \to +\infty$. Since ε^{0K} represents isotropic compression of the boundaries (including the compression in the Z-direction) and the cylinder spans the sample, i.e., it is not confined to a finite volume, but is continuous from one boundary to the other, we must obtain $\kappa^{(e)} \to +\infty$. Thus F(s) must have a pole at s=0. This argument is not limited to a specific microgeometry: Whenever the $C^{(1)}$ material spans the entire sample, elastostatic resonances with eigenvalues $s_\alpha = 0$ must be present.

If we consider an X- or a Y-cylinder then its dipolar resonances are obtained from the Z-resonances by a simple rotation of the reference frame.

In order to obtain the CMTA's for the effective elastic moduli of the 3D system of cylinders under consideration, we must evaluate the lattice sums $Q_{\beta,\alpha}$ of (IV.12) for all the dipolar resonances which were described above. Since we are dealing with long-range (dipole-dipole) interactions,

these summations must be performed following the "prescriptions" of Sec. C. Some details of the calculations are given in App.C. The resulting lattice sums $Q_{XCL,XCL'}$ $Q_{ZST+,YSL-}$, etc., form a symmetric matrix, half of which is presented in Fig. IV.4. The large number of vanishing elements in this matrix allows it to be diagonalized rather easily. Moreover, we actually do not need to diagonalize the entire matrix all at once. For any specific choice of ε^0 we only need that part of $Q_{\beta,\alpha}$ which contains (a) eigenstates which have non-zero scalar products with $\tilde{\varepsilon}^0$ and (b) eigenstates which are degenerate with them. We shall derive expressions which are accurate up to and including order p_1^2, and we will include in our calculations only those eigenstates of type (b) which lead to non-vanishing matrix elements $Q_{\beta,\alpha}$ with eigenstates of type (a) (all the other eigenstates of type (b) do not affect the solution to order p_1^2).

Choosing $\varepsilon^0 = \varepsilon^{0\kappa}$ we will obtain an expression for $\kappa^{(e)}$. There are six dipolar resonances, namely all CT and CL resonances, which have non-zero scalar products with $\tilde{\varepsilon}^{0\kappa}$. Thus we only need a 6 x 6 part of the $Q_{\beta,\alpha}$ matrix. Moreover, only a 3 x 3 part of that matrix, which corresponds to the ε^{XCT}, ε^{YCT} and ε^{ZCT} eigenstates, does not vanish. The entire problem thus reduces to a diagonalization of that 3 x 3 matrix. The result has a similar form to that of a single cylinder (see (IV.48)) except that one of the poles is shifted

$$\kappa^{(e)} = \kappa^{(2)} + \frac{p_1 \delta\kappa\delta\mu}{3(\delta\lambda+\delta\mu)} + \frac{p_1 \delta\kappa^2(\delta\lambda+\delta\mu)}{1 + \frac{(1-p_1)(\delta\lambda+\delta\mu)}{\lambda^{(2)}+2\mu^{(2)}}} \quad . \tag{IV.49}$$

This expression satisfies the zero and first moment sum rules (III.52) and (III.68) exactly.

Choosing $\varepsilon^0 = \varepsilon^{0\mu}$ we can obtain one of the effective shear moduli, namely $\mu^{(e)}$. Only 3 dipolar resonances, namely ε^{ZST-}, ε^{YSL-} and ε^{XSL+}, have non-zero scalar products with $\tilde{\varepsilon}^{0\mu}$. There are 11 additional eigenstates which are degenerate with some of those 3 eigenstates. However, their matrix elements $Q_{\beta,\alpha}$ with either ε^{ZST-} or ε^{YSL-} or ε^{XSL+} vanish, and

XCL	YCL	ZCL	XCT	YCT	ZCT	XST+	YST+	ZST+	XST-	YST-	ZST-	XSL+	YSL+	ZSL+	XSL-	YSL-	ZSL-	
0	0	0	0	0	0	0	0	0	0	0	0	0	0	0	0	0	0	XCL
	0	0	0	0	0	0	0	0	0	0	0	0	0	0	0	0	0	YCL
		0	0	0	0	0	0	0	0	0	0	0	0	0	0	0	0	ZCL
			A	A	A	0	B	-B	0	0	0	0	0	0	0	0	0	XCT
				A	A	-B	0	B	0	0	0	0	0	0	0	0	0	YCT
					A	B	-B	0	0	0	0	0	0	0	0	0	0	ZCT
						C	D	D	0	0	0	0	0	0	0	0	0	XST+
							C	D	0	0	0	0	0	0	0	0	0	YST+
								C	0	0	0	0	0	0	0	0	0	ZST+
									E	0	0	0	2F	0	0	0	2F	XST-
										E	0	0	0	2F	2F	0	0	YST-
											E	2F	0	0	0	2F	0	ZST-
												F	0	0	0	0	0	XSL+
													F	0	0	0	0	YSL+
														F	0	0	0	ZSL+
															F	0	0	XSL-
																F	0	YSL-
																	F	ZSL-

$$A \equiv -\frac{1}{3} s_{CT} p_1$$

$$B \equiv \frac{p_1 \sqrt{\delta\mu(\delta\lambda+\delta\mu)}}{3(\lambda^{(2)}+2\mu^{(2)})}$$

$$\{\frac{E}{C}\} \equiv -s_{ST}\left[\frac{1}{3}p_1 \pm \frac{\lambda^{(2)}+\mu^{(2)}}{\lambda^{(2)}+3\mu^{(2)}}[1.92(\frac{1}{3}p_1)^2 - 1.60(\frac{1}{3}p_1)]\right]$$

$$D \equiv s_{ST}\frac{2\mu^{(2)}p_1}{3(\lambda^{(2)}+3\mu^{(2)})}$$

$$F \equiv \frac{1}{3} s_{SL} p_1$$

Fig. IV.4 Half of the (symmetric) matrix $Q_{\beta,\alpha}$ of the lattice sums of dipole-dipole interactions. The upper line and the right column of the matrix denote the dipolar states α and β in $Q_{\beta,\alpha}$.

therefore it can be shown that they do not affect the result to order p_1^2. The final result, which we obtain by solving the secular equation (IV.11) using standard perturbations methods [64], is

$$\mu^{(e)} = \mu^{(2)} + p_1\delta\mu\left\{\frac{\mu^{(2)} + \frac{8}{3}p_1(\lambda^{(2)}+2\mu^{(2)})}{3\mu^{(2)} + \frac{(3-p_1)\delta\mu}{2(\lambda^{(2)}+2\mu^{(2)})} + \frac{0.80\ p_1\delta\mu(\lambda^{(2)}+\mu^{(2)})}{\lambda^{(2)}+2\mu^{(2)}}} + \right.$$

$$\left. + \frac{2\mu^{(2)} + \frac{8}{3}p_1(\lambda^{(2)}+2\mu^{(2)})}{3\mu^{(2)} + \frac{1}{2}(3-p_1)\delta\mu}\right\}, \qquad \text{(IV.50)}$$

where we kept only the terms which affect the result up to order p_1^2.

Finally, if we choose $\varepsilon^0=\varepsilon^{0m}$, we obtain an expression for an additonal shear modulus $m^{(e)}$. This time 7 dipolar resonances, namely ε^{XCL}, ε^{YCL}, ε^{XST+}, ε^{YST+}, ε^{ZST+}, ε^{XCT} and ε^{YCT}, are important, i.e. have non-zero scalar products with $\tilde{\varepsilon}^{0m}$. The resonance ε^{ZCT} must also be included in the calculation since it has non-vanishing matrix elements with ε^{XCT} and ε^{YCT}, and has the same eigenvalue as those states. Because of this degeneracy, the state ε^{ZCT} contributes to $m^{(e)}$ corrections of order p_1^2. Other resonances, which are degenerate with the resonances listed above, do not contribute in that order because their interactions with the "important" resonances vanish. Thus the solution of the secular equation (IV.11) requires diagonalization of an 8 x 8 matrix. Part of this matrix, which includes ε^{XCL} and ε^{YCL}, is trivial (vanishes), thus we really only have to diagonalize a 6 x 6 matrix which includes two groups of degenerate states. By applying standard perturbation methods [64] we arrive at the following result:

$$m^{(e)} = \mu^{(2)} + \frac{1}{2}\frac{\delta\mu\delta\kappa}{\delta\lambda+\delta\mu} +$$

$$+ \frac{\frac{1}{2}p_1\delta\mu\left(1 + \frac{\frac{4}{3}p_1\mu^{(2)}\delta\mu}{2\mu^{(2)}\delta\lambda - (\mu^{(2)}+\lambda^{(2)})\delta\mu}\right)}{1 + \frac{\delta\mu[(3-p_1)(\lambda^{(2)}+3\mu^{(2)}) - 1.60\,p_1(\lambda^{(2)}+\mu^{(2)})]}{6\mu^{(2)}(\lambda^{(2)}+2\lambda^{(2)})}} - \frac{p_1\delta\mu}{3(\lambda^{(2)}+2\mu^{(2)})}$$

$$+ \frac{\frac{1}{6}p_1\frac{\delta\mu^2}{\delta\lambda+\delta\mu}\left(1 - \frac{4p_1(\delta\lambda+\delta\mu)}{2\mu^{(2)}\delta\lambda - (\mu^{(2)}+\lambda^{(2)})\delta\mu}\right)}{1 + \frac{\delta\lambda+\delta\mu}{\lambda^{(2)}+2\mu^{(2)}}} \quad , \tag{IV.51}$$

in which we kept only the terms that contribute to $m^{(e)}$ up to and including order p_1^2. This expression was derived assuming that there is no accidental degeneracy between ST and CT states (i.e C≠A in Fig. IV.4). When such an accidental degeneracy appears, the perturbation expansion used above must be modified appropriately.

The average shear modulus, μ_{av} (see (III.73)), i.e., a linear combination of (IV.50) and (IV.51), satisfies the zero and first moment sum rules (III.52) and (III.69) exactly, in spite of the fact that these are only approximate expressions for $m^{(e)}$ and $\mu^{(e)}$. In the case of such complicated expressions, as (IV.49)-(IV.51), sum rules provide us with a useful independent check that no algebraic mistake was made in the derivation of the effective elastic constants.

We are not aware of any numerical solution of the model, which was considered in this section, and it is therefore not easy to estimate the accuracy of our perturbative solution. By analogy, with the results of the previous section, we believe that the CMTA's (IV.49)-(IV.51) are quite accurate up to rather high values of p_1. In order to improve upon our results we must solve for <u>all</u> eigenstates of the cylinders and evaluate the

overlap integrals, which include 3D integrations over functions of the type $F_\ell(q\rho)e^{iqZ}e^{i\ell\phi}$, which were mentioned at the beginning of this section. We shall not evaluate these corrections. However, we would like to make a few remarks regarding the possible order of these corrections. All the other, i.e. non-dipolar, resonances with q=0 decrease with distance ρ from the cylinder axis faster than $1/\rho^2$. Thus, as in the 2D case of Sec.D, they could lead to corrections of order p_1^3. However, due to the symmetry of the problem, we believe that the corrections will in fact start at some higher order. The $q\neq 0$ states form a (quasi) continuous band of eigenstates, which, one might think, would invalidate our approach. However, since $Q_{\beta,\alpha}$ includes summation over inclusions which are equally spaced at the lattice spacing b, the matrix element will include integrals of the form $\sum_j \int f(\rho,\phi)e^{iq(Z-jb)}dV$, which vanish unless $q=\frac{2\pi}{b}n$ $(n = 0,\pm1,\pm2,\ldots)$. Thus we are left only with a discrete set of q's that are able to interact. (The fact that the eigenstates of this set themselves have vanishing matrix elements with any eigenstate with $q\neq\frac{2\pi}{b}n$ can be proven in the same way.) All $q\neq 0$ eigenstates decrease exponentially with distance from the cylinder axis because they are described by modified Bessel functions of the second kind. However, the interaction between a dipolar resonance on one cylinder and $F_\ell(q\rho)e^{iqZ}e^{i\ell\phi}$ state on a neighbouring cylinder will depend mainly on the normalization constant of the latter state: Since $q=\frac{2\pi}{b}n$, the argument of the function F_ℓ will be of order of unity for small n. In an electrostatic problem with the same microgeometry [78] we found that the corrections are $O(p_1^3)$. However, as we mentioned before, further work must be done in order to estimate the corrections to CMTA's.

F. DISCUSSION

In this chapter we applied our general approach to several multi-grain systems with well defined microgeometries. We succeeded in deriving various approximations to the effective elastic moduli of those composites which are correct, in most cases, up to a high order in p_1. We used single grain resonances to construct resonances of the entire system. Somewhat analogously, the T-matrix approach [22] uses t-matrices of single grains to

construct the total T-matrix. It is in going from the individual inclusion to the array of inclusions that we use a procedure that is entirely different from that used in the T-matrix approach. Our formalism uses only two-grain interactions (and their sums $Q_{\beta,\alpha}$), while the T-matrix approach expands the total scattering amplitude in a series whose successive terms describe multiple scattering by a successively larger number of grains. In a certain sense, our approach divides the interactions according to their strength, but in each order the calculations are exact, i.e., all multiple scatterings are taken into account. Our method takes full advantage of the symmetry of the grain and the symmetry of the composite. Those symmetries are responsible for the appearance of the numerous vanishing terms in the $Q_{\beta,\alpha}$ matrices. Thus $\kappa^{(e)}$ of a hexagonal array of parallel cylinders could be found up to order p_1^{11} in our approach merely by diagonalizing a single 2 x 2 matrix. In order to achieve the same order of accuracy using the T-matrix approach, we would have to evaluate 11 terms in the multiple-scattering series!

For non-periodic (e.g. random) systems the original secular equation (IV.6) must be used instead of the simplified equation (IV.11). Even for such systems our formalism is quite convenient. E.g., we can claim, without performing any further calculations, that the CMTA (IV.27) for $\kappa^{(e)}$ is correct at least up to and including order p_1^2 for any "well stirred" system of parallel, identical, non-overlapping circular-cylinder inclusions. (By the term "well stirred" we mean a system in which the (random) locations of the grains are completely independent, except for the restriction that they must be non-overlapping. In such a system, p_1 is the <u>only</u> relevant parameter.) The subspace of the secular equation (IV.6), which includes the compression dipole interactions of different grains, will be diagonal because those interactions always vanish (see (IV.13b)). The interactions between any compression dipole and a shear dipole will be of order p_1 (see (IV.13g)). Thus the problem can be solved by a perturbation series. If we keep only the terms that affect the solution up to and including order p_1^2, we must actually treat that part of the secular equation which contains only the compression dipoles. The solution will therefore coincide with $\kappa^{(e)}$ for the periodic (square or hexagonal) arrays of cylinders.

A quasi-random distribution of cylinders can also be handled effectively, as it was done in the electrostatic problem [79], by a following procedure: N inclusions are placed at random positions, but without overlapping, in a cell, which is then repeated infinitely many times in all directions. This problem can be solved numerically to any desired accuracy for eigenvalues and eigenstates, using overlap integrals between the pairs of inclusions which are evaluated analytically (e.g., (IV.13)). A set of weights F_α and poles s_α (see (III.21)) is thus obtained for one particular choice of the locations of the inclusions. In an infinite random system, or in ensemble average of the quasi-random system, we expect to obtain a continuous ditribution of poles, i.e. (III.21) will have the form

$$F(s) = \int \frac{f(x)}{s-x}\, dx \quad . \tag{IV.52}$$

If we repeat the numerical calculation of F_α and s_α, described above, for several random choices of the locations of the inclusions in the unit cell, then we can superimpose the different pole spectra to obtain an approximation for the continuous function f(x) in the form of a histogram. This method was shown to be very effective in the electrostatic case [79] even when the repeated unit cell is small and a quite small number of different random configurations is chosen (in the electrostatic case each cell contained only 4 inclusions and 60 different configurations were solved).

CHAPTER V. EXTENSION OF THE THEORY AND DERIVATION OF BOUNDS

A. INTRODUCTION

In principle, exact values for the effective elastic constants can be obtained only when the microgeometry of the composite is known precisely. In many cases, however, the precise microgeometry is not known, e.g. when the composite has a certain randomness in its microstructure. In that case, exact theories are limited to the derivation of rigorous bounds on the effective elastic constants.

The simplest bounds on the effective elastic constants were obtained by Hill [15], who proved that the Voigt [16] and Reuss [17] estimates of the effective elastic constants are actually upper and lower bounds, respectively, on those constants. The proof of these bounds by Hill is based on some classical variational principles, and the bounds themselves are equal to the volume averages of compliance and stiffness tensors, i.e. $\langle S \rangle_{av}^{-1} \leqslant C^{(e)} \leqslant \langle C \rangle_{av}$, and therefore only the volume fractions (≡ one point correlation functions) of the components need to be known.

More detailed geometrical information, i.e. a knowledge of higher order correlation functions, allows the derivation of improved (more stringent) bounds. Hashin and Shtrikman [80] discovered some new variational principles which led to tighter bounds on the effective elastic moduli [18,80,81]. These bounds were also derived using different methods by Hill [13,82] and Walpole [83] (Walpole's treatment removed the restriction $C^{(1)} - C^{(2)} \geqslant 0$ on the stiffness tensors of the components which appeared in the original analysis of Hashin and Shtrikman). Although Hashin-Shtrikman-type bounds generally require the knowledge of the two-point correlation function [40], in the case of isotropic composites a knowledge of the volume fractions suffices. Beran and Molyneux [84] and McCoy [85] incorporated three-point correlation function in the derivation of still tighter bounds. Recently, some of these bounds were modified and improved [86]. Variational principles have sometimes also been used for the deri-

vation of various bounds in the context of a scattering-theory-like approach [22,87].

In this chapter we use the spectral representation (III.21) to derive various bounds on the effective elastic moduli [28]. We use the methods which were developed and applied by Bergman [88] for the derivation of bounds on the effective dielectric constants of composites. The main differences between the elastostatic problem and the electrostatic problem arise from the tensorial nature of the elastic moduli, which can never be ignored. By contrast, the dielectric constants could be treated as scalars, at least in the case of isotropic components [46].

In Sec.B we use our formalism to derive some of the simple known bounds, and we also extend the validity of the Hashin-Shtrikman bounds to include composites with an arbitrary (i.e., not necessarily isotropic or cubic) microgeometry. A more general and more flexible formalism is introduced in Sec.C. This is applied in Secs.D and E to derive improved bounds that require information of a new type about the composites. This information is in the form of known values of the effective elastic constants for a composite with the same microgeometry but different constituents. Such information can be obtained either by measurement or by another calculation. It is clearly information of a "physical" nature about the composite, as opposed to the purely geometrical information that is contained in the correlation functions which are also sometimes used to obtain improved bounds.

B. SIMPLE BOUNDS ON THE EFFECTIVE ELASTIC MODULI

In this section we will derive some simple bounds on the effective elastic moduli of a two-component composite [28]. Even in the case of the known bounds (Voigt and Hashin-Shtrikman-type bounds) this is not just another alternative derivation, since we extend the range of validity of the Hashin-Shtrikman bounds to composites made of isotropic components but with an arbitrary microgeometry. We also show how our method can be extended simply to a derivation of higher order bounds.

Whenever the microgeometry of a composite is not known precisely we cannot, in general, calculate the locations of the poles s_α and their weights F_α in (III.21). Nevertheless, if we treat F_α and s_α as unknown free parameters, we can find rigorous upper and lower bounds on the effective elastic moduli. Both F_α and s_α are not completely free: they must satisfy inequalities (III.29), (III.31) and equalities which arise from the sum rules (III.50).

One way to obtain bounds on F(1) is by a direct variation of the free parameters F_α and s_α in (III.21), subject to the constraints which were mentioned above. However, there is a much more convenient procedure for obtaining these bounds, which will be described below.

A knowledge of the volume fraction p_1 of the $C^{(1)}$ material, and thus a knowledge of the zero order sum rule M_0 (see (III.51)), is sufficient for the derivation of a simple bound on $C^{(e)}$ as follows: From the inequality (III.29) and the fact that the poles s_α satisfy $s_\alpha < 1$, it follows that

$$F(1) = \sum_\alpha F_\alpha \left(1 + \frac{s_\alpha}{1-s_\alpha}\right) \leqslant \sum_\alpha F_\alpha = M_0 \ . \tag{V.1}$$

In the usual notation we thus get

$$\varepsilon^0 C^{(e)} \varepsilon^0 \leqslant \varepsilon^0 C^{(e)} \varepsilon^0 + p_1 \varepsilon^0 \delta C \varepsilon^0 = \varepsilon^0 \langle C \rangle_{av} \varepsilon^0 \tag{V.2}$$

which is the well known Voigt bound [15].

The Reuss bound [15], which is complementary to Voigt's bound, is derived in App.D. The derivation requires a parametrization of the local elastic compliance tensor with the variable s, as was done for the elastic stiffness tensor in (III.1). This requires the knowledge of a different sum rule, which can be obtained by using the generalized formalism which will be presented in the following sections.

The knowledge of higher order moments M_n ($n \geqslant 1$) would enable us to derive more restrictive bounds. Once M_1 (see (III.53)-(III.57)) is known,

we can use it as an additional constraint on F_α and s_α. The improved bounds which arise from the additional constraint can be found without any variational calculation by examining the function

$$D(s) \equiv \frac{1}{M_0} - \frac{1}{sF(s)} \quad , \tag{V.3}$$

which has a structure similar to that of F(s) and can also be written as a sum of simple poles

$$D(s) = \sum_\alpha \frac{D_\alpha}{s-d_\alpha} \quad . \tag{V.4}$$

The poles d_α are the zeros of F(s), and there is also a pole at s=0, unless F(s) has a pole at that point. The zero moment sum rule for F(s) has been incorporated in the definition of D(s) and is responsible for the fact that $D \to 0$ as $s \to \infty$, as can be seen by expanding (V.3) in powers of 1/s:

$$D(s) = \frac{1}{M_0} - \frac{1}{s(\frac{M_0}{s} + \frac{M_1}{s^2} + \ldots)} = \frac{M_1}{sM_0^2} + \ldots , \tag{V.5}$$

where (III.49) and (III.50) were used. The first moment sum rule of F(s) now determines the zero moment sum rule of D(s) since, by expanding (V.4) in powers of 1/s and comparing the result with (V.5), we obtain

$$\sum_\alpha D_\alpha = \frac{M_1}{M_0^2} \quad . \tag{V.6}$$

Similarly, higher order moments of D(s) can be related to higher moments of F(s). It can easily be shown that all residues D_α in (V.4) are negative

$$\frac{1}{D_\alpha} = -\frac{d}{ds}[sF(s)]\Big|_{s=d_\alpha} = \sum_\beta \frac{F_\beta s_\beta}{(d_\alpha - s_\beta)^2} < 0 \quad , \tag{V.7}$$

where we used the inequality (III.29). The poles d_α of D(s) are subject to the same restrictions as the poles of F(s) (see (III.31)).

The bounds on D(1) can now easily be found. For $\delta C \geqslant 0$, all $d_\alpha \leqslant 0$, and we obtain

$$D(1) = \sum_{\alpha} \frac{D_\alpha}{1-d_\alpha} \geqslant \sum_{\alpha} D_\alpha = \frac{M_1}{M_0^2} \tag{V.8}$$

or, returning to the function F,

$$F(1) \geqslant \frac{M_0^2}{M_0 - M_1} . \tag{V.9}$$

If we interchange the roles of $C^{(1)}$ and $C^{(2)}$, and thus define a different pair of functions F'(s) and D'(s) and different moments M'_0 and M'_1, we can repeat the entire procedure. However, now $\delta C \leqslant 0$, i.e. $0 \leqslant d_\alpha < 1$, and the inequalities corresponding to (V.8) and (V.9) are reversed. Thus we obtain

$$F'(1) \leqslant \frac{M_0'^2}{M_1' - M_0'} . \tag{V.10}$$

In order to translate these inequalities into explicit lower and upper bounds for $C^{(e)}$ we must be able to evaluate M_1 explicitly. In Ch.III.E we have shown that for $\varepsilon^0 = \varepsilon^{0\kappa}$, the first moment sum rule is given by (III.68) for an arbitrary mixture of isotropic components. Thus for such a choice of ε^0 we obtain from (III.52), (III.68), (V.9) and (V.10) the following bounds on the effective bulk modulus:

$$\frac{p_1}{1 + (1-p_1)(\kappa^{(1)}-\kappa^{(2)})/(\kappa^{(2)}+2\frac{d-1}{d}\mu^{(2)})} \leqslant \frac{\kappa^{(e)} - \kappa^{(2)}}{\kappa^{(1)} - \kappa^{(2)}} \leqslant$$

$$= \tag{V.11}$$

$$\leqslant \frac{p_1}{1 - (1-p_1)(\kappa^{(1)}-\kappa^{(2)})/(\kappa^{(1)}+2\frac{d-1}{d}\mu^{(1)})} ,$$

where d is the dimensionality of the system. In the case of isotropic microgeometry these are the well-known Hashin-Shtrikman bounds [13,18,80,81], the validity of which was extended in the past also to the cases of cubic [13] and elipsoidal [89] symmetries. However, by our method of derivation, it is clear that they really apply irrespective of the symmetry of the microgeometry! As far as we know this fact has not been recognized before [90].

For a different choice of ε^0, namely $\varepsilon^0 = \varepsilon^{0\mu}$, the first moment sum rule

is given by (III.69) for an isotropic mixture of isotropic components. Thus for this choice of ε^0 we obtain from (III.52), (III.69), (V.9) and (V.10) the following bounds on the effective shear modulus of an isotropic mixture of isotropic components:

$$\frac{p_1}{1 + 2(1-p_1)(\mu^{(1)}-\mu^{(2)})(\kappa^{(2)}+2\mu^{(2)})/[(d+2)\mu^{(2)}(\kappa^{(2)}+2\frac{d-1}{d}\mu^{(2)})]} \leqslant \frac{\mu^{(e)} - \mu^{(2)}}{\mu^{(1)} - \mu^{(2)}} \leqslant$$

$$\leqslant \frac{p_1}{1 + 2(1-p_1)(\mu^{(1)}-\mu^{(2)})(\kappa^{(1)}+2\mu^{(1)})/[(d+2)\mu^{(1)}(\kappa^{(1)}+2\frac{d-1}{d}\mu^{(1)})]} , \qquad (V.12)$$

which are the usual Hashin-Shtrikman bounds [13,18,80,81]. However, by an appropriate redefinition of $\mu^{(e)}$ the validity of these bounds can also be extended to arbitrary microgeometries. In Ch.III.E we have shown that the expression (III.69) for the first moment sum rule remains valid for an arbitrary microgeometry if we replace $\mu^{(e)}$ by μ_{av} defined by(III.73). Thus the bounds (V.12) are also valid for arbitrary microgeometries if we replace $\mu^{(e)}$ in (V.12) by μ_{av}!

The bounds (V.11) and (V.12), which are valid for arbitrary dimensionality d, were originally discovered and derived for 3D isotropic mixtures [13,18] and later for 2D istotropic mixtures [81]. The Hashin-Shtrikman bounds are valid only in the case of (positive or negative) semidefinite δC. (Note that D_α is negative for both positive and negative d_α, i.e. the inequality analogous to (III.29) is not valid for the poles and residues of D(s). Thus in the case of non-definite δC we cannot perform a calculation similar to (V.8).) When this is not the case, then the less stringent Walpole bounds [83] can be derived by a modification of the above formalism. However, these bounds are more easily obtained from a more general formalism, which will be presented in the next sections.

Finally, we would like to mention that when higher order moments M_n ($n \geqslant 2$) are known, the entire procedure can be repeated. We can define a new function of s, which is obtained from D(s) in the same way that D(s) was obtained from F(s) in (V.3), and which thus has the same pole structure.

The bounds arising from that function, incorporating the additional information, will naturally be more stringent than the Hashin-Shtrikman bounds.

C. EXTENSION OF THE THEORY

In this section we generalize the functional dependence (III.3) of $C(\vec{r};s)$ on the argument s [28], and analyze the analytic properties of the spectral representation of F(s) (locations of the poles and signs of their weights) and also obtain the moment sum rules. A simple implementation [28] of the extended formalism for the derivation of Walpole bounds is explained at the end of this section, while a somewhat modified formalism is used in App.D to derive the Reuss bound. An application of the formalism to the derivation of improved bounds will be presented in the following sections.

In order to improve the Hashin-Shtrikman-type bounds it is usually necessary to have more detailed information on the microstructure of the composite. On way to obtain such information is through a knowledge of the corresponding effective elastic constant of another composite, which is made of different components but has the same or a sufficiently similar microgeometry (e.g., both composites are produced by the same technological process). If an elastic constant of both composites is represented by the same function F(s), taken at different values of the argument s, say s=1 and $s=s_+$, then a knowledge of the effective elastic constant of the s_+ material can be expressed in the form

$$F(s_+) = \sum_\alpha \frac{F_\alpha}{s_+ - s_\alpha} \qquad \text{(V.13)}$$

which becomes an additional constraint in the derivation of bounds on F(1).

However, the form (III.3) is not flexible enough for such treatment. The argument s does not affect the $C^{(2)}$ tensor and restricts the values of the $C^{(1)}$, tensor to lie on a straight line in the space of elastic constants (see (III.4)). We shall, therefore, replace (III.3) by a more general form. We shall also extend the formalism to handle composites made

of more than two components.

We will represent the microgeometry of a multi-component composite by a set of step functions $\{\theta_n\}$, where θ_n defines the microgeometry of the n-th component as in (III.2). Sometimes we will find it convenient to split the elastic stiffness tensor of the n-th component $C^{(n)}$ into a sum of several symmetric positive definite tensors

$$C^{(n)} = \sum_{\gamma} C^{(n\gamma)} \quad , \tag{V.14}$$

as we did in the isotropic case in (II.33) and in the cubic case in (II.31), where γ took the values κ, μ, m. We again define a new stiffness tensor, that depends on the continuous parameter s:

$$C(\vec{r};s) = C^{(o)} + \sum_{n\gamma} v_{n\gamma}\theta_n(\vec{r})(C^{(n\gamma)} - C^{(o\gamma)}) \equiv C^{(o)} + \sum_{n\gamma} v_{n\gamma}\theta_n \delta C^{(n\gamma)} \quad , \tag{V.15}$$

$$v_{n\gamma} \equiv 1/[(s-1)/b_{n\gamma} + 1], \tag{V.16}$$

where $C^{(o)}$ is an arbitrary (symmetric positive definite) tensor, and $b_{n\gamma}$ are constants. For s=1, also $v_{n\gamma}=1$ and this expression reduces to the actual $C(\vec{r})$. However, when s varies, the stiffness tensor in each component moves along a line in the space of elastic constants which, in general, will not be straight. The effective elastic constants now have an analytic structure as functions of s which is similar to (III.21), namely

$$F(s) \equiv \varepsilon^o(C^{(e)} - C^{(o)})\varepsilon^o = \sum_{\alpha} \frac{F_\alpha}{s-s_\alpha} \tag{V.17}$$

However, as things stand now, both s_α and F_α will, in general, be complex numbers. In order to facilitate their manipulation we, therefore, restrict the choice of $C^{(o)}$ so that <u>all</u> $\delta C^{(n\gamma)} \geqslant 0$ (or <u>all</u> $\delta C^{(n\gamma)} \leqslant 0$) and we restrict the constants $b_{n\gamma}$ to be real numbers satisfying $b_{n\gamma} \geqslant 1$ ($0 < b_{n\gamma} \leqslant 1$). We shall prove that under these restrictions, all F_α and s_α are real numbers and that they are confined to certain intervals.

We start from the observation that $v_{n\gamma}$ in (V.15) plays a similar role

to that of 1/s in (III.3). Thus the entire proof will follow closely the investigation of the properties of F(s) in Ch.III.C. Let $s=s_\alpha$ be a pole of F(s). For that value of s, there exists a resonance solution $\varepsilon^{(\alpha)}$ which satisfies a differential equation analogous to (III.23), from which we can show exactly in the same way as it was done in Ch.III.C, that the following integral, which is a generalization of (III.25a), must vanish

$$\int \varepsilon^{(\alpha)*} (C^{(o)} + \sum_{n\gamma} v_{n\gamma}(s_\alpha)\ \theta_n \delta C^{(n\gamma)}) \varepsilon^{(\alpha)} dV = 0 \quad . \tag{V.18}$$

If we restrict ourselves to case of positive $b_{n\gamma}$ in (V.16) and <u>all</u> $\delta C^{(n\gamma)} \geqslant 0$ (or <u>all</u> $\delta C^{(n\gamma)} \leqslant 0$) then by considering the imaginary part of (V.18)

$$\sum_{n\gamma} \frac{|v_{n\gamma}(s_\alpha)|^2 \operatorname{Im} s_\alpha}{b_{n\gamma}} \int \theta_n \varepsilon^{(\alpha)*} \delta C^{(n\gamma)} \varepsilon^{(\alpha)} dV = 0 \quad , \tag{V.19}$$

we arrive at the conclusion that $\operatorname{Im} s_\alpha = 0$. Note that the essential point in this proof was <u>not</u> the <u>specific</u> choice of $v_{n\gamma}$ in (V.16) but rather the fact that for complex s the imaginary parts of <u>all</u> $v_{n\gamma}$ had the same sign. Clearly, there are additional possible choices of $v_{n\gamma}$ which have the same property. We have tried several additional possibilities, which complicated the formalism but did not improve the final results. We shall discuss this point again at the end of the chapter.

Rewriting (V.18) in the form

$$\int \varepsilon^{(\alpha)*} \sum_{n\gamma} [v_{n\gamma}(s_\alpha) \theta_n C^{(n\gamma)} + (1 - v_{n\gamma}(s_\alpha)) \theta_n C^{(o)}] \varepsilon^{(\alpha)} dV = 0 \quad , \tag{V.20}$$

we note that there can be no poles in the region $s_\alpha \geqslant 1$ (because $0 < v_{n\gamma}(s_\alpha) \leqslant 1$). Moreover, from (V.18) and (V.20) we find that all $s_\alpha \leqslant 0$ in the case where all $\delta C^{(n\gamma)} \geqslant 0$ and $b_{n\gamma} \geqslant 1$, and that all $0 \leqslant s_\alpha < 1$ in the case where all $\delta C^{(n\gamma)} \leqslant 0$ and $0 < b_{n\gamma} \leqslant 1$. Since all the poles s_α are real and the function F(s) must be real (at least) in the physical region $s \geqslant 1$, we conclude that the weights F_α of the poles are also real. Later on we shall determine also the signs of F_α.

The parameters F_α and s_α in (V.17) satisfy moment sum rules analogous to (III.50). The n-th moment can be found by calculating the (n+1)-th derivative of F(s) with respect to $w \equiv 1/s$

$$M_n \equiv \sum_\alpha F_\alpha s_\alpha^n = \frac{1}{(n+1)!} \frac{d^{n+1}F}{dw^{n+1}} \Big|_{w=0} \quad . \tag{V.21}$$

This follows from an expansion of F(s) in (V.17) in powers of w. Thus, in order to evaluate the n=0 and n=1 moments we must find the first and second derivatives of F at w=0. We do this by using the following representation for F(s):

$$F(s) = \frac{1}{V} \int \varepsilon C(\vec{r};s) \varepsilon \, dV - \varepsilon^0 C^{(0)} \varepsilon^0 \, . \tag{V.22}$$

The first variation of that expression is:

$$\Delta F = \frac{2}{V} \int \Delta\varepsilon C \, \varepsilon \, dV + \frac{1}{V} \int \varepsilon \, \Delta C \, \varepsilon \, dV \quad . \tag{V.23}$$

The first integral in (V.23) can be shown to vanish by transforming it to a surface integral and using the fact that $\Delta \vec{u} \equiv 0$ on the surface. Using (V.15) to evaluate C in terms of the variation of $v_{n\gamma}$, we finally get

$$\Delta F = \frac{1}{V} \sum_{n\gamma} \Delta v_{n\gamma} \int \theta_n \varepsilon \delta C^{(n\gamma)} \varepsilon \, dV \quad . \tag{V.24}$$

In the limit w=0 ($v_{n\gamma}$=0) the sample becomes homogeneous, i.e. $\varepsilon = \varepsilon^0$ and it is now straightforward to obtain M_0 from (V.21), (V.24) and (V.16)

$$\begin{aligned} M_0 &= \frac{1}{V} \int \varepsilon^0 \sum_{n\gamma} \theta_n b_{n\gamma} \delta C^{(n\gamma)} \varepsilon^0 dV = \\ &= \sum_{n\gamma} p_n b_{n\gamma} \varepsilon^0 \delta C^{(n\gamma)} \varepsilon^0 \, , \end{aligned} \tag{V.25}$$

where p_n is the volume fraction of the n-th component.

We also note that if all $\delta C^{(n\gamma)} \geqslant 0$ ($\delta C^{(n\gamma)} \leqslant 0$) in (V.24) then all the partial derivatives $\partial F/\partial v_{n\gamma}$ are positive (negative). Under the restrictions on the form of $v_{n\gamma}$, the derivatives $dv_{n\gamma}/dw$ are always positive for real w, therefore $dF/dw > 0$ ($dF/dw < 0$). From this it follows that all $F_\alpha > 0$ ($F_\alpha < 0$). Thus we summarize the restrictions on the locations and weights of the poles by the following set of inequalities:

$$s_\alpha \leqslant 0, \qquad \text{when all } \delta C^{(n\gamma)} \geqslant 0, \tag{V.26a}$$

$$0 \leqslant s_\alpha < 1, \text{ when all } \delta C^{(n\gamma)} \leqslant 0, \tag{V.26b}$$

$$F_\alpha \cdot s_\alpha \leqslant 0, \text{ in both cases .} \tag{V.26c}$$

Note that (V.26c) has a more restricted range of validity than the analogous result (III.29) for two-component composites: Inequality (III.29) is valid even for non-definite δC, while here for non-definite $\delta C^{(n\gamma)}$ we cannot even claim that F_α and s_α are real.

The second variation of F is obtained from (V.24):

$$\tfrac{1}{2}\Delta^2 F = \frac{1}{V} \sum_{n\gamma} \Delta v_{n\gamma} \int \theta_n \, \Delta\varepsilon \, \delta C^{(n\gamma)} \varepsilon \, dV \ . \tag{V.27}$$

We cannot evaluate this expression in the general case. However, for w=0 ($v_{n\gamma}=0$, $\varepsilon=\varepsilon^0$) the variation $\Delta\varepsilon$ must satisfy the following inhomogeneous differential equation.

$$\partial_j \, C^{(o)}_{ijk\ell} \, \Delta\varepsilon_{k\ell} = -\partial_j \Big(\sum_{n\gamma} \theta_n \Delta v_{n\gamma} \, \delta C^{(n\gamma)}_{ijk\ell} \, \varepsilon^o_{k\ell} \Big) \ , \tag{V.28}$$

while the displacement vector $\Delta\vec{u}$, which corresponds to $\Delta\varepsilon$, vanishes at the boundaries. The solution of (V.28) and the vanishing boundary condition on $\Delta\vec{u}$ can be written with the help of the tensor Green's function G (see (A.1)-(A.5), where the r.h.s. of (A.1) should be replaced by the r.h.s. of (V.28))

$$\Delta\varepsilon_{k\ell}(\vec{r}) = \int \sum_{n\gamma} \theta_n(\vec{r}')\ \Delta v_{n\gamma} G_{k\ell mn}(\vec{r},\vec{r}';C^{(o)})\,\delta C_{mnrt}\varepsilon^o_{rt}\ dV' \ . \qquad (V.29)$$

Substituting the result in (V.27) we get

$$\tfrac{1}{2}\Delta^2 F\Big|_{v_{n\gamma}=0} = \frac{1}{V}\iint \sum_{nm\gamma\beta} \theta_n(\vec{r}')\theta_m(\vec{r})\Delta v_{n\gamma}\Delta v_{m\beta}\varepsilon^o_{rt}\ \delta C^{(m\beta)}_{rtij} G_{ijk\ell}(\vec{r},\vec{r}')\delta C^{(n\gamma)}_{k\ell ps}\varepsilon^o_{ps}\, dV dV' \ . \qquad (V.30)$$

Note that integrals of this type have already been evaluated in Ch.III.E. Following the same line of reasoning, we rewrite (V.30) in the following form:

$$\tfrac{1}{2}\Delta^2 F\Big|_{v_{n\gamma}=0} = \varepsilon^o\Big(\sum_{nm\gamma\beta} \Delta v_{m\beta}\Delta v_{n\gamma}\delta C^{(m\beta)}\Big)\int f_{mn}(\vec{r})\, G(\vec{r})\, dV\ \delta C^{(n\gamma)}\Big)\varepsilon^o \ , \qquad (V.31)$$

where

$$f_{mn}(\vec{r}) = \frac{1}{V}\int \theta_m(\vec{r}+\vec{r}')\ \theta_n(\vec{r}')\ dV' - p_m p_n \ . \qquad (V.32)$$

Expressions (III.55) and (III.56) are special cases of (V.31) and (V.32), repectively. With the help of these results it is now a straightforward matter to calculate d^2F/dw^2 at w=0. Since

$$\frac{d^2F}{dw^2} = \sum_{nm\gamma\beta} \frac{\partial^2 F}{\partial v_{n\gamma}\partial v_{m\beta}}\cdot\frac{dv_{n\gamma}}{dw}\cdot\frac{dv_{m\beta}}{dw} + \sum_{n\gamma}\frac{\partial F}{\partial v_{n\gamma}}\cdot\frac{d^2 v_{n\gamma}}{dw^2} \ , \qquad (V.33)$$

we obtain from (V.21), (V.24), (V.31) and (V.33)

$$M_1 = \sum_{mn\beta\gamma}\Big[\varepsilon^o\ \delta C^{(m\beta)}\int f_{mn}(\vec{r})\ G(\vec{r})\, dV\ \delta C^{(n\gamma)}\varepsilon^o b_{m\beta} b_{n\gamma}\Big] - \qquad (V.34)$$

$$- \sum_{n\gamma}\big[p_n\varepsilon^o\delta C^{(n\gamma)}\varepsilon^o b_{n\gamma}(1-b_{n\gamma})\big] \ .$$

As in the case of a two-component composite (see Ch.III.E) the integrals in this equation can always be evaluated for an isotropic mixture of isotropic components. Thus for $\varepsilon^o = \varepsilon^{o\gamma}$ where $\gamma = \kappa$ or $\gamma = \mu$, we obtain

$$M_1^{(\gamma)} = - \sum_{mn} p_m (\delta_{mn} - p_n) \delta\gamma^{(m)} \delta\gamma^{(n)} E^{(\gamma)}(C^o) b_{n\gamma} b_{m\gamma} - \\ - \sum_n p_n \delta\gamma^{(n)} b_{n\gamma} (1 - b_{n\gamma}) \quad , \tag{V.35}$$

where $\delta\gamma^{(n)} \equiv \gamma^{(n)} - \gamma^{(o)}$, $E^{(\gamma)}(C^{(o)})$ is defined by (III.68b) or (III.69b) with $\kappa^{(2)}$, $\mu^{(2)}$ replaced by $\kappa^{(o)}$, $\mu^{(o)}$, and the term $p_m(\delta_{mn} - p_n)$ is just the value of $f_{mn}(0)$. This result for M_1 can be extended to the case of non-isotropic microgeometries, similarly to the way in which it was done for a two-component composite in Ch.III.E. In this case, M_0 of (V.25) also has a somewhat simpler form:

$$M_0^{(\gamma)} = \sum_n p_n b_{n\gamma} \delta\gamma^{(n)} \quad . \tag{V.36}$$

Using this more general formalism, we are now able to derive Walpole's bounds, i.e., we can treat the case of non-definite $C^{(1)} - C^{(2)}$, by a suitable choice of $C^{(o)}$ and $b_{n\gamma}$. In the isotropic case, for instance, we choose $(\kappa^{(o)}, \mu^{(o)}) = (\min(\kappa^{(1)}, \kappa^{(2)}), \min(\mu^{(1)}, \mu^{(2)}))$ or $(\kappa^{(o)}, \mu^{(o)}) = (\max(\kappa^{(1)}, \kappa^{(2)}), \max(\mu^{(1)}, \mu^{(2)}))$ and all $b_{n\gamma} = 1$. For such a choice all $\delta C^{(n\gamma)} \geqslant 0$ (all $\delta C^{(n\gamma)} \leqslant 0$) and we can derive the bounds on $F(1)$ in the same way as in the previous section. The resulting bounds are similar to (V.11) and (V.12) but with $(\kappa^{(1)}, \mu^{(1)})$ replaced by $(\max(\kappa^{(1)}, \kappa^{(2)}), \max(\mu^{(1)}, \mu^{(2)}))$ and $(\kappa^{(2)}, \mu^{(2)})$ replaced by $(\min(\kappa^{(1)}, \kappa^{(2)}), \min(\mu^{(1)}, \mu^{(2)}))$. These bounds can be extended to cases of non-isotropic mixtures of isotropic materials, as was done in the previous section.

In principle, this approach can be implemented even for a composite whose components are non-isotropic: We must choose $C^{(o)}$ to be as large as possible (as small as possible) under the restrictions $\delta C^{(1)} \geqslant 0$, $\delta C^{(2)} \geqslant 0$ ($\delta C^{(1)} \leqslant 0$, $\delta C^{(2)} \leqslant 0$) and we must take all $b_{n\gamma} = 1$. The bounds on $C^{(e)}$ are again obtained from (V.9) and (V.10) in terms of M_0 and M_1. The main problem is of course, how to calculate M_1. Unfortunately, there is no

prescription for such a calculation in the general case other than (V.34).

Another advantage of the parametric representation (V.15), (V.16) is that it enables us to represent different composites (but having the same microgeometry) by the same function F(s) at different values of s, as was explained earlier. In the next section we shall derive improved bounds under the assumption that such representation is possible, while detailed examples will be given in Sec.E.

The method of derivation of the moment sum rules, which was presented in this section is more general and flexible than the method presented in Ch.III.E. In App.D we shall apply an analogous method to derive Voigt's bound.

D. IMPROVED BOUNDS FROM ADDITIONAL INFORMATION - THEORY

In this section we shall exploit the additional constraint (V.13) to derive improved bounds on the effective elastic constants. We shall discuss only the case when all the $\delta C^{(n\gamma)}$ appearing in (V.15) are positive semidefinite. In that case, all the poles $s_\alpha \leqslant 0$ and their residues $F_\alpha > 0$. The case of all $\delta C^{(n\gamma)} \leqslant 0$ in (V.15) is completely analogous.

Although the entire calculation can be performed using the function F(s), it is convenient to introduce a new related function

$$H(s) \equiv F(s)/(F(s) + \varepsilon^0 C^{(0)} \varepsilon^0) = 1 - \varepsilon^0 C^{(0)} \varepsilon^0 / \varepsilon^0 C^{(e)} \varepsilon^0 \ . \qquad (V.37)$$

Clearly, the function H(s) includes the same information about the system as does F(s). Furthermore, we will now show that it also has a similar analytic structure, namely,

$$H(s) = \sum_\alpha \frac{H_\alpha}{s - h_\alpha} \ , \qquad (V.38)$$

where the poles h_α and the residues H_α are all real and satisfy

$$s' \leqslant h_\alpha \leqslant 0, \quad H_\alpha > 0. \tag{V.39}$$

These poles and residues also satisfy certain sum rules. In order to demonstrate these properties, we note first that the poles h_α must be zeros of the denominator $F(s) + \varepsilon^0 C^{(0)} \varepsilon^0$ and that, due to the structure of $F(s)$, these zeros must lie on the negative real axis. At these zeros, both $F(s)$ and its derivative are negative, and thus the residues H_α must be positive. The lower bound s' on h_α arises by noting that even for negative s, as long as $C(\vec{r};s)$ or (V.15) is positive semidefinite in all components, $C^{(e)}$ will also be positive semidefinite, and consequently $F(s) + \varepsilon^0 C^{(0)} \varepsilon^0 > 0$. This will certainly be true for any s which is sufficiently negative. If we denote by s' the most negative value of s for which $C(\vec{r};s)$ ceases to be positive semidefinite, then clearly all zeros of $F(s) + \varepsilon^0 C^{(0)} \varepsilon^0$ must lie to its right. By expanding (V.37) and (V.38) in powers of $1/s$ and equating the coefficients, we obtain the following moment sum rules for $H(s)$ in terms of corresponding quantities of $F(s)$:

$$M_{0H} \equiv \sum_\alpha H_\alpha = M_0 / \varepsilon^0 C^{(0)} \varepsilon^0 \quad , \tag{V.40a}$$

$$M_{1H} \equiv \sum_\alpha H_\alpha h_\alpha = M_1 / \varepsilon^0 C^{(0)} \varepsilon^0 - M_{0H}^2 \quad , \text{ etc.} \tag{V.40b}$$

We can now manufacture bounds on $H(s)$ in much the same way as we did for $F(s)$, and these can of course be translated into bounds on either $F(s)$ or $\varepsilon^0 C^{(e)} \varepsilon^0$. We note that since $H(1)$ is a monotonically increasing function of $F(1)$, therefore the upper (lower) bound on $H(1)$ leads to an upper (lower) bound on $F(1)$.

The analytical properties of $F(s)$ and $H(s)$ are very convenient for the construction of rigorous bounds on the effective elastic moduli. Whenever only partial information on the microgeometry of the sample is available, the weights F_α and the locations s_α of the poles of $F(s)$ in (V.17) cannot be determined exactly. However, they must satisfy a number of constraints which fall into two categories, (a) equalities such as sum rules (V.21) or a constraint introduced by the additional information (V.13), and (b) inequalities such as (V.26). A similar statement is valid

for the weights H_α and locations h_α of the poles of H(s) in (V.38) (see (V.39) and (V.40) and note that from the knowledge of $F(s_+)$ it follows that $H(s_+)$ is also known and thus a constraint on H(s) analogous to (V.13) is valid). In order to derive bounds on the effective moduli we attempt to minimize or maximize H(1) and F(1) by varying the weigts and the locations of the poles of F(s) and H(s) subject to certain constraints.

The first variation of (V.17), ignoring the constraints, is given by

$$\Delta F(s) = \sum_\alpha \left(\frac{\Delta F_\alpha}{s - s_\alpha} + \frac{F_\alpha \Delta s_\alpha}{(s - s_\alpha)^2}\right). \tag{V.41}$$

If we assume that the zero and first moment sum rules on F(s) and the value of $F(s_+)$ are known, then the constraints (V.21) and (V.13) can be written in the following differential form:

$$\Delta M_0 = 0 = \sum_\alpha \Delta F_\alpha \quad , \tag{V.42a}$$

$$\Delta M_1 = 0 = \sum_\alpha (F_\alpha \Delta s_\alpha + s_\alpha \Delta F_\alpha) \quad , \tag{V.42b}$$

$$\Delta F(s_+) = 0 = \sum_\alpha \left(\frac{\Delta F_\alpha}{s_+ - s_\alpha} + \frac{F_\alpha \Delta s_\alpha}{(s_+ - s_\alpha)^2}\right) . \tag{V.42c}$$

These differential forms can now be used to eliminate, say, the variation of one pole (denoted s_0) and the variations of two weights (denoted F_0 and F_1) from (V.41), leaving us with

$$\begin{aligned}\Delta F(s) = {} & \sum_{\alpha>1} \Delta F_\alpha \left(\frac{s_\alpha - s_0}{s - s_0}\right)^2 \frac{(s-s_+)(s_1-s_\alpha)}{(s-s_\alpha)(s_+-s_\alpha)(s-s_1)} \\ & + \sum_{\alpha>1} F_\alpha \Delta s_\alpha \frac{s_1 - s_\alpha}{(s-s_0)^2} \left[\frac{s_0 + s_\alpha - 2s}{(s-s_\alpha)^2} - \frac{(s_+ - s_1)(s_0 + s_\alpha - 2s_+)}{(s_+ - s_\alpha)^2 (s - s_1)}\right] \\ & + F_1 \Delta s_1 \left[\frac{(s_0 - s_1)}{(s-s_0)(s-s_1)}\right]^2 \frac{s_+ - s}{s_+ - s_1} \quad .\end{aligned} \tag{V.43}$$

Until now we did not specify which poles are denoted by s_0, s_1, etc. We can choose s_1 to be the largest pole. Then for $s_+ > s$, the coefficients of the variations ΔF_α ($\alpha>1$) in the first sum of (V.43) are negative, and therefore F(s) can be increased by taking $\Delta F_\alpha < 0$, for $\alpha>1$. Since E_α cannot be negative, the maximum will be obtained for $E_\alpha=0$ ($\alpha=2,3,\ldots$). The coefficient of the variation Δs_1 is positive, and therefore F(s) will be further increased by increasing s_1 up to its maximal possible value $s_1=0$. Thus the upper bound on F(s) has the form

$$F_{\text{bound}}(s) = \frac{F_0}{s - s_0} + \frac{F_1}{s} . \tag{V.44}$$

The values of the three parameters, F_0, F_1 and s_0 are determined by the zero and first moment sum rules and by the information on $F(s_+)$, i.e. they must satisfy

$$F_0 + F_1 = M_0 , \tag{V.45a}$$

$$F_0 s_0 = M_1 , \tag{V.45b}$$

$$\frac{F_0}{s_+ - s_0} + \frac{F_1}{s_+} = F(s_+) . \tag{V.45c}$$

Solving this system of equations for F_0, F_1 and s_0, and substituting the solution into (V.44) the following upper bound on F(1) is obtained:

$$F_{\text{bound}}(1) = M_0 + 1/\left[\frac{1-s_+}{M_1} + \frac{1}{s_+ F(s_+) - M_0}\right] . \tag{V.46}$$

For $s_+ < s$ we can find lower bound on F(s) by repeating the entire procedure and by using analogous arguments. Thus (V.46) is the lower bound on F(1) for the case $s_+<1$.

The complementary bound, i.e. the lower (upper) bound on F(1) for $s_+>1$ ($s_+<1$), can be found by similar arguments which are applied to H(s). Elimination of three parameters in the variation of H(s) will lead to a result which can be obtained from (V.43) by performing the replacements $F(s) \to H(s)$, $s_0 \to h_0$, $s_1 \to h_1$, $s_\alpha \to h_\alpha$, $F_0 \to H_0$, $F_1 \to H_1$, $F_\alpha \to H_\alpha$. This time we choose h_1 to be the smallest, i.e. most negative, pole. Then for

$s_+ > s$ the coefficients of the variations ΔH_α are positive, and therefore $H(s)$ will be decreased by taking $\Delta H_\alpha < 0$, for $\alpha > 1$. Since all H_α cannot be negative, the minimum will be obtained for $H_\alpha = 0$ ($\alpha = 2,3,\ldots$). The coefficient of Δh_1 is positive, and therefore $H(s)$ will be further decreased if we decrease h_1 down to the most negative possible value $h_1 = s'$ (see (V.39)). Thus the lower bound on $H(s)$ has the form

$$H_{bound}(s) = \frac{H_0}{s - h_0} + \frac{H_1}{s - s'} \tag{V.47}$$

Values of the three parameters, H_0, H_1 and h_0 are now determined by the sum rules (V.40) and by the information on $H(s_+)$, i.e. they must satisfy

$$H_0 + H_1 = M_{0H} \,, \tag{V.48a}$$

$$H_0 h_0 + H_1 s' = M_{1H} \,, \tag{V.48b}$$

$$\frac{H_0}{s_+ - h_0} + \frac{H_1}{s_+ - s'} = H(s_+) \,. \tag{V.48c}$$

(Compare (V.47) and (V.48) with (V.44) and (V.46), respectively.) Solving this system of equations for H_0, H_1, h_0 and substituting the solution into (V.47) the following lower bound on $H(1)$ is obtained

$$H_{bound}(1) = \frac{M_{0H}}{1-s'} + 1/\left[\left(\frac{1-s_+}{M_{1H} - s' M_{0H}} + \frac{1}{H(s_+)(s_+ - s') - M_{0H}}\right)\cdot(1-s')\right] \tag{V.49}$$

Similarly, we can show that for $s_+ < 1$, this expression provides an upper bound on $H(1)$.

The bounds (V.46) and (V.49) are always more stringent than the Hashin-Shtrikman bounds. The improvement which is obtained from the additional information, i.e. the knowledge of $F(s_+)$, can be quite considerable, as will be shown in some examples in the following section. We should keep in mind that M_0, M_1, M_{0H}, M_{1H}, s_+ and s' which appear in (V.46) and (V.49) depend on the choice of $b_{n\gamma}$ in (V.16). Thus, the improved bounds on the effective elastic constants depend on $b_{n\gamma}$ and they should be optimized, i.e. made as narrow as possible, in each case.

The bounds (V.46) and (V.49) can be used even in the case when $F(s_+)$ is not known exactly: If we only know that $F(s_+)$ is somewhere in the range $[F'_+,F''_+]$, then by inserting the appropriate end of that range into (V.46) and (V.49) we can still derive an improved bound (provided that the range of $F(s_+)$ itself is narrower than the Hashin-Shtrikman bounds, otherwise no additional information is actually supplied).

E. IMPROVED BOUNDS FROM ADDITIONAL INFORMATION - EXAMPLES

In this section we implement the theoretical results of the two previous sections. Improved bounds [28] on the effective elastic moduli are obtained for several examples of specific composites. The considerable improvement in the bounds obtained, as well as some limitations of the theory, are demonstrated.

We start with an example of the parametric representation (V.15) and (V.16), which will be used later on for the derivation of an improved bound. We consider two mixtures of isotropic components. The first one is composed of $C^{(1)} = (\kappa^{(1)},\mu^{(1)})$ and $C^{(2)}=(\kappa^{(2)},\mu^{(2)})$, and the second one is composed of $C_+^{(1)} = (\kappa_+^{(1)},\mu_+^{(1)})$ and $C_+^{(2)} = C^{(2)}$. We will restrict ourselves to the case $C^{(1)}-C^{(2)} \geqslant 0$. We start by choosing $C^{(o)}=C^{(2)}$ in (V.15) and requiring that for some value $s = s_+ \neq 1$ the $C^{(1)}$ material be replaced by $C_+^{(1)}$. Thus the parameters in (V.16) must be chosen so as to satisfy

$$\kappa_+^{(1)} = \kappa^{(2)} + (\kappa^{(1)} - \kappa^{(2)})/[(s_+-1)/b_{1\kappa} + 1] \quad , \tag{V.50a}$$

$$\mu_+^{(1)} = \mu^{(2)} + (\mu^{(1)} - \mu^{(2)})/[(s_+-1)/b_{1\mu} + 1] \quad . \tag{V.50b}$$

If we treat s_+ as given, then the b's in (V.50) are determined by

$$b_{1\kappa} = (\kappa_+^{(1)} - \kappa^{(2)})(s_+-1)/(\kappa^{(1)} - \kappa_+^{(1)}) \quad , \tag{V.51a}$$

$$b_{1\mu} = (\mu_+^{(1)} - \mu^{(2)})(s_+-1)/(\mu^{(1)} - \mu_+^{(1)}) \quad . \tag{V.51b}$$

Since both $b_{1\kappa}$ and $b_{1\mu}$ must be greater than 1 in this case, these equa-

tions can be used only when the following inequalities are simultaneously valid

$$(\kappa_+^{(1)} - \kappa^{(1)})(\mu_+^{(1)} - \mu^{(1)}) \geqslant 0 \tag{V.52}$$

$$\kappa_+^{(1)} > \kappa^{(2)} \quad , \quad \mu_+^{(1)} > \mu^{(2)} \tag{V.53}$$

$$s_+ \geqslant 1 + \max \left(\frac{\kappa^{(1)} - \kappa_+^{(1)}}{\kappa_+^{(1)} - \kappa^{(2)}} \, , \, \frac{\mu^{(1)} - \mu_+^{(1)}}{\mu_+^{(1)} - \mu^{(2)}} \right) , \quad \text{for } \kappa^{(1)} - \kappa_+^{(1)} > 0 \tag{V.54a}$$

$$0 \leqslant s_+ \leqslant 1 + \min \left(\frac{\kappa^{(1)} - \kappa_+^{(1)}}{\kappa_+^{(1)} - \kappa^{(2)}} \, , \, \frac{\mu^{(1)} - \mu_+^{(1)}}{\mu_+^{(1)} - \mu^{(2)}} \right) , \quad \text{for } \kappa^{(1)} - \kappa_+^{(1)} < 0 \tag{V.54b}$$

Inequalities (V.52) and (V.53) limit the range of applicability of this particular implementation of the formalism. Different choices of $C^{(o)}$ (e.g. $C^{(o)}=C^{(1)}$) allow us to circumvent the limitations arising from (V.53) (or a similar pair of inequalities), but an inequality similar to (V.52) will always appear. Thus there will be pairs of composites for which representation of an elastic modulus by a single function F(s) is impossible. Nevertheless, the improved bounds can be derived even in those cases by a two-stage procedure which will be explained later on in this section.

The extent to which the new bounds are an improvement over the Hashin-Shtrikman bounds can be demonstrated by the following numerical example: Suppose we have a 50%-50% isotropic mixture of isotropic components $C^{(1)} = (\kappa^{(1)}, \mu^{(1)}) = (10,4)$ and $C^{(2)}=(1,2)$. The Hashin-Shtrikman bounds (V.11) and (V.12) on the effective elastic constants of such a composite are

$$3.02 \leqslant \kappa^{(e)} \leqslant 4.48 \, , \tag{V.55a}$$

$$2.78 \leqslant \mu^{(e)} \leqslant 2.89 \, . \tag{V.55b}$$

Suppose we know that $C_+^{(e)} = (\kappa_+^{(e)}, \mu_+^{(e)}) = (7,4.5)$ for a mixture with the same microgeometry but with the $C^{(1)}$ material replaced by $C_+^{(1)} = (30,10)$.

Using this information in (V.46) and (V.49) we obtain the following new bounds

$$3.41 \leqslant \kappa^{(e)} \leqslant 3.99, \tag{V.56a}$$

$$2.82 \leqslant \mu^{(e)} \leqslant 2.86, \tag{V.56b}$$

which are clearly much narrower than (V.55). In the previous section we have already mentioned that the bounds (V.46) and (V.49) depend on the particular choices of $b_{n\gamma}$ in (V.16). The b's themselves depend on s_+ (see (V.51)). The above result was obtained after a numerical optimization of the bounds achieved by allowing s_+ to vary in the range defined by (V.54b). The lowest upper bound was obtained when $s_+ \to 0$ and the highest lower bound was obtained when s_+ was equal to its maximum allowed value. We stress that we were only able to obtain these optimum values of s_+ empirically.

The extent to which we can improve over the Hashin-Shtrikman bounds depends strongly on the differences between the elastic constants of the two materials. This fact can be demonstrated by the following example: Let us examine again a 50%-50% mixture of isotropic materials in which $C^{(2)} = (\kappa^{(2)},\mu^{(2)}) = (2,0.75)$ and $C^{(1)}=(x\kappa^{(2)},x\mu^{(2)})$, where x is a continuous variable which enables the properties of the $C^{(1)}$ material to be varied continuously. Suppose we know that for $x=x_+\equiv 8$, i.e. for $C_+^{(1)}=(16,6)$, the effective bulk modulus is $\kappa_+^{(e)}=5$. Fig. V.1 depicts the dependence on x of the improved bounds. The upper and lower bounds naturally coincide for $x=x_+$, and begin to diverge when x becomes larger or smaller than x_+. However, even when x is far away from x_+ the bounds are still considerably narrower than the Hashin-Shtrikman bounds.

At the beginning of this section we mentioned cases in which we cannot represent two different composites by the same function F(s). Nevertheless, we can derive an improved bound even in those cases by a two-stage procedure which is demonstrated by the following example: If we have two isotropic composites made of isotropic components in which the $C^{(2)}$ material is the same but $C^{(1)}$ is different from $C_+^{(1)}$, and if $\kappa^{(2)} < \kappa^{(1)} < \kappa_+^{(1)}$, $\mu^{(2)} < \mu_+^{(1)} < \mu^{(1)}$, then the inequality (V.52) is not satisfied and both

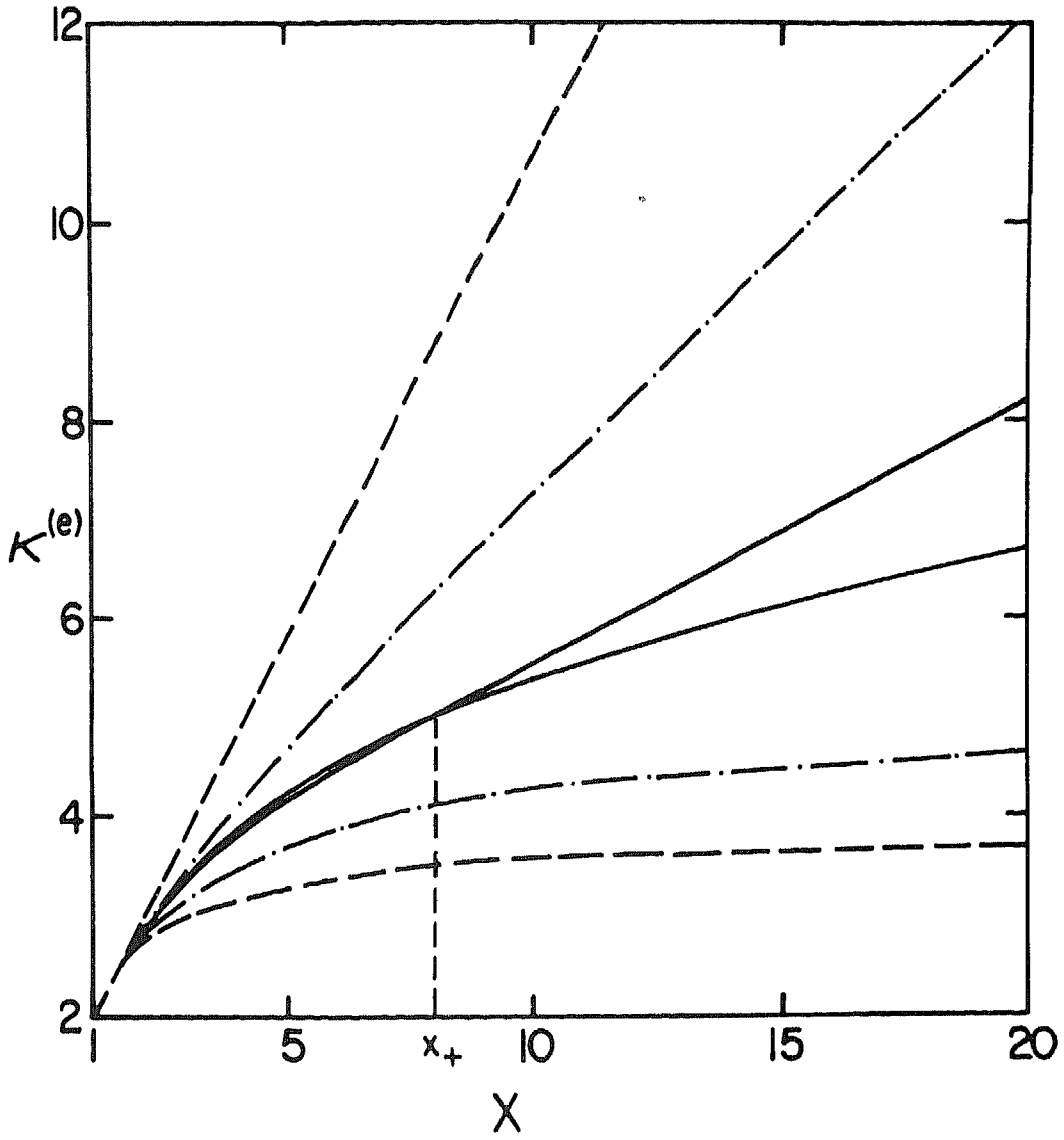

Fig. V.1. Improved upper and lower bounds on the effective bulk modulus $\kappa^{(e)}$ of a two-component (50%-50%) composite made of isotropic components $C^{(2)} = (\kappa^{(2)}, \mu^{(2)}) = (2, 0.75)$, $C^{(1)} = (x\kappa^{(2)}, x\mu^{(2)})$, as a function of x. The dashed lines are the Voigt (upper) and the Reuss (lower) bounds. The dot-dashed lines are the two Hashin-Shtrikman bounds. The solid lines are our improved bounds, obtained by including the additional information that for $x = x_+ \equiv 8$, i.e., for $C^{(1)} = C_+^{(1)} = (16,6)$, the effective bulk modulus is $\kappa_+^{(e)} = 5$. The improvement is most striking for x near x_+, but it is quite considerable even far away from that point. Note that all the bounds in this figure apply in the case of a two-component composite with an arbitrary microgeometry.

composites cannot be represented by the same function F(s) associated with (V.15). However, we can introduce a hypothetical third mixture in which $C_*^{(1)} = (\kappa^{(1)}, \mu_+^{(1)})$. The knowledge of $C_+^{(e)}$ can now be used to first derive improved bounds on the $C^{(2)}$, $C_*^{(1)}$ composite, and those bounds can be used in the next stage to derive improved bounds on the $C^{(2)}$, $C^{(1)}$ composite. Note that at each stage the inequality (V.52) holds.

Finally, we would like to stress that suitable choices of $C^{(o)}$ enable us to treat very general cases, including the case of non-definite $C^{(1)}-C^{(2)}$.

F. DISCUSSION

We have presented a new approach to the calcuation of rigorous bounds on the effective elastic constants of a composite material. Using this approach, we rederived some of the known bounds and extended the range of their validity to lower symmetries. We then showed that our formalism can also be used to include new types of information about the system in order to improve the bounds on the effective elastic constants. Specifically, we showed that a knowledge of the effective elastic constants of one composite can be used to improve the bounds on the elastic constants of another composite with the same microgeometry. The bounds thus obtained can be considerably narrower than the Hashin-Shtrikman bounds. Other types of information, including both equalities and inequalities, can also be incorporated in the derivation of exact bounds. The possibility of incorporating non-geometrical information in the derivation of improved bounds may be important from a practical point of view, because the high order correlation functions of the composite are usually very difficult to obtain, even for very simple microgeometries.

It should be kept in mind that the improved bounds which were derived in the previous section are the best possible for a given parametric representation (V.15) and (V.16) of $C(\vec{r};s)$. We used a particularly simple representation, but even then we still had to optimize the bounds numerically with respect to the value of the one parameter s_+. Although

the optimum values of s_+ turned out empirically (i.e., by the numerical experiments) to be very simple (i.e., either $s_+=0$ or $s_+=$ the maximum possible value) for the case we considered, we were not able to derive a generally applicable analytical result for the optimal value of s_+. Thus this remains an open problem. Moreover, there is a possibility that a more general parametric representation of $C(\vec{r};s)$ would lead to even more stringent bounds on $C^{(e)}$ from the same information. We have in fact tried to use a generalized form of (V.16), namely

$$v_{n\gamma} = a_{n\gamma} + b_{n\gamma} s + \frac{c_{n\gamma}}{d_{n\gamma}-s}, \tag{V.57}$$

which under several (different) sets of restrictions on the constants $a_{n\gamma}$, $b_{n\gamma}$, $c_{n\gamma}$ and $d_{n\gamma}$, produces a function $F(s)$ which has similar properties to those described in Sec.C. The entire formalism (especially the moment sum rules M_0 and M_1) then became much more complicated. However, no additional improvement of the bounds was achieved: Numerical experiments showed that at the optimal point the constants in (V.57) assumed such values that (V.57) was reduced to the simpler expression (V.16).

The representation of $C^{(e)}$ as a sum of simple poles can also be applied in the case of viscoelastic materials, i.e. when the elastic stiffness tensor is complex. A similar extension of the dielectric theory to complex dielectric constants [91] has led to considerable progress in the derivation of bounds on complex dielectric constants. It seems, however, that in the case of viscoelasticity, one must use a representation that is more general than (V.16) (or (V.57)) in order to endow $C(\vec{r};s)$ with sufficient freedom to move about in the space of <u>complex</u> elastic constants when s is varied.

In summary, we believe that the new approach to the derivation of rigorous bounds on the elastic moduli of a composite material which was presented here is a very fruitful and promising one. While some of its uses and implications for various situations, where only partial information is available about the microscopic structure of the composite, have been explored, further work along these lines will surely lead to more new and interesting results.

CHAPTER VI. GENERAL CONCLUSIONS

The representation of an effective elastic constant as a sum of simple poles has turned out to be an admirably convenient method for the systematic evaluation of effective elastic moduli, as well as for the derivation of rigorous bounds. The degree of accuracy to which the effective constants can be evaluated is much higher than can be obtained with reasonable effort by any other analytical method. Thus, for well-defined microgeometries, our method not only provides new insight into the elastostatic problem, but also leads to better and simpler practical calculations of the effective elastic constants.

When the microgeometry is not known precisely, we can use the spectral representation for the derivation of rigrous bounds. In this way, we rederived some of the known bounds and extended the range of validity of the Hashin-Shtrikman bounds. However, the main advantage of the pole representation is in the possibility of using various kinds of information of a non-geometrical nature in order to derive improved bounds.

The few examples which were presented in this Thesis clearly only serve to indicate the enormous potential of the method. We believe that further work both on the general theory and on specific applications will be very fruitful, and will lead to the solution of more, presently unresolved, problems.

APPENDIX A. INTEGRAL EQUATION FOR THE STRAIN TENSOR IN A COMPOSITE MATERIAL

In this appendix we derive the integral equation for the strain ε in a composite material and investigate the main properties of the integral operator. This derivation can be found in many places [21-25], some of them very detailed [40]. Since the integral representation plays a major role in our work, we reproduce it briefly for easy reference.

From (II.1), (II.9) and (II.10) we obtain the following differential equation for the displacement vector $\vec{u}$ in the composite

$$C^{(o)}_{ijkl}\partial_j\partial_l u_k = -\partial_j c_{ijkl}\partial_l u_k, \tag{A.1}$$

where $C^{(o)}$ and $c(\vec{r})$ are the spatially constant and varying parts, respectively, of the local elastic stiffness tensor of a composite. This equation must be supplemented by boundary conditions on $\vec{u}$. For a homogeneous elastic medium ($c(\vec{r}) \equiv 0$) the solution of (A.1), denoted by $\vec{u}^h(\vec{r})$, can be found using standard elastostatic methods. For homogeneous boundary conditions (II.18), this solution is particularly simple (see Ch.II.B).

For a homogeneous elastic medium we can define a Green function $g_{mi}(\vec{r},\vec{r}')$, which gives the i component of the displacement vector at the point $\vec{r}'$ due to a δ-function point force in m direction at $\vec{r}$, when the displacement is assumed to vanish at the boundaries of the sample. This tensor must satisfy

$$C^{(o)}_{ijkl}\partial'_j\partial'_l\, g_{mi}(\vec{r},\vec{r}') + \delta_{mk}\delta(\vec{r}-\vec{r}') = 0 \quad . \tag{A.2a}$$

$$g_{mi}(\vec{r},\vec{r}') = 0, \text{ for } \vec{r}' \text{ on the boundary.} \tag{A.2b}$$

The solutions of the differential equation (A.1) can be built from $\vec{u}^h(\vec{r})$ plus a correction term which vanishes on the boundaries. It can be verified by a direct substitution into (A.1) that

$$u_m(\vec{r}) = u^h_m(\vec{r}) + \int g_{mi}(\vec{r},\vec{r}')\,\partial'_j[c_{ijkl}(\vec{r}')\,\partial'_l u_k(\vec{r}')]dV'. \qquad (A.3)$$

Thus from (II.1) and (A.3) we obtain the following integral equation for the strain tensor

$$\begin{aligned}\varepsilon_{mn} &= \varepsilon^h_{mn} + \tfrac{1}{4}\int[(\partial_n g_{mi} + \partial_m g_{ni})\partial'_j(c_{ijkl}\varepsilon_{kl}) + \\ &+ (\partial_n g_{mj} + \partial_m g_{nj})\partial'_i(c_{ijkl}\varepsilon_{kl})]\,dV' = \\ &= \varepsilon^h_{mn} + \int G_{mnij}\,c_{ijkl}\varepsilon_{kl}\,dV',\end{aligned} \qquad (A.4)$$

$$G_{mnij}(\vec{r},\vec{r}') \equiv \tfrac{1}{4}(\partial_n\partial'_j g_{mi} + \partial_m\partial'_j g_{ni} + \partial_n\partial'_i g_{mj} + \partial_m\partial'_i g_{nj}), \qquad (A.5)$$

where at the first stage of (A.4) we used the symmetry of (A.3) under the interchange of the indices $i \leftrightarrow j$, while at the next stage Gauss' theorem was applied together with the boundary conditions (A.2b). We shall call G the Green tensor of the problem.

The equality

$$\int g_{nk}(\vec{r}',\vec{r})C^{(o)}_{ijkl}\partial_l\partial_j\, g_{mi}(\vec{r}'',\vec{r})\,dV = \int g_{mi}(\vec{r}'',\vec{r})C^{(o)}_{ijkl}\partial_l\partial_j\, g_{nk}(\vec{r}',\vec{r})\,dV \qquad (A.6)$$

can be verified by applying Gauss' theorem twice and by using the boundary conditions (A.2b). Using (A.2a) and the symmetry of $C^{(o)}_{ijkl}$ (see (II.3)) in (A.6) we prove the following symmetry property (reciprocity) for g:

$$g_{nm}(\vec{r},\vec{r}') = g_{mn}(\vec{r}',\vec{r}). \qquad (A.7)$$

From (A.5) and (A.7) we find that G also has some symmetry properties:

$$G_{ijkl}(\vec{r},\vec{r}') = G_{ijlk}(\vec{r},\vec{r}') = G_{jikl}(\vec{r},\vec{r}') = G_{klij}(\vec{r}',\vec{r}). \qquad (A.8)$$

An additional property of G can be found if we note that

$$\int \partial'_j g_{mi}(\vec{r},\vec{r}')\,dV' = \oint n_j g_{mi}(\vec{r},\vec{r}')\,dS' = 0, \tag{A.9}$$

where we transformed the volume integral to the surface integral ($\vec{n}$ is a unit vector normal to the boundary) and used (A.2b) on the surface. From (A.5) and (A.9) we find that

$$\int G_{ijkl}(\vec{r},\vec{r}')\,dV' = 0, \tag{A.10}$$

whenever the integral is performed over the entire volume of the sample.

For an unbounded domain, i.e. for an infinite sample, both g and G become translationally invariant

$$g_{ij}(\vec{r},\vec{r}') = g_{ij}(\vec{r}-\vec{r}'), \tag{A.11a}$$

$$G_{ijkl}(\vec{r},\vec{r}') = G_{ijkl}(\vec{r}-\vec{r}'). \tag{A.11b}$$

The entire formalism remains unchanged except for the boundary conditions (A.2b) which are replaced by requirement that

$$\lim_{|\vec{r}-\vec{r}'|\to\infty} g_{ij}(\vec{r}-\vec{r}') = 0. \tag{A.12}$$

The equation (A.2a) now contains only one variable. (Note that $\partial'_j g = -\partial_j g$ in this case.) Its Fourier transform has the following form

$$C^{(o)}_{ijkl} k_l k_j \tilde{g}_{mi}(\vec{k}) = \delta_{mk}\ , \tag{A.13}$$

while the connection (A.5) in k-space becomes

$$\tilde{G}_{mnij}(\vec{k}) = -\tfrac{1}{4}[\tilde{g}_{mi}(\vec{k})k_n k_j + \tilde{g}_{ni}(\vec{k})k_m k_j + \tilde{g}_{mj}(\vec{k})k_n k_i + \tilde{g}_{nj}(\vec{k})k_m k_i)]\ , \tag{A.14}$$

where $\hat{g}$ and $\tilde{\hat{G}}$ denote the Fourier transforms of the corresponding tensors. For an isotropic $C^{(o)}$, i.e. for

$$C^{(o)}_{ijkl} = \lambda^{(o)} \delta_{ij}\delta_{kl} + 2\mu^{(o)} I_{ijkl} \tag{A.15}$$

(see (II.22)), we can easily solve (A.13) for $\hat{g}(\vec{k})$. We thus find that

$$\hat{g}_{mn}(\vec{k};C^{(o)}) = \frac{1}{\mu^{(o)}} \left(\frac{\delta_{mn}}{k^2} - \frac{\lambda^{(o)}+\mu^{(o)}}{\lambda^{(o)}+2\mu^{(o)}} \cdot \frac{k_m k_n}{k^4}\right) . \tag{A.16}$$

From (A.14) and (A.16) we obtain the Fourier transform $\hat{\tilde{G}}$ of the problem (see (III.58)).

Note that all the results which were derived in this appendix are independent of the space dimensionality. This dimensionality will enter the expressions only when we express the Lamé constant $\lambda^{(o)}$ in terms of the bulk and the shear moduli (see (II.25)).

APPENDIX B. AN ALTERNATIVE FORMALISM FOR THE GENERAL APPROACH

In this appendix we present a modification of the formalism which was presented in Ch.III.B. This acutally was the original form of our approach [27] to the problem of the calculation of the effective elastic constants of composites.

The Green's tensor $G_{ijkl}(\vec{r},\vec{r}')$ which appears in the integral equation (III.8) is symmetric under the interchanges $i\leftrightarrow j$, $k\leftrightarrow l$, and under the joint interchange $i,j,\vec{r} \leftrightarrow k,l,\vec{r}'$ (see (A.8)). However, the entire integral operator $\hat{G}$ (III.10) is not symmetric. We now symmetrize it with the help of the "square root tensor" of δC, denoted by K_{ijkl}

$$KK = \delta C \quad . \tag{B.1}$$

Note that K has the same symmetries (II.3) as the elastic stiffness tensor, but is not real unless δC is positive semidefinite. For negative semi-definite δC, we obtain a purely imaginary K. We now define

$$\rho \equiv K\varepsilon \quad , \tag{B.2}$$

$$H \equiv KGK \, . \tag{B.3}$$

Multiplying (III.8) by K from the left we arrive at the following integral equation

$$\rho_{ij} = \rho^{o}_{ij} + \frac{1}{s}\int \theta_1(\vec{r}')H_{ijkl}(\vec{r},\vec{r}')\rho_{kl}(\vec{r}')\, dV' \quad , \tag{B.4}$$

or, in the more concise symbolic bra-and-ket notation

$$|\rho\rangle = |\rho^{o}\rangle + \frac{1}{s}\hat{H}|\rho\rangle, \tag{B.5}$$

which is analogous to (III.9).

We now introduce a scalar product

$$\langle \rho | \rho' \rangle \equiv \int \theta(\vec{r}) \rho_{ij}^{*}(\vec{r}) \rho'_{ij}(\vec{r})\, dV \quad . \tag{B.6}$$

(Compare this definition with (III.11) and (III.12).) The operator $\hat{H}$ is symmetric, but in general non-hermitian, under this product. If δC is positive (negative) semidefinite, i.e. K is real (pure imaginary) then $\hat{H}$ is real and symmetric, i.e. hermitian.

The rest of the derivation is completely analogous to that of Ch.III.B: We rewrite (III.6) in the form

$$F(s) = \frac{1}{sV} \langle \rho^{o*} | \rho \rangle, \tag{B.7}$$

which is analogous to (III.13). Then we formally solve (B.5) (see (III.14)) and rewrite (B.7) in the form

$$F(s) = \frac{1}{V} \langle \rho^{o*} | \frac{1}{s - \hat{H}} | \rho^{o} \rangle, \tag{B.8}$$

which is analogous to (III.15). We proceed by defining right and left eigenstates of $\hat{H}$ (see (III.16) and (III.17)), denoted $\rho^{(\alpha)}$ and $\rho'^{(\alpha)}$, respectively, and use the bi-orthogonal set of these eigenstates to expand the identity operator (see (III.20)). If $\{\rho^{(\alpha)}\}$ is a set of right eigenstates, then $\{\rho^{(\alpha)*}\}$ is a set of left eigenstates of $\hat{H}$, because $\hat{H}$ is a symmetric operator. However, the bi-orthogonality of the two sets is not guaranteed in degenerate subspaces, and therefore a bi-orthogonalization procedure still has to be performed in these subspaces. Finally, we bring (B.8) to the form (III.21), where the weights of the poles F_α, are given by

$$F_\alpha \equiv \frac{1}{V} \langle \rho^{o*} | \rho^{(\alpha)} \rangle \langle \rho'^{(\alpha)} | \rho^{o} \rangle \quad , \tag{B.9}$$

which is analogous to (III.22).

Clearly, there is a one-to-one correspondence between the formalism presented in Ch.III.B and the modification presented here. E.g., the eigenstates $\varepsilon^{(\alpha)}$ of a single isotropic cylindrical inclusion imbedded in an

infinite isotropic medium, which were derived in Ch.III.D, can be easily transformed into the eigenstates $\rho^{(\alpha)}$ of $\hat{H}$ (as they appeared in our original paper [27]) by multiplying them by the K tensor, which in the isotropic case is

$$K_{ijkl} = \frac{1}{\sqrt{2}} (\sqrt{\delta\kappa} - \sqrt{\delta\mu})\delta_{ij}\delta_{kl} + \sqrt{2\delta\mu}\, I_{ijkl} \quad . \tag{B.10}$$

Although the formalism which was presented here has some minor formal advantages (e.g., sometimes $\hat{H}$ is hermitian), it appears that in practical calculations [28,29], it is more convenient to use the form of Ch.III.B.

APPENDIX C. EVALUATION OF LATTICE SUMS IN A 3D MODEL

In this appendix we discuss the evaluation of the lattice sums $Q_{\beta,\alpha}$ of the 3D dipole-dipole interactions for the model which was described in Ch.IV.E. The results of those calculations were depicted in Fig.IV.4.

A single cylindrical inclusion has 6 dipolar resonances and there are 3 possible orientations of the cylinder. Thus, the dipole-dipole part of the $Q_{\beta,\alpha}$ matrix of (IV.12) has $18^2=324$ elements. However, the number of possibly different lattice sums is reduced to 57 if we take account of the fact that $Q_{\beta,\alpha}= Q_{\alpha,\beta}$ is a symmetric matrix, and that some of the elements can be obtained from others by rotating the reference frame: E.g., $Q_{XCT,XCT} = Q_{YCT,YCT}$, $Q_{YCT,XST+} = Q_{ZCT,YST+}$, etc.

All the interactions of CL states vanish, because $s_{CL} = 0$ (see (IV.47)). Thus the first three lines in Fig. IV.4 vanish trivially. The diagonal elements denoted by C and E in Fig. IV.4 have been calculated in the 2D problem of the periodic square array of parallel cylinders: $Q_{XST\pm,XST\pm}$, $Q_{YST\pm,YST\pm}$ and $Q_{ZST\pm,ZST\pm}$ can be obtained directly from $Q_{\pm B2,\pm B2}$ of (IV.29), because these elements include summation of the interaction of parallel cylinders and we are actually treating a 2D problem. Note that, in these and in subsequent results, p_1 which appeared in (IV.29) is replaced by $\frac{1}{3}p_1$, because a set of cylinders which point in one direction is a subset consisting of 1/3 of the total number of cylinders in the 3D problem. The lattice sums $Q_{XSL\pm,XSL\pm}$, $Q_{YSL\pm,YSL\pm}$ and $Q_{ZSL\pm,ZSL\pm}$ can also be easily evaluated: Although in, say, a Z-cylinder the non-vanishing component of the displacement vector is u_3, it depends only on the X and Y coordinates, and we actually treat a 2D problem, which can be handled by the methods presented in Ch.IV.C, i.e. (IV.21) can be used.

The remaining components of the $Q_{\beta,\alpha}$ are non-trivial and do not reduce to a 2D calculation. In order to evaluate the lattice sum of interactions between states which belong to mutually perpendicular cylinders, we must use the procedure of Ch.IV.C, in a somewhat modified form. Suppose we are interested in $Q_{X\beta,Z\alpha}$, where β and α are some dipolar

resonances. Fig.C.1 shows the cross section of the system depicted in Fig.IV.3 in the X,Y plane. The black circles are the cross sections of Z-cylinders, while the shaded area (including the black rectangle) is the cross section of one X-cylinder.

It is convenient to represent the lattice sum (IV.12) in the following form:

$$Q_{X\beta,Z\alpha} = s_\alpha \langle \varepsilon^{c(X\beta)} \mid \theta_c \left(\sum_a \mid \varepsilon^{a(Z\alpha)}\right\rangle), \tag{C.1}$$

where a and c enumerate the cylinders. Thus we are actually interested in the overlap integral between <u>one</u> X-cylinder dipolar resonance β and the <u>sum</u> of dipolar resonances α over all Z-cylinders. We shall not evaluate this overlap over the entire X-cylinder, but only over a part of it of length b (= lattice spacing), i.e. the integral will be evaluated only in the blackened portion of the X-cylinder shown in Fig.C.1. Due to the periodicity in the X-direction, the resulting partial overlap integral must clearly be equal to $(Q_{X\beta,Z\alpha} \cdot b)/(s_\alpha \cdot L)$.

The strain ε created by the α resonances of all the Z-cylinders must be treated in a similar fashion to that which was described in Ch.IV.C: We split ε into a "near" and a "far" contributions (see (IV.16)) and replace the "far" contribution by a "macroscopic (volume averaged) near" contribution (see (IV.18)). The strain produced by the "macroscopic near" region is equal to the strain of the α state inside the Z-cylinder multiplied by the volume fraction (see (IV.19)), which in our case is $\frac{1}{3}p_1$.

As an example of such a calculation, we evaluate $Q_{XST+,ZCT}$:

$$\frac{Q_{XST+,ZCT}\cdot b}{s_{CT}\cdot L} = A_{ST}\, A_{CT}\, R^2 \int \left[\begin{pmatrix} 0 \\ 1 \\ -1 \\ 0 \\ 0 \\ 0 \end{pmatrix} \delta C \sum_{w_o} \begin{pmatrix} -Re \\ Re \\ 0 \\ Im \\ 0 \\ 0 \end{pmatrix} \frac{1}{(w-w_o)^2} \right] dV \quad , \tag{C.2}$$

where the first column represents ε^{XST+} (compare with ε^{ZST+} in (IV.41)) inside the X-cylinder, $\frac{1}{(w-w_o)^2}$ together with the column vector to its left

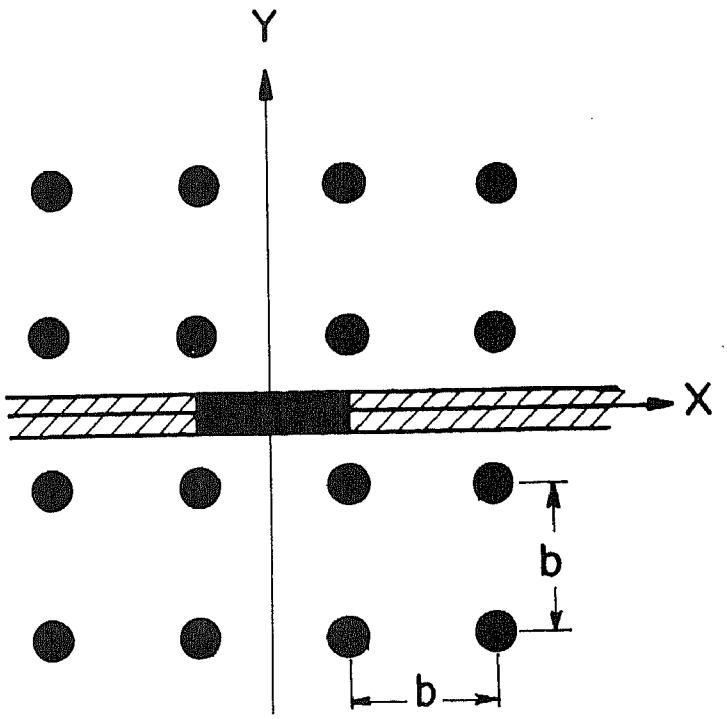

Fig. C.1 Cross section of the system depicted in Fig. IV.3 and described in Ch.IV.E., in the X,Y plane. The black circles denote the cross section of a square array with lattice spacing b of parallel Z-cylinders. The shaded area (including the black rectangle) denotes the cross section of one X-cylinder. The black rectangle inside it denotes the part of the X-cylinder over which the overlap integrals are evaluated.

represents the tail of the ε^{ZCT} state (see (IV.39)) outside the Z-cylinder located at $w_o = X_o + iY_o$, the summation is performed over all locations w_o of the Z-cylinders, and the 3D integral is performed inside the blackened portion of the X-cylinder (see Fig.C.1). We now replace the contribution of the far cylinders by a "macroscopic near" contribution (see (IV.18) and (IV.19)) and obtain

$$\frac{Q_{XST+,ZCT}^{\cdot b}}{s_{CT}^{\cdot L}} = A_{ST}A_{CT}R^2\int\Big[\begin{pmatrix}0\\1\\-1\\0\\0\\0\end{pmatrix}\delta C \sum_{\substack{w_o\\ near}}\begin{pmatrix}-Re\\Re\\0\\Im\\0\\0\end{pmatrix}\frac{1}{(w-w_o)^2}\Big]\,dV -$$

$$-\frac{1}{3}p_1 A_{ST}A_{CT}\int\begin{pmatrix}0\\1\\-1\\0\\0\\0\end{pmatrix}\delta C\begin{pmatrix}1\\1\\0\\0\\0\\0\end{pmatrix}dV =$$

$$= A_{ST}A_{CT}R^2\,2\delta\mu\int\Big[\sum_{\substack{w_o\\ near}}Re\frac{1}{(w-w_o)^2}\Big]\,dV - \frac{1}{3}p_1 bA_{ST}A_{CT}2\delta\mu\pi R^2 =$$

$$= -\frac{p_1 b}{3L}\sqrt{\frac{\delta\mu}{\delta\lambda+\delta\mu}}\quad , \tag{C.3}$$

where we used (IV.39b) and (IV.41b), as well as the result of the following integral

$$\int\sum_{\substack{w_o\\ near}}Re\,\frac{1}{(w-w_o)^2}\,dXdYdZ = -\frac{1}{3}p_1 b\pi \tag{C.4}$$

over the blackened region of the X-cylinder (see Fig.C.1). This integral was evaluated by the following considerations: Let us treat $Re\frac{1}{(w-w_o)^2}$ as the <u>electric</u> field of a 2D unit dipole located at the point w_o. If we perform the dX integration in (C.4) we obtain the potential difference between $X = -\frac{1}{2}b$ and $X = \frac{1}{2}b$. It can be shown by standard

electrostatic methods [39] that the average field created by such a square array of dipoles with lattice spacing b inside a very large circle (as required by the definition of the "near" region (see Ch.IV.C)) is $-\pi/b^2$. Thus the potential difference between $X = -\frac{1}{2}b$ and $X = \frac{1}{2}b$ will be $-\pi/b$. The additional integrations (dYdZ) in (C.4) will contribute πR^2, and the final result of that integral will be $-\pi^2R^2/b = -\frac{1}{3}\pi p_1 b$, from which (C.3) follows.

The example presented above is a typical calculation: all the other 3D lattice sums can be evaluated in a similar way.

APPENDIX D. DERIVATION OF THE REUSS BOUND

In this appendix we modify the formalism which was presented in Ch.V.C and use this modification to derive the Reuss bound [15] on the elastic stiffness tensor.

As in Ch.V.C we represent the microgeometry of a multi-component composite by a set of step functions $\{\theta_n\}$, where θ_n defines the microgeometry of the n-th component as in (III.2). However, this time we define a compliance tensor, that depends on the continuous parameter s:

$$S(\vec{r};s) = S^{(o)} + \frac{1}{s}\sum_n \theta_n(\vec{r})(S^{(n)} - S^{(o)}) \equiv$$

$$\equiv S^{(o)} + \frac{1}{s}\sum_n \theta_n \delta S^{(n)} \quad , \tag{D.1}$$

where $S^{(o)}$ is an arbitrary (symmetric postive definite) tensor. If we define

$$C(\vec{r};s) \equiv S^{-1}(\vec{r};s) \quad , \tag{D.2a}$$

$$C^{(o)} \equiv S^{(o)^{-1}} \quad , \tag{D.2b}$$

then the elastic constants will have the same analytic structure as (V.17), i.e.

$$F(s) \equiv \varepsilon^o(C^{(e)} - C^{(o)})\varepsilon^o = \sum_\alpha \frac{F_\alpha}{s-s_\alpha} \quad . \tag{D.3}$$

In general, both s_α and F_α will be complex. However, once we restrict the choice of $S^{(o)}$ so that <u>all</u> $\delta S^{(n)} \geqslant 0$ (or <u>all</u> $\delta S^{(n)} \leqslant 0$), these parameters become real numbers: Let $s = s_\alpha$ be a pole of F(s). As in Ch.V.C we can show that there exists a resonance state $\varepsilon^{(\alpha)}$ for which

$$\int \varepsilon^{(\alpha)*} C(\vec{r};s_\alpha)\varepsilon^{(\alpha)} dV = 0 \tag{D.4}$$

(see (V.15)). Suppose we choose $S^{(o)}$ so that all $\delta S^{(n)}$ are positive definite. Assume that Im $s_\alpha > 0$. Then we would obtain from (D.1) that Im $S(\vec{r};s_\alpha)$ is negative definite. Since $C(\vec{r};s_\alpha)$ is the inverse of $S(\vec{r};s_\alpha)$, i.e. the eigenvalues of the $C(\vec{r};s_\alpha)$ matrix are the reciprocals of the eigenvalues of $S(\vec{r};s_\alpha)$ matrix, we would find that Im $C(\vec{r};s_\alpha)$ is positive definite. This conclusion would contradict (D.4), and therefore the assumption that Im $s_\alpha > 0$ was wrong. Similarly, we can prove that Im s_α cannot be negative. Thus s_α is a real number. The entire proof can be repeated for negative definite $\delta S^{(n)}$. The weights F_α are real for the same reasons as in Ch.V.C.

As long as $S(\vec{r};s)$ assumes physical values, i.e. is positive definite, there can be no poles in F(s). Therefore, from (D.1) we obtain that

$$s_\alpha \leqslant 0, \qquad \text{when } \underline{\text{all}}\ \delta S^{(n)} \geqslant 0, \tag{D.5a}$$

$$0 \leqslant s_\alpha < 1, \quad \text{when } \underline{\text{all}}\ \delta S^{(n)} \leqslant 0. \tag{D.5b}$$

The parameters F_α and s_α of (D.3) also satisfy moment sum rules, which can be calculated from (V.21), i.e.

$$M_n \equiv \sum_\alpha F_\alpha s_\alpha^n = \frac{1}{(n+1)!} \cdot \frac{d^{n+1}F}{dw^{n+1}}\bigg|_{w=0} , \tag{D.6}$$

where $w = 1/s$. Thus, in order to evaluate the $n = 0$ moment we must find the first derivative of F at $w = 0$. We start from a calculation of the first variation of F with repect to w. As in Ch.V.C (see (V.22) and (V.23)) we obtain

$$\Delta F = \frac{1}{V} \int \varepsilon \Delta C \varepsilon \, dV \quad . \tag{D.7}$$

From (D.1) and (D.2) we obtain

$$\Delta C = \Delta(S^{-1}) = -S^{-1}\Delta S\, S^{-1} = -C(\sum_n \theta_n \delta S^{(n)})C\,\Delta w, \tag{D.8}$$

$$\Delta F = -\frac{\Delta w}{V}\int \varepsilon\, C(\sum_n \theta_n \delta S^{(n)})C\varepsilon \quad . \tag{D.9}$$

In the limit $w = 0$ ($s = \infty$) the sample becomes homogeneous, i.e. $\varepsilon = \varepsilon^o$ and it is now straightforward to obtain M_o from (D.6) and (D.9)

$$\begin{aligned} M_o &= -\frac{1}{V}\int \varepsilon^o C^{(o)}(\sum_n \theta_n \delta S^{(n)})C^{(o)}\varepsilon^o\, dV = \\ &= -\sum_n p_n\, \varepsilon^o C^{(o)}\delta S^{(n)} C^{(o)}\varepsilon^o = -\varepsilon^o C^{(o)}\langle \delta S\rangle_{av} C^{(o)}\varepsilon^o = \\ &= -\varepsilon^o C^{(o)}\langle S\rangle_{av} C^{(o)}\varepsilon^o + \varepsilon^o C^{(o)}\varepsilon^o \quad . \end{aligned} \tag{D.10}$$

We also note that if <u>all</u> $\delta S^{(n)} \geqslant 0$ ($\delta S^{(n)} \leqslant 0$) in (D.9), then the derivative dF/dw is always negative (positive). From this it follows that all $F_\alpha < 0$ ($F_\alpha > 0$). Thus we obtain from (D.5)

$$F_\alpha \cdot s_\alpha \geqslant 0 \ , \tag{D.11}$$

when <u>all</u> $\delta S \geqslant 0$ or <u>all</u> $\delta S^{(n)} \leqslant 0$, as opposed to (V.26c).

As in Ch.IV.D, it is convenient to introduce a new related function

$$H(s) \equiv F(s)/(F(s) + \varepsilon^o C^{(o)}\varepsilon^o) = 1 - \varepsilon^o C^{(o)}\varepsilon^o/\varepsilon^o C^{(e)}\varepsilon^o \tag{D.12}$$

This function has an analytical structure analogous to that of $F(s)$ (see (V.38)). The poles of h_α of this function and their weights H_α satisfy

$$h_\alpha \leqslant 0, \qquad \text{when } \underline{\text{all}}\ \delta S^{(n)} \geqslant 0, \tag{D.13a}$$

$$0 \leqslant h_\alpha < 1, \quad \text{when } \underline{\text{all}}\ \delta S^{(n)} \leqslant 0, \tag{D.13b}$$

$$H_\alpha \cdot h_\alpha \geqslant 0, \quad \text{in both cases.} \tag{D.13c}$$

The proof of (D.13) is the same as in Ch.IV.D with one exception: The inequality (D.11) has an opposite sign to (V.26c) and therefore (D.13a) replaces $H_\alpha \cdot h_\alpha \leqslant 0$, which was obtained before (see (V.39)).

The Reuss bound can now be derived along the same lines as the Voigt bound in Ch.V.B. (see (V.1) and (V.2)):

$$H(1) = \sum_\alpha H_\alpha \left(1 + \frac{s_\alpha}{1-s_\alpha}\right) \geqslant \sum_\alpha H_\alpha = M_{OH}, \tag{D.14}$$

where the zero moment M_{OH} of H(s) is given by (V.37). This can be re-written in the form

$$H(1) = \frac{F(1)}{F(1) + \varepsilon^0 C^{(o)} \varepsilon^{(o)}} = 1 - \frac{\varepsilon^0 C^{(o)} \varepsilon^0}{\varepsilon^0 C^{(e)} \varepsilon^0} \geqslant \tag{D.15}$$

$$\geqslant \frac{M_0}{\varepsilon^0 C^{(o)} \varepsilon^0} = 1 - \frac{\varepsilon^0 C^{(o)} \langle S \rangle_{av} C^{(o)} \varepsilon^0}{\varepsilon^0 C^{(o)} \varepsilon^0},$$

where (V.40a) and (D.10) were used. Thus we obtain

$$\varepsilon^0 C^{(e)} \varepsilon^0 \geqslant \frac{(\varepsilon^0 C^{(o)} \varepsilon^0)^2}{\varepsilon^0 C^{(o)} \langle S \rangle_{av} C^{(o)} \varepsilon^0} \tag{D.16}$$

If we choose

$$C^{(o)} = A \cdot \langle S \rangle_{av}^{-1}, \tag{D.17}$$

where the positive constant A must be small enough (or large enough) to ensure that all $\delta S^{(n)} \leqslant 0$ (or all $\delta S^{(n)} \geqslant 0$), then we obtain from (D.16) and (D.17)

$$\varepsilon^0 C^{(e)} \varepsilon^0 \geqslant \varepsilon^0 \langle S \rangle_{av}^{-1} \varepsilon^0, \tag{D.18}$$

which is the Reuss bound.

Finally, we would like to note that the parametrization of F(s) in (D.1) is a particular case of the parametrization of the type (V.15) and (V.16). The simple form (D.1) sufficed for our purposes. However, the generalized parametrization may have additional applications, analogous to those presented in Ch.V.D.

BIBLIOGRAPHY

1. L. Holliday in "Composite Materials" (ed. by L. Holliday) ch. I, Elsevier Publishing Co., Amsterdam, 1966.

2. D.K. Hale, J. Mater. Science 11 (1976), 2105.

3. See, e.g.,
   a. "Composite Materials" (ed. by L. Holliday), Elsevier Publishing Co., Amsterdam, 1966;

   b. "Fundamental Aspects of Fiber Reinforced Plastic Composites" (ed. by R.T. Schwartz and H.S. Schwartz), Interscience Publishers, New York, 1968;

   c. F.S. Galasso "High Modulus Fibers and Composites", Gordon and Breach Science Publishers, New York, 1969;

   d. "Fibrous Composites" (ed. by I.N. Frantsevich and D.M. Karpinos), Israel Program for Scientific Translations, Jerusalem, 1972 (Translated from Russian: "Kompozitsionnye Materialy Voloknistogo Stroeniya", Naukova Dumka, Kiev, 1970).

4. "Applications of Composite Materials" (ed. by M.J. Salkind and G.S. Holister), American Soc. for Testing Materials, Philadelphia, 1973; see also Ref. 3c.

5. "Composite Materials" - vol. 3 "Engineering Applications of Composites" (ed. by B.R. Noton), Academic Press, New York, 1974.

6. S.K. Garg, V. Svalbonas and G.A. Gurtman, "Analysis of Structural Composite Materials" Sec. I.1, Marcel Dekker, New York, 1973.

7. Z. Hashin, "Theory of Fiber Reinforced Materials", NASA, Langeley Research Center, Hampton, Virginia, 1970.

8. a. V.M. Levin, Mech. Solids 2 (1967), 58 (Translation from Russian: Mekhanika Tverdogo Tela 2 (1967), 88);

   b. B.W. Rosen and Z. Hashin, Int. J. Engng. Sc. 8 (1970), 157.

9. a. Z. Hashin, J. Appl. Mech. 32 (1965), 630;

   b. Z. Hashin, AIAA J. 4 (1966), 1411;

   c. Z. Hashin, Int. J. Solids Structures 6 (1970), 539.

10. A review of the traditional approaches to the problem of effective elastic constants, as well as an exhaustive list of references, can be found in:
   a. J.P. Watt, G.F. Davies and R.J. O'Connell, Rev. Geophys. Space Phys. 14 (1976), 541; see also Refs. 6 and 7;

   b. J.R. Willis, "Elasticity of Composites", SUDAM Rep. No. 80 - 2, Stanford University, California, 1980;

   c. J.R. Willis in "Advances in Appl. Mech." (ed. by Chia - Shun Yih), vol. 21, p. 1, Academic Press, New York, 1981.

11. Z. Hashin, J. Appl. Mech. 29 (1962), 143.

12. Z. Hashin and B.W. Rosen, J. Appl. Mech. 31 (1964), 223.

13. R. Hill, J. Mech. Phys. Solids 11 (1963), 357.

14. A summary of many numerical solutions, as well as numerous references on different models and different numerical techniques, can be

found in Ref. 6.

15. R. Hill, Proc. Phys. Soc. London A65 (1952), 349.
See also Ref. 13.

16. a. W. Voigt, Ann. Phys. 38 (1889), 573;

b. W. Voigt, Lehrbuch der Kristallphysik, Teubner, Leipzig, 1928.

17. A. Reuss, Z. Angew. Math. Mech. 9 (1929), 49.

18. Z. Hashin and S. Shtrikman, J. Mech. Phys. Solids 10 (1963), 127.

19. a. D.A. Bruggeman, Ann. Phys. Leipzig 29 (1937) 160 (the result for the effective shear modulus in this article is incorrect);

b. J.M. Dewey, J. Appl. Phys. 18 (1947), 578;

c. J.D. Eshelby, Proc. Roy. Soc. London A241 (1957), 376;

d. Z. Hashin in "Proceedings of the International Union of Theoretical and Applied Mechanics Symposium on Nonhomogeneity in Elasticity and Plasticity" (ed. by W. Olszak), p. 463, Pergamon Press, New York, 1959;

e. L.J. Walpole, Quart. J. Mech. Appl. Math. 25 (1972), 153;

f. J.R. Willis and J.R. Acton, Quart. J. Mech. Appl. Math. 29 (1976), 163;
and many others.

20. a. B. Budiansky, J. Mech. Phys. Solids 13 (1965), 223;

b. R. Hill, J. Mech. Phys. Solids 13 (1965), 213;
For additional references see Ref. 10a.

21. J. Korringa, J. Math. Phys. 14 (1973), 509.

22. R. Zeller and P.H. Dederichs, Phys. Stat. Solidi (b) 55 (1973), 831.

23. J.E. Gubernatis and J.A. Krumhansl, J. Appl. Phys. 46 (1975), 1875.

24. E. Kröner, J. Mech. Phys. Solids 25 (1977), 137.

25. a. J.E. Gubernatis, E. Domany and J.A. Krumhansl, J. Appl. Phys. 48 (1977), 2804;

b. J.E. Gubernatis, E. Domany, J.A. Krumhansl and M. Huberman, J. Appl. Phys. 48 (1977), 2812;

c. J.E. Gubernatis, E. Domany and R.M. Thomson, J. Appl. Phys. 50 (1979), 3338;

d. J.E. Gubernatis, J. Appl. Phys. 50 (1979), 4046.

26. a. J.R. Willis, J. Mech. Phys. Solids 28 (1980), 287;

b. J.R. Willis, J. Mech. Phys. Solids 28 (1980), 307.

27. Y. Kantor and D.J. Bergman, J. Mech. Phys. Solids 30 (1982), 355.

28. Y. Kantor and D.J. Bergman, to appear in J. Mech. Phys. Solids.

29. Y. Kantor and D.J. Bergman, Appl. Phys. Lett. 41 (1982), 932.

30. D.E. Lloyd, in Ref. 3a, p. 91.

31. K. Newman, in Ref. 3a, p. 336.

32. J.J. Bikerman, "The Science of Adhesive Joints", Academic Press, New York, 1961.

33. See, e.g., G.F. Davies, J. Phys. Chem. Solids 34 (1973), 841.

34. For main equations of elastostatics and properties of linear homogeneous materials, see e.g.

    a. I.S. Sokolnikoff, "Mathematical Theory of Elasticity", Ch. 1 - 3, McGraw-Hill, New York, 1956;

    b. A.E.H. Love, "A Treatise on the Mathematical Theory of Elasticity", Ch. 1 - 5, Dover, New York, 1944;

    c. L.D. Landau and E.M. Lifshitz, "Theory of Elasticity", Ch. 1, Pergamon Press, Oxford, 1970. (Translated from Russian: "Teoriya Uprugosti", Nauka, Moskva, 1965.)

35. See, e.g., p. 29 in Ref. 31a.

36. See, e.g.,
    a. N.M. Parikh in "Fiber Composite Materials", p. 131, American Soc. for Metals, Metals Park, Ohio, 1965;

    b. "Composite Materials" - vol. 6 "Interfaces in Polymer Matrix Composites" (ed. by L.J. Broutman and R.H. Krock), Academic Press, London, 1974.

37. V.D. Kupradze, "Potential Methods in the Theory of Elasticity", Israel Program for Scientific Translations, Jerusalem, 1965. (Translation from Russian: "Metody Potentsiala v Teorii Uprugosti", Fizmatgiz, Moskva, 1963.)

38. I.M. Gelfand and G.E. Shilov, "Generalized Functions" - vol. 1, Academic Press, New York, 1964. (Translated from Russian: "Obobshchennye Funktsii", Fizmatgiz, Moskva, 1958.)

39. N.W. Ashcroft and N.D. Mermin, "Solid State Physics", Ch. 27, Holt, Rinehart and Winston, New York, 1976.

40. E.g., C. - T.D. Wu and R.L. McCullough in "Developments in Composite Materials - 1" (ed. by G.S. Holister), p. 119, Science Publishers, London, 1977.

41. E. Kröner, "Statistical Continuum Mechanics", Springer, New York, 1972.

42. An extensive discussion as well as numerous examples of the properties and applications of the homogeneous boundary conditions can be found in Sec. 3.2 - 3.4 in Ref. 7.

43. See, e.g., Ch. 5 in Ref. 34a.

44. R. Hill, J. Mech. Phys. Solids 12 (1964), 199.

45. a. R.J. Elliot, J.A. Krumhansl and P.L. Leath, Rev. Mod. Phys. 46 (1974), 465;

b. F. Yonezawa and K. Morigaki, Prog. Theor. Phys. Suppl. 53 (1974), 1.

46. D.J. Bergman, Phys. Rev. B19 (1979), 2359.

47. D.J. Bergman, J. Phys. C12 (1979), 4947.

48. For the properties of bi-orthogonal sets of functions, see P.M. Morse and H. Feshbach, "Methods of Theoretical Physics", pp. 884 and 919, McGraw-Hill, New York, 1953.

49. D.J. Bergman and Y. Kantor, unpublished (1981).

50. See Ch. VII in Ref. 37.

51. The analysis of $s_\alpha = 0$ eigenstates in both electrostatic and elastostatic cases was given by D.J. Bergman, in "Proceedings of the Summer School on Homogenization (Chartres, France, July, 1983)", to be published, 1983.

52. See, e.g., H. Goldstein, "Classical Mechanics", p. 124, Adisson-Wesley Publishing Co., Reading, Massachusetts, 1971.

53. For the equations of transformation of strain tensor see, e.g., Ref. 34.

54. J.D. Eshelby, Proc. Roy. Soc. London A241 (1957), 376.

55. An analogous subtraction of a constant term was used by
a. J. Korringa, J. Math. Phys. 14 (1973), 509;

b. J.R. Willis and J.R. Acton, Quart. J. Mech. Appl. Math. 29 (1976), 163;

c. J.R. Willis, J. Mech. Phys. Solids 25 (1977), 185.

56. See Refs. 10b, 37 and the references therein.

57. See, e.g., Ch. 7 in Ref. 7.

58. See, e.g., S.W. Tsai, D.F. Adams and D.R. Doner, "Effect of Constituent Material Properties on the Strength of Fiber-Reinforced Composite Materials", Air Force Materials Lab. Rep., 1966.

59. "Fiber Composite Materials", Amer. Soc. for Metals, Metals Park, Ohio, 1965.

60. J.D. Forest and J.L. Christian, p. 134 in Ref. 4.

61. G. Pickett, p. 13 in Ref. 3b.

62. a. C.H. Chen and S. Cheng, J. Comp. Mater. 1 (1967), 30;

b. R.R. Rizzo, J. Comp. Mater. 3 (1969), 202.

63. C.H. Chen and S. Cheng, J. Appl Mech. 37 (1970), 186.

64. E.g., L.I. Schiff, "Quantum Mechanics", pp. 244 - 251, McGraw-Hill, New York, 1968.

65. See Ch. 5 in Ref. 6 and references therein.

66. See, e.g., Ch. 8 in Ref. 39.

67. See, e.g., Ch. 10 in Ref. 39.

68. Scattering-theory approaches to the elastodynamic problem can be found in Refs. 25 and 26.

69. a. G.K. Batchelor, Ann. Rev. Fluid Mech. 6 (1974), 227;

b. D.J. Jeffrey, Proc. Roy. Soc. London A338 (1974), 503;

c. J.R. Willis and J.R. Acton, Quart. J. Mech. Appl. Math. 29 (1976), 163.

70. A standard approach to the electrostatic problem of dipole-dipole interactions can be found in Ref. 39, while the same approach in the "language" of electrostatic resonances is presented in Ref. 46.

71. See, pp. 250 - 274 in Ref. 7.

72. a. R. Hill, J. Mech. Phys. Solids 13 (1965), 189;

b. L.J. Walpole, J. Mech. Phys. Solids 17 (1969), 235;

c. L.J. Walpole, Quart. J. Mech. Appl. Math. 25 (1972), 153.

73. An analysis of this approximation as well as list of references on its original derivations can be found in R. Landauer in "AIP Conf. Proc. No. 40" (ed. by C.W. Garland and D. Tanner), p. 2, AIP, New York, 1978; See also Ch. 27 in Ref. 39, and Ref. 46.

74. See pp. 179, 294 - 296 in Ref. 7.

75. In the original publication an algebraic mistake was made in this expression (Eq. 5.14 in Ref. 27).

76. A. Gray and G.B. Mathews, "A Treatise on Bessel Functions and Their Applications to Physics", Ch. XV, Dover Publications, New York, 1966.

77. See, Ch. II in Ref. 76.

78. Y. Kantor and D.J. Bergman, unpublished (1982).

79. Y. Kantor and D.J. Bergman, J. Phys. C15 (1982), 2033.

80. a. Z. Hashin and S. Shtrikman, J. Franklin Inst. 271 (1961), 336;

b. Z. Hashin and S. Shtrikman, J. Mech. Phys. Solids 10 (1962), 335.

81. Z. Hashin, J. Mech. Phys. Solids 13 (1965), 119.

82. R. Hill, in "Prog. in Appl. Phys., The Prager Anniversary Volume",

p. 99, MacMillan, New York, 1963.

83. a. L.J. Walpole, J. Mech. Phys. Solids 14 (1966), 151;

b. L.J. Walpole, J. Mech. Phys. Solids 14 (1966), 289.

84. J.M. Beran and J. Molyneux, Quart. J. Appl. Math. 24 (1960), 107.

85. J.J. McCoy in "Recent Advances in Engineering Science" (ed. by A.C. Eringen), p. 235, Gordon and Breach, New York, 1970.

86. a. G.W. Milton, Phys. Rev. Lett. 46 (1981), 542;

b. G.W. Milton and N. Phan-Thien, Proc. Roy. Soc. London A380 (1982), 305.

87. P.H. Dederichs and R. Zeller, Z. Physik 259 (1973), 103.

88. a. D.J. Bergman, in "AIP Conference Proceedings No. 40" (ed. by J.W. Garland and D. Tanner), p. 46, Amer. Inst. Phys., New York, 1978;

b. D.J. Bergman, Phys. Rep. 43 (1978), 377.

89. J.R. Willis, J. Mech. Phys. Solids 25 (1977), 185.

90. See, e.g., Refs. 13, 83, 72b.

91. a. D.J. Bergman, Phys. Rev. Lett. 44 (1980), 1285;

b. D.J. Bergman, Phys. Rev. B23 (1981), 3058;

c. D.J. Bergman, Ann. Phys. 38 (1982), 78.

חקירת הקבועים האלסטיים האפקטיביים

של חומרים מורכבים

חבור לשם קבלת תואר "דוקטור לפילוסופיה"

מאת

יעקב קנטור

הוגש לסנאט של אוניברסיטת תל-אביב

אלול תשמ"ג

עבודה זו נעשתה בהדרכת

פרופסור דוד ברגמן

ת ק צ י ר

במסגרת תיזה זו מוצגת גישה חדשה להערכה שיטתית של הקבועים האלסטיים האפקטיביים של חומרים מורכבים ולקבלת חסמים מדוייקים עליהם. בעזרת גישה דמויית תורת הפיזור מפתחים את הפתרון של הבעיה האלסטוסטטית באמצעות קבוצת מצבים עצמיים של אופרטור אינטגרלי מסויים. המצבים האלה הינם הרזוננסים האלסטוסטטיים של הדגם, כלומר הם מייצגים מצבים שבהם מתקיימים מאמצים ומעוותים פנימיים בדגם למרות העובדה ששפת הדגם אינה מעוותת. כל קבוע אלסטי אפקטיבי מוצג כסכום של קטבים פשוטים. מיקומם של הקטבים נקבע ע"י הערכים הלא פיסיקליים של הקבועים האלסטיים של מרכיבי החומר שמאפשרים קיום הרזוננסים. משקלו של כל קוטב נקבע מתוך ידיעת טבזור המעוות המפורט במצב של רזוננס.

חישוב הרזוננסים של מערכת רב גרגירית נעשה במספר שלבים. בתחילה מוצאים את הרזוננסים של גרגירים בודדים המבודדים משאר הגרגירים ולאחר מכן בונים את הרזוננסים של הדגם כולו כהרכבה של רזוננסים של גרגירים מבודדים. אני מיישם את התהליך למערכים דו-ממדיים (מרובע ומשושה) של גלילים. בעזרת תורת ההפרעות של מטריצות אני מפתח את הקבועים האלסטיים בחזקות של הרכוז הנפחי של הגלילים p_1. הפיתוחים מגיעים עד לסדר p_1^7 (p_1^{11}) עבור קבוע הדחיסה של מערך מרובע (משושה) ועד לסדר p_1^5 עבור קבועי הגזירה של שני המערכים. אני מראה כי קירוב דמוי קלאוזיאוס-מוסוטי נותן הערכה טובה של הפתרון המדוייק עבור המיקרוגיאומטריות שהוזכרו לעיל. אני מקבל קירוב כזה גם למערכת תלת-מימדית של גלילים עגולים המסודרים כך שלמערכת יש סימטריה קובית.

אני משתמש בהצגת הקבוע האלסטי האפקטיבי כסכום של קטבים פשוטים גם במקרים שבהם קיים רק מידע חלקי על מיקרוגיאומטריה של החומר. אני מתיחס למיקומם ולמשקלם של הקטבים כאל פרמטרים ווריאציוניים ומתרגם את הסוגים השונים של המידע על החומר לאילוצים על הפרמטרים האלה, כגון כללי הסכום על ספקטרום הקטבים. מספר חסמים ידועים משוחזרים בשיטות האלה. התוצאות החדשות כוללות הרחבת תחום תחולתם של חסמי חשין-שטריקמן לחומרים מורכבים בעלי מיקרוגיאומטריה שרירותית במקרים שפונקצית הקורלציה הדו-נקודתית של המיקרוגיאומטריה איננה ידועה. מידע על הקבועים האלסטיים האפקטיביים של חומר מורכב אחד מנוצל לשיפור החסמים על הקבועים האלסטיים האפקטיביים של חומר מורכב אחר בעל אותה המיקרוגיאומטריה.

אני דן במספר יישומים אפשריים נוספים של התיאוריה למערכות קווזי-אקראיות ולחומרים מורכבים וויסקו-אלסטיים. נתנת השווה בין התיאוריה שלי לבין הגישות האחרות לבעיה של חישוב הקבועים האלסטיים (האפקטיביים) של חומר מורכב.

תוכן העניינים